

**Aus der Medizinischen Klinik und Poliklinik IV
der Ludwig-Maximilians-Universität München
Direktor: Prof. Dr. med. Martin Reincke**

Application of engineered mesenchymal stem cells as therapeutic vehicles for the treatment of solid tumors: HIF1 α -based targeting and the influence of thyroid hormones

**Dissertation
zum Erwerb des Doktorgrades der Medizin
an der Medizinischen Fakultät der
Ludwig-Maximilians-Universität zu München**

vorgelegt von

Nicole Salb, geb. Schöbinger

aus München

2018

**Mit Genehmigung der Medizinischen Fakultät
der Universität München**

Berichterstatter:	Prof. Dr. Peter Jon Nelson
Mitberichterstatter:	Prof. Dr. Heiko Hermeking Prof. Dr. Ralph Mocikat
Dekan:	Prof. Dr. med. dent. Reinhard Hicel
Tag der mündlichen Prüfung:	04.10.2018

Table of Contents

Summary	V
Zusammenfassung	VII
1. Introduction.....	1
1.1. New approaches for cancer treatment	1
1.2. Role of MSCs within tumor microenvironments	1
1.2.1. The importance of tumor stroma for tumor growth and progression	1
1.2.2. Biology of human MSCs	3
1.2.3. Potential clinical application of MSCs in cancer therapy and other fields ..	4
1.2.4. Use of engineered MSCs as vehicles for cancer therapy	4
1.3. Role of thyroid hormones in tumor microenvironments and MSC biology	7
1.4. MSCs as vehicles for cancer therapy: Hypoxia as possible new mechanism for selective transgene induction	10
1.5. Rationale of this study	12
1.6. Specific aims and scope	13
2. Materials and Methods	14
2.1. Materials.....	14
2.1.1. Cell culture.....	14
2.1.1.1. Media and supplements, dyes and other reagents	14
2.1.1.2. Cell lines and primary cells	15
2.1.2. Bacteria/Microbiology	17
2.1.3. Buffers and solutions	17
2.1.3.1. SDS-PAGE and western blot	18
2.1.3.2. Molecular biology	19
2.1.3.3. Microbiology.....	19
2.1.3.4. Histological and immunohistological staining	20
2.1.3.5. Cell culture	20
2.1.3.6. Other buffers and solutions	20
2.1.4. Antibodies for FACS and WB	21
2.1.5. Enzymes.....	22
2.1.6. Size standards for electrophoresis	22
2.1.7. Primers/Oligonucleotides.....	22
2.1.8. Plasmids and vectors	23
2.1.9. Kits	23
2.1.10. Chemicals.....	24
2.1.11. Disposables and other materials	25
2.1.12. Other laboratory equipment (devices)	26

2.1.13. Software	27
2.2. Methods	28
2.2.1. Cell culture.....	28
2.2.1.1. General cell culture	28
2.2.1.2. Freezing and thawing of cells.....	28
2.2.1.3. Cell quantification.....	28
2.2.1.4. Isolation of primary MSCs	28
2.2.1.5. Characterization of MSCs and HUH7 (FACS, differentiation, immortalization)	29
2.2.1.5.1. FACS analysis of characteristic surface markers	29
2.2.1.5.2. Differentiation and histochemical staining	30
2.2.1.5.3. Immortalization	31
2.2.1.6. Stripping of fetal calf serum.....	32
2.2.1.7. Production of HUH7 conditioned medium (CM)	32
2.2.1.8. Stimulation of MSCs with hypoxia, thyroid hormones and HUH7 conditioned medium (CM)	32
2.2.1.9. Transient transfection and luciferase reporter assay	33
2.2.1.9.1. Transient transfection using electroporation and lipofectamine® reagent.....	33
2.2.1.9.2. Dual Luciferase assay	34
2.2.1.10. Stable transfection of MSCs.....	34
2.2.1.11. Mycoplasma test	34
2.2.2. Microscopy of cells	34
2.2.3. Microbiology	34
2.2.3.1. Preparation of agar plates.....	34
2.2.3.2. Freezing and thawing of bacteria	34
2.2.3.3. Preparation of competent E.coli DH5α.....	35
2.2.3.4. Purification of up to 20µg plasmid DNA	35
2.2.3.5. Purification of up to 10mg plasmid DNA	35
2.2.4. Molecular biology.....	35
2.2.4.1. Restriction digestion of DNA	35
2.2.4.2. Separation of DNA fragments by agarose gel electrophoresis.....	36
2.2.4.3. Determination of DNA and RNA concentrations	36
2.2.4.4. Ligation of DNA fragments	36
2.2.4.5. DNA sequencing	36
2.2.4.6. Analysis of gene expression	36
2.2.4.6.1. Isolation of RNA	36
2.2.4.6.2. Reverse transcription	36
2.2.4.6.3. Quantitative real-time-PCR (qRT-PCR).....	37
2.2.5. Cloning strategies for luciferase reporter constructs.....	39
2.2.6. Protein biochemical methods.....	41

2.2.6.1. Protein extraction	41
2.2.6.2. BCA-Assay Protein quantification	42
2.2.6.3. SDS-Page and western blot.....	43
2.2.7. Chemotaxis assay	44
2.2.7.1. Chemotaxis assay preparation.....	45
2.2.7.2. Video microscopy.....	46
2.2.7.3. Chemotaxis analysis using Image J (plugins: Manual tracking, Chemotaxis tool)	46
2.2.7.4. Chemotactic and chemokinetic parameters	46
2.2.8. Tumor spheroid model.....	49
2.2.8.1. Spheroid formation.....	49
2.2.8.2. Frozen section of HUH7 tumor spheroids	50
2.2.8.3. HE staining of HUH7 tumor spheroids	50
2.2.8.4. Staining of necrotic and hypoxic areas in HUH7 and HT29 tumor spheroids	50
2.2.8.5. CMFDA staining of MSCs	51
2.2.8.6. Invasion of CMFDA stained MSCs.....	51
2.2.9. MTT-Assay	51
2.2.10. Statistical analysis	51
2.2.10.1. Rayleigh test for vector data	52
3. Results.....	53
3.1. Synthetic HIF1 α -responsive promoter in MSC-based gene-therapy of solid cancers	53
3.1.1. Utilizing the hypoxia response system in MSCs	53
3.1.2. HIF1 α protein level in MSCs increases under hypoxic conditions	53
3.1.3. Hypoxic activation of synthetic HIF1 α -responsive promoter and its comparison to the human RANTES/CCL5 gene promoter	53
3.1.4. Hypoxia in HUH7 and HT29 tumor spheroids.....	55
3.1.5. MSCs show a strong tropism for the center of HUH7 tumor spheroids ...	57
3.2. Unresponsiveness of the HUH7 tumor cell line to non-genomic thyroid hormone effects.	58
3.3. Non-genomic thyroid hormone effects on MSC hypoxia response	59
3.3.1. Thyroid hormones increase normoxic HIF1 α protein level in MSCs in a Tetrac dependent manner	59
3.3.2. Thyroid hormones increase activation of synthetic HIF1 α -responsive promoter in normoxia in a Tetrac dependent manner	61
3.3.3. Influence of thyroid hormones and HUH7 tumor cell conditioned medium (CM) on the steady state mRNA expression of known HIF1 α target genes	62
3.4. Thyroid hormones enhance chemotaxis and chemokinesis of MSCs in a Tetrac dependent manner.....	65

3.5. Effects of thyroid hormones, HUH7 tumor cell conditioned medium (CM) and oxygen level on MSC viability	72
4. Discussion	75
4.1. New targeting strategies for MSC-based cancer gene therapy	75
4.1.1. Existing protocols do not target hypoxic tumor stroma	75
4.1.2. Establishing tools to target hypoxic solid tumors	76
4.2. Non-genomic thyroid hormone effects on MSC biology in the context of Hepatocellular Carcinoma (HCC)	77
4.2.1. Potential effect of thyroid hormones on MSC proliferation.....	79
4.2.2. Potential effects of thyroid hormones on MSC differentiation	79
4.2.3. MSC hypoxia response: HIF1 α protein level and HIF1 α -driven reporter gene activation	80
4.2.4. MSC chemotaxis	81
4.2.5. MSC tumor spheroid invasion, <i>in vivo</i> homing and activation of transgenes in tumor stroma.....	81
4.3. Hypoxia targeting and thyroid hormones during MSC-based cancer gene therapy	82
4.3.1. Using hypoxia targeting for MSC-based cancer gene therapy.....	82
4.3.2. Influence of thyroid hormones on MSC-based cancer gene therapy	83
4.3.3. Tetrac as antitumor agent.....	83
4.3.4. Possible therapeutic improvements by prestimulation of MSCs with thyroid hormones	84
4.4. Outlook.....	84
4.4.1. Effects of chronic tumor disease on patient's thyroidal status and relevance for MSC therapy.....	84
4.4.2. Current limitations and risks of MSC-based cancer therapy and application of thyroid hormones	84
5. Addendum	86
5.1. Abbreviations and Symbols.....	86
5.2. List of Figures	89
5.3. List of Tables.....	90
6. References	91
7. Publications	100
8. Acknowledgements	100
Eidesstattliche Versicherung	101

Summary

Cancer is one of the top causes of mortality and morbidity despite our medical advances, thus new therapeutic concepts are needed. Solid tumors are composed of malignant cells within a tumor stroma. This microenvironment has become focus of ongoing cancer therapy research. Engineered versions of mesenchymal stem cells (MSCs) using suicide genes are a new approach under development for the therapy of solid tumors.

MSCs are multipotent progenitor cells residing in many tissues including the bone marrow and play an important role in tissue homeostasis as well as wound healing. The signals produced by a solid tumor resemble those from chronic non-healing wounds. Thus, MSCs show a natural tropism for solid cancers and act as progenitors for many of the cell types that make up the tumor stroma. These characteristics have been exploited in a Trojan horse-like approach to deliver exogenously administered MSCs carrying anticancer agents (e.g. suicide genes) into the tumor environment. After homing into the tumor, MSCs are activated by tumor signals. These signals can also be used to selectively activate specific gene promoters to focus the gene transcription of suicide genes to the tumor leaving other tissues relatively unaffected. To date, the RANTES/CCL5 promoter has been the most effective tumor-specific promoter. The general approach, which uses the herpes simplex virus thymidine kinase (HSV-TK) in combination with ganciclovir as a suicide gene system, has advanced to clinical trials for progressed gastrointestinal tumors.

Our laboratory has recently developed a new MSC-based approach using the thyroidal sodium iodide symporter (NIS), which shows enhanced therapeutic efficiency through the active uptake of radionuclides and can also be used for diagnostic purposes. The use of this gene system for non-thyroidal tumors requires protection of the thyroid gland from uptake of radionuclides by thyroid hormone pre-treatment, which reduces NIS surface expression on thyroidal cells. *In vivo* experiments have not shown adverse effects of this treatment, however the effects of this biology on MSC cells have not been examined in detail. Thyroid hormones affect cells long-term by modulating gene transcription (genomic) but there is also an action that occurs over the cell surface receptor integrin $\alpha\beta3$ (non-genomic), which is expressed by MSCs.

The rationale of this thesis was to find ways to maximize the therapeutic efficiency of engineered MSC-based cancer therapy when using the NIS gene. This included the characterization of the biologic mechanisms of thyroid hormones on MSC biology and further assessing a new tumor specific promoter targeting approach.

The observation of especially aggressive, often therapy resistant and fast growing tumors like hepatocellular carcinoma (HCC), which still impose therapeutic challenges, showing hypoxic areas led to the idea of hypoxia targeting. So far, these areas, where tumor growth outpaces neoangiogenesis had not been targeted by MSC based suicide gene therapy. To this end, an in house designed synthetic hypoxia responsive promoter was used to evaluate therapeutic efficiency *in vitro* in comparison to RANTES/CCL5 promoter.

Non-genomic thyroid hormone effects on MSC biology and therapeutic efficiency of the new targeting strategy were evaluated *in vitro* as well. Examination included effects on proliferation, differentiation, gene activation, migration and hypoxia response system of MSCs. It was possible to distinguish effects on the tumor stroma versus direct effects on the tumor as used tumor cell line HUH7 (HCC derived) does not express integrin $\alpha\beta3$.

Results of this thesis show significantly stronger activation of the new promoter under hypoxic conditions *in vitro* compared to the RANTES/CCL5 promoter, which does not

activate in hypoxia *in vitro* at all. Additionally MSCs carrying the hypoxia responsive promoter invade hypoxic areas of an *in vitro* tumor spheroid model and show hypoxia regulated gene activation therein. This provides sustainable proof that hypoxia targeting is a promising targeting strategy for MSC based suicide gene therapy. However, the synthetic hypoxia responsive promoter still shows limitations for *in vivo* use. It has the advantage of targeting hypoxic areas very specifically and efficiently while it does not activate in other areas of the tumor than hypoxic areas. The required tandem repeat build up to ensure specific targeting leads to instability *in vivo*. Therefore, the HIF1 α -responsive promoter does not yet reach the level of therapeutic efficiency RANTES/CCL5 promoter shows *in vivo* even though it surpasses the level *in vitro* under hypoxic conditions. Moreover, the targeting of metastases remains to be evaluated. Nevertheless further research in the direction of hypoxia targeting seems to be promising as further results of this thesis show that non-genomic thyroid hormone effects upregulate hypoxia response and hypoxia regulated gene expression (e.g. VEGFa, IL6) in MSCs. In addition, this thesis provides proof that thyroid hormones enhance MSC chemotaxis and tumor homing *in vitro* over the integrin $\alpha v \beta 3$ pathway. These insights into the detailed mechanisms of thyroid hormone effects on MSC biology imply that potential side effects by means of the thyroid hormone pretreatment are controllable and do not limit positive effects on therapeutic efficiency like upregulation of hypoxia response and enhancement of tumor homing. The findings also suggest that before any therapeutic use of MSCs in other therapeutic contexts it seems to be attractive to assess the patient's thyroidal status and possible influence on the therapeutic efficiency.

Further research is necessary to refine hypoxia targeting and increase therapeutic efficiency *in vivo*. The next step is to find a native and therefore *in vivo* stable, promoter responsive to hypoxia and other tumor signals, which is equally positively influenced by thyroid hormone treatment. This thesis reveals VEGFa and IL6 as possible candidates and further experiments beyond the scope of this thesis are already being conducted in this direction.

Zusammenfassung

Krebserkrankungen sind trotz allen medizinischen Fortschrittes immer noch eine der Hauptursachen von Mortalität und Morbidität, sodass neue therapeutische Konzepte gebraucht werden. Solide Tumore bestehen aus malignen Zellen in einem Tumorstroma. Dieses Tumormikromilieu ist in den Fokus der laufenden Krebstherapieforschung gerückt. Derzeit werden gentechnisch veränderte mesenchymale Stammzellen (MSC) entwickelt, die einen neuen Therapieansatz für solide Tumore darstellen.

MSCs sind multipotente Vorläuferzellen, die in vielen Geweben vorkommen unter anderem im Knochenmark und eine wichtige Rolle bei der Regulation der Gewebehomöostase und Wundheilung spielen. Die Signale, die ein solider Tumor produziert, ähneln denen chronischer, nicht verheilender Wunden. Daher zeigen MSCs eine natürliche zielgerichtete Migration in solide Tumore und dienen dort als Vorläufer für viele Zellarten des Tumorstromas. Diese Eigenschaften können genutzt werden, um extern verabreichte MSCs wie trojanische Pferde beladen mit Krebsmedikamenten (z.B. Suizidgenen) in den Tumor migrieren zu lassen. Nach Einwanderung in den Tumor werden MSCs von Tumorsignalen aktiviert. Diese Signale können auch genutzt werden um selektiv so genannte tumorspezifische Genpromotoren zu aktivieren und damit die Transkription von Suizidgenen auf den Tumor zu begrenzen. Somit bleiben andere Gewebe nahezu unbeeinträchtigt. Bisher ist der RANTES/CCL5 Promoter der effektivste tumorspezifische Promoter. Dieser Ansatz, der die Herpes Simplex Virus Thymidin Kinase (HSV-TK) in Kombination mit Ganciclovir als Suizidgensystem nutzt, wird bereits in klinischen Studien bei fortgeschrittenen gastrointestinalen Tumoren untersucht.

In unserem Labor wurde vor kurzem ein neuer MSC-basierter Ansatz entwickelt, der den thyreoidalen Natrium-Iodid-Symporter (NIS) nutzt, welcher verbesserte therapeutische Effizienz zeigt durch die aktive Aufnahme von Radionukliden und auch für diagnostische Zwecke verwendet werden kann. Der Einsatz dieses Gens für nicht-thyreoidalen Krebs erfordert jedoch den Schutz der Schilddrüse vor Aufnahme von Radionukliden. Dies wird durch Vorbehandlung mit Schilddrüsenhormonen erreicht, welche die Oberflächenexpression von NIS auf thyreoidalen Zellen verringert. Erste *in vivo* Experimente zeigten keine nachteiligen Effekte der Behandlung, jedoch wurden bisher die Effekte auf MSC Zellen nicht im Detail untersucht. Schilddrüsenhormone beeinflussen Zellen langfristig durch Modulation der Gentranskription (genomisch), aber es gibt auch Effekte vermittelt durch den Zelloberflächenrezeptor Integrin $\alpha\beta3$ (nicht-genomisch), der von MSCs exprimiert wird.

Der Grundgedanke dieser Arbeit war es, die therapeutische Effizienz der MSC-basierten Krebstherapie, insbesondere bei Nutzung von NIS, zu maximieren. Dies beinhaltet einerseits die Charakterisierung der biologischen Effekte von Schilddrüsenhormonen auf die Biologie der MSCs sowie die Evaluation eines neuen tumorspezifischen Promoters für das Targeting.

Die Beobachtung, dass vor allem aggressive, oft therapieresistente und schnell wachsende Tumore wie das Hepatozelluläre Karzinom (HCC), die immer noch eine therapeutische Herausforderung darstellen, große hypoxische Areale aufweisen, führte zur Idee des Hypoxie-gerichteten Targetings. Bisher wurden diese Bereiche, in denen das Tumorwachstum schneller erfolgt als die Neoangiogenese, nicht gezielt angesteuert durch MSC-basierte Suizidgentherapie. Um das zu ändern wurde ein hausinterner, synthetischer Hypoxie-reagibler Promoter benutzt um die therapeutische Effizienz *in vitro* im Vergleich zum RANTES/CCL5 Promoter zu evaluieren.

Nicht-genomische Schilddrüsenhormoneffekte auf MSCs und auf die therapeutische Effizienz der neuen Targetingstrategie wurden ebenfalls *in vitro* untersucht. Die Un-

tersuchung beinhaltet Effekte auf die Proliferation, Differenzierung, Genaktivierung, Migration und Hypoxieantwort in MSCs. Direkte Effekte auf Tumorzellen konnten von Effekten auf das Tumorstroma unterschieden werden durch Auswahl einer Integrin $\alpha\beta3$ -negativen HCC Tumorzelllinie (HUH7) als Tumormodell.

Die Ergebnisse dieser Arbeit zeigen signifikant stärkere Aktivierung des neuen Promoters unter hypoxischen Bedingungen *in vitro*, während der RANTES/CCL5 Promoter *in vitro* keine Aktivierung in Hypoxie zeigt. Zusätzlich wandern MSCs, die den Hypoxie-reagiblen Promoter tragen, in hypoxische Areale eines *in vitro* Tumorspheroidmodells ein und zeigen dort Hypoxie-regulierte Genaktivierung. Dies liefert den tragfähigen Beweis, dass Hypoxietargeting einen vielversprechenden Ansatz für die MSC-basierte Suizidgentherapie darstellt. Der synthetische Hypoxie-reagible Promoter zeigt jedoch noch Limitierungen im *in vivo*-Gebrauch. Sein Vorteil besteht darin, dass er hypoxische Areale sehr spezifisch und effizient ansteuert, während er in anderen Tumorbereichen keine Aktivierung zeigt. Dies erfordert einen Aufbau im Sinne eines Tandem Repeats, welcher *in vivo* zu Promoterinstabilität führt. Eine Konsequenz davon ist, dass die Effizienz des HIF1 α -reagiblen Promoters noch nicht das Effizienzlevel des RANTES/CCL5 Promoters *in vivo* erreicht, obwohl er ihn *in vitro* unter hypoxischen Bedingungen übertrifft. Weiterhin bleibt zu evaluieren, ob der neue Promoter auch Metastasen erreicht. Trotzdem scheinen weitere Nachforschungen im Bereich des Hypoxietargeting vielversprechend zu sein, da weitere Ergebnisse dieser Arbeit zeigen, dass nicht-genomische Schilddrüsenhormoneffekte die Hypoxieantwort und Hypoxie-regulierte Genexpression (z.B. VEGFa, IL6) in MSCs hochregulieren. Zusätzlich liefert diese Arbeit Beweise, dass Schilddrüsenhormone über das Integrin $\alpha\beta3$ die MSC Chemotaxis und Einwanderung in Tumore *in vitro* verbessern. Diese Einblicke in die genauen Mechanismen der Schilddrüsenhormoneffekte auf die MSC Biologie implizieren, dass potentielle Nebenwirkungen durch eine Schilddrüsenhormonvorbehandlung kontrollierbar sind und die positiven Effekte auf die therapeutische Effizienz, wie die Hochregulierung der Hypoxieantwort und verbessertes Tumorphoming, nicht limitieren. Weiterhin deuten die Erkenntnisse darauf hin, dass vor jeglichem therapeutischen Einsatz von MSCs in anderen therapeutischen Feldern eine Untersuchung des Schilddrüsenstatus des Patienten und potenzieller Einflüsse auf die therapeutische Effizienz von Nutzen zu sein scheint. Weitere Forschung ist notwendig um das Hypoxietargeting zu verfeinern und die therapeutische Effizienz *in vivo* zu erhöhen. Der nächste Schritt ist, einen nativen, und daher *in vivo* stabilen, Promoter zu finden, der auf Hypoxie und weitere Tumorsignale reagiert und gleichermaßen positiv beeinflussbar ist durch Schilddrüsenhormonvorbehandlung. Diese Arbeit zeigt VEGFa and IL6 als mögliche Kandidaten auf und weitere Experimente in diese Richtung über den Rahmen dieser Arbeit hinausgehend werden bereits durchgeführt.

1. Introduction

1.1. New approaches for cancer treatment

Despite our medical advances, cancer still represents one of the leading causes of morbidity and mortality worldwide imposing an economic burden on healthcare systems (Rajab et al. 2013, Stewart 2014). Much effort has gone into the search for novel cancer treatments to replace or augment the established options of chemotherapy, surgery and radiotherapy.

Particularly aggressive, often therapy resistant and fast growing solid tumors such as hepatocellular carcinoma (HCC) create therapeutic challenges. These neoplasias are composed of malignant cells within a tumor stroma. The tumor stroma has become the focus of ongoing cancer therapy research. Cell-based therapy represents one of the most promising new cancer treatment approaches. Engineered mesenchymal stem cells (MSCs) are currently under development as vehicles for the delivery of antitumor agents or suicide transgenes to reduce tumor load (Hagenhoff et al. 2016). HCC is a good model cancer for investigations in this direction. HCC is a solid, primary liver tumor, which generally occurs in the context of an underlying liver disease. It is one of the most common tumors and can be very difficult to treat. The main risk factor for HCC is liver cirrhosis, which also enhances the formation and growth of tumors elsewhere in the body (Yang et al. 2011, Heindryckx et al. 2015). When detected in early stages the five-year survival is above 50 percent (Lee et al. 2006). Most of the time however, the cancer has already progressed and is largely therapy resistant. Therefore, new therapeutic approaches consider targeting the interactions between malignant cells and the tumor stroma.

1.2. Role of MSCs within tumor microenvironments

1.2.1. The importance of tumor stroma for tumor growth and progression

MSC-based therapy targets the tumor stroma, which consists of supporting cells that include fibroblasts, endothelial cells, pericytes and lymphocytes. For each solid tumor, this microenvironment is vital for the survival and growth of neoplastic cells and it can influence malignancy and invasiveness (De Wever et al. 2003, Zischek et al. 2009). Tumor or cancer associated fibroblasts (TAF/CAF) play an important role in tumor biology. Spaeth et al. reported that MSCs originating from the bone marrow or from locally resident MSC populations can differentiate into TAF as a response to tumor-derived signals. (Spaeth et al. 2009)

Exogenously administered MSCs are able to engraft into tumors and can contribute to tumor stroma (Hung et al. 2005).

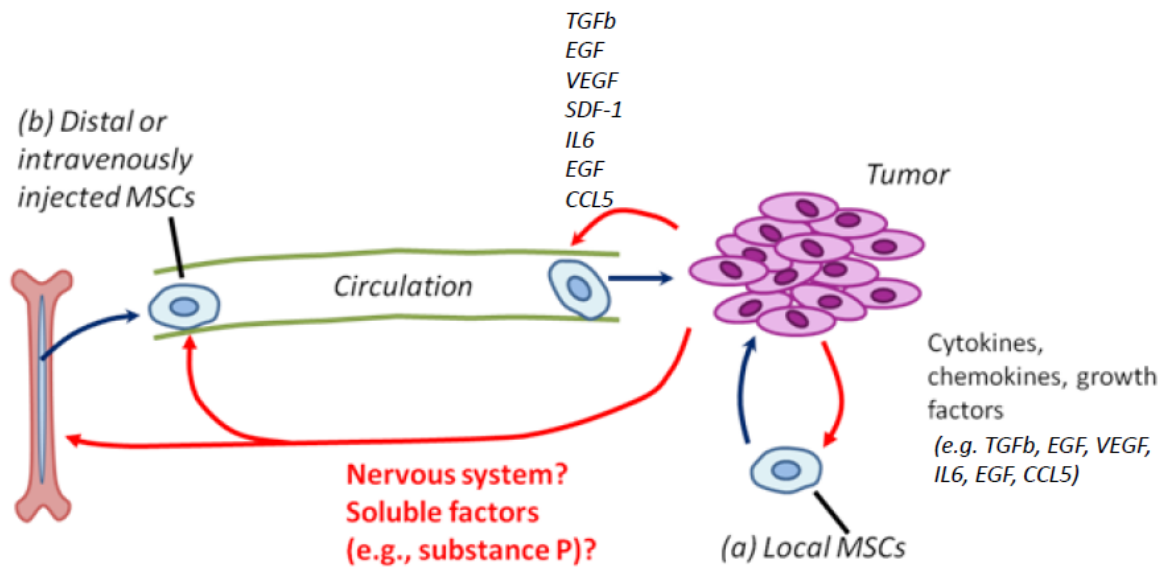


Figure 1: MSC sources for tumor stroma: Local (a), distal or exogenous (b) MSCs are recruited to tumor stroma via tumor-derived cytokines, chemokines and growth factors. Subsequently, they differentiate e.g. into tumor-associated fibroblasts (TAF). Red arrows show regulatory interactions of tumor cells on MSC biology; dark blue arrows show cell movements and action of MSCs on tumor cells. [adapted from (Barcellos-de-Souza et al. 2013, Droujinine et al. 2013)]

TAF produce diverse growth factors including HGF, IL6, VEGFa and TGF β that strongly contribute to the formation of tumor stroma (Figure 1). They promote disordered, rapid tumor growth that is associated with an increased tumor aggressiveness and poor prognostic outcome (Yang et al. 2011). Furthermore, MSCs can promote metastases e.g. in breast cancer through the enhancement of metastatic niches and the induction of mesenchymal to epithelial or epithelial to mesenchymal transition (Barcellos-de-Souza et al. 2013). For these reasons, the tumor stroma has become an important new target in the therapy of solid tumors (De Wever et al. 2003, Ahmed et al. 2008).

In HCC, the stroma regulates malignant transformation, survival, progression and invasiveness (Yang et al. 2011, Heindryckx et al. 2015). It has been targeted by antibodies such as the antiangiogenic Bevacizumab (Heindryckx et al. 2015) or the hypoxia activated prodrug (Q6) (Liu et al. 2014).

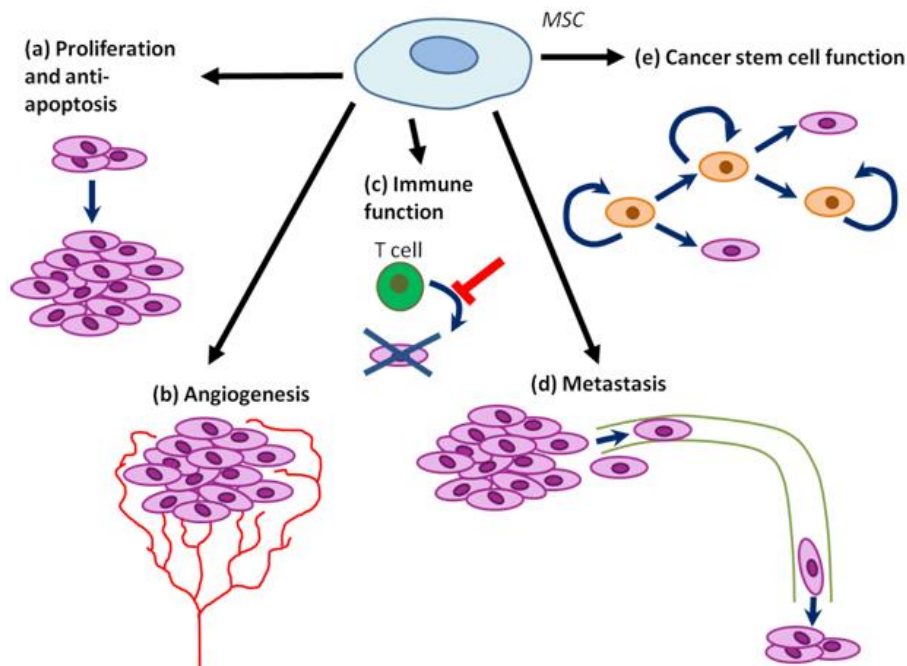


Figure 2: MSC tumor promoting functions: (a) MSCs promote tumor cell proliferation and inhibit cell death. (b) MSCs promote angiogenesis within tumors. (c) MSCs inhibit some immune functions, while promoting others. (d) MSCs promote tumor metastasis. (e) MSCs may regulate cancer stem cell self-renewal and differentiation. [adapted from (Droujinine et al. 2013)]

1.2.2. Biology of human MSCs

MSCs are referred to as mesenchymal stromal cells or marrow stromal cells (Horwitz et al. 2005, Salem et al. 2010). They are multipotent, non-hematopoietic progenitor cells that have the capacity of self-renewal and differentiation, thus supporting maintenance and remodeling in diverse tissues including the tumor stroma (Zischek et al. 2009, Niess et al. 2011, Maxson et al. 2012). As there are no single markers available to characterize MSCs, the International Society for Cellular Therapy has determined minimum criteria to characterize this heterogeneous cell population (Dominici et al. 2006): Human MSCs are plastic-adherent under standard culture conditions, they show expression of CD105, CD73 and CD90 and lack the hematopoietic markers CD34, CD45, CD14, CD19 and HLA-DR. Following the administration of specific stimuli, the cells are able to differentiate into osteocytes, adipocytes and chondrocytes *in vitro*. (Dominici et al. 2006, Salem et al. 2010)

Within the scope of this thesis, human MSCs, isolated from the bone marrow of healthy donors, met the minimum criteria for human MSCs. Chondrogenic differentiation was not explored individually for every isolate due to very complex experimental set up and subordinate relevance to the topic. However, it can be assumed that untested samples are able to differentiate in this pathway as all other characteristics match.

While found in adult bone marrow, where MSCs reside in low frequency within hypoxic niches, they can also be isolated from adipose tissue, umbilical cord blood and other tissues such as brain, kidney and liver (Fritz et al. 2008).

MSCs migrate into various healthy tissues such as secondary lymphatic tissue, spleen, gut, salivary gland, skin and lung as part of normal tissue homeostasis. While specific homing may occur, fine structure and microvessels are also thought to transiently entrap MSCs in lung, liver and spleen. (Hagenhoff et al. 2016)

Chemokine and cytokine signaling recruit MSCs to sites of increased cell turnover, in general, and injuries in particular (Karp et al. 2009). The signals include CXCL12,

CX3CL1, CXCL16, CCL3, CCL19 and CCL21 (Salem et al. 2010). MSCs exogenously applied show equally strong recruitment to sites of injury (Bao et al. 2012).

The signals produced by a solid tumor resemble those of a chronic wound. It has been suggested that the body sees cancer as something like a “chronic injury that does not heal” (Dvorak 2015). For this reason, MSCs show a strong, natural tropism for solid neoplasia and microscopic tumor lesions (Hung et al. 2005, Spaeth et al. 2008, Dvorak 2015), which can be enhanced for example through stimulation with TNF α (Hagenhoff et al. 2016).

MSCs’ immunoprivileged nature uniquely suits them as vehicles for cell-based cancer treatment. MSCs are reported to inhibit T-cell function and to be resistant to natural killer cell cytotoxicity (Bao et al. 2012). This is partly due to their lack of major histocompatibility complex II (MHC II) and helps make rejection issues rare (Rajab et al. 2013, Hagenhoff et al. 2016).

The biosafety of MSCs has been examined and yielded controversial results regarding the tumorigenic potential of MSCs (Lazennec et al. 2008, Hagenhoff et al. 2016). This question needs to be further elucidated for the future clinical application of these cells. To date, only minor adverse effects have been seen in clinical trials (D’souza et al. 2015).

1.2.3. Potential clinical application of MSCs in cancer therapy and other fields

The clinical potential of MSCs has become evident over the last two decades and a wide field of applications (Reiser et al. 2005). MSCs are suitable vectors for the delivery of therapeutic agents in many different settings. Potential applications for MSCs include treatment of graft-versus-host disease, tissue repair including cerebral injury, bone fracture and myocardial infarction as well as muscular dystrophy (Spaeth et al. 2008). MSCs are also being evaluated in the treatment of renal disease, Crohn’s disease, osteogenesis imperfecta, amyotrophic lateral sclerosis (Salem et al. 2010), acute lung injury, asthma, sepsis and multiple sclerosis (Dimarino et al. 2013, D’souza et al. 2015). MSCs have been tested for lymphatic regeneration (Conrad et al. 2009). The use of MSCs as vehicles for cell-based cancer therapy ranges among the most promising applications. MSCs show great potential to enhance tumor-specificity and reduce side effects of therapies in comparison to conventional cancer treatments.

1.2.4. Use of engineered MSCs as vehicles for cancer therapy

The tumors shown to recruit exogenously administered MSCs include gastrointestinal and gynecological neoplasia as well as gliomas, melanomas and sarcomas (Hagenhoff et al. 2016). Various approaches have been developed to target tumor stroma therapeutically via MSC-based delivery of anticancer agents. Among these agents are immune-modulating agents like Interferon β (Studený et al. 2004), cytotoxic agents or growth factor antagonists like TRAIL (Grisendi et al. 2015). Combining this approach with radiation therapy increases the therapeutic efficiency of MSC-based therapeutic concepts (Hagenhoff et al. 2016).

When MSCs are recruited to the tumor microenvironment containing cytokines, chemokines and growth factors, the milieu initiates a specific response in the MSCs to these signals. MSCs can differentiate into fibroblasts or enhance angiogenesis depending on the needs of the tumor and in this way can promote tumor growth (Spaeth et al. 2009). While on the surface this appears to limit their potential utility as therapeutic vehicles, their natural ability to penetrate deeply into tumor microenvironments can be exploited in a “Trojan horse”-like (Bao et al. 2012) therapy approach. The differentiation can be used to activate specific gene promoters and thus, the expression of transgenes can be largely limited to the tumor stroma (Conrad

et al. 2007). This can act to limit potential side effects of the therapy as intravenously administered MSCs can also home into healthy tissues (Bao et al. 2012).

The combination of tumor tropism and the capacity to differentiate make MSCs a potentially efficient system for the delivery of suicide gene systems into tumors (Rajab et al. 2013).

The suicide gene systems evaluated to date include: cytosine deaminase combined with 5-FU (5-Fluorouracil), carboxyl esterase with irinotecan (CE/CPT-11), varicella zoster virus thymidine kinase with 6-methoxypurine arabinonucleoside (Vzvtk/Aram), nitro-reductase (Nfsb) with 5-Aziridiny-2,4-dinitrobenzamide (NTR/CB1954) and carboxy-peptidase G2 with CMDA (CPG2/CMDA) (Rajab et al. 2013). These systems have been evaluated in experimental glioblastoma multiforme (Sasportas et al. 2009), mesothelioma, gastrointestinal cancer, prostate cancer and gynecologic cancers (Rajab et al. 2013).

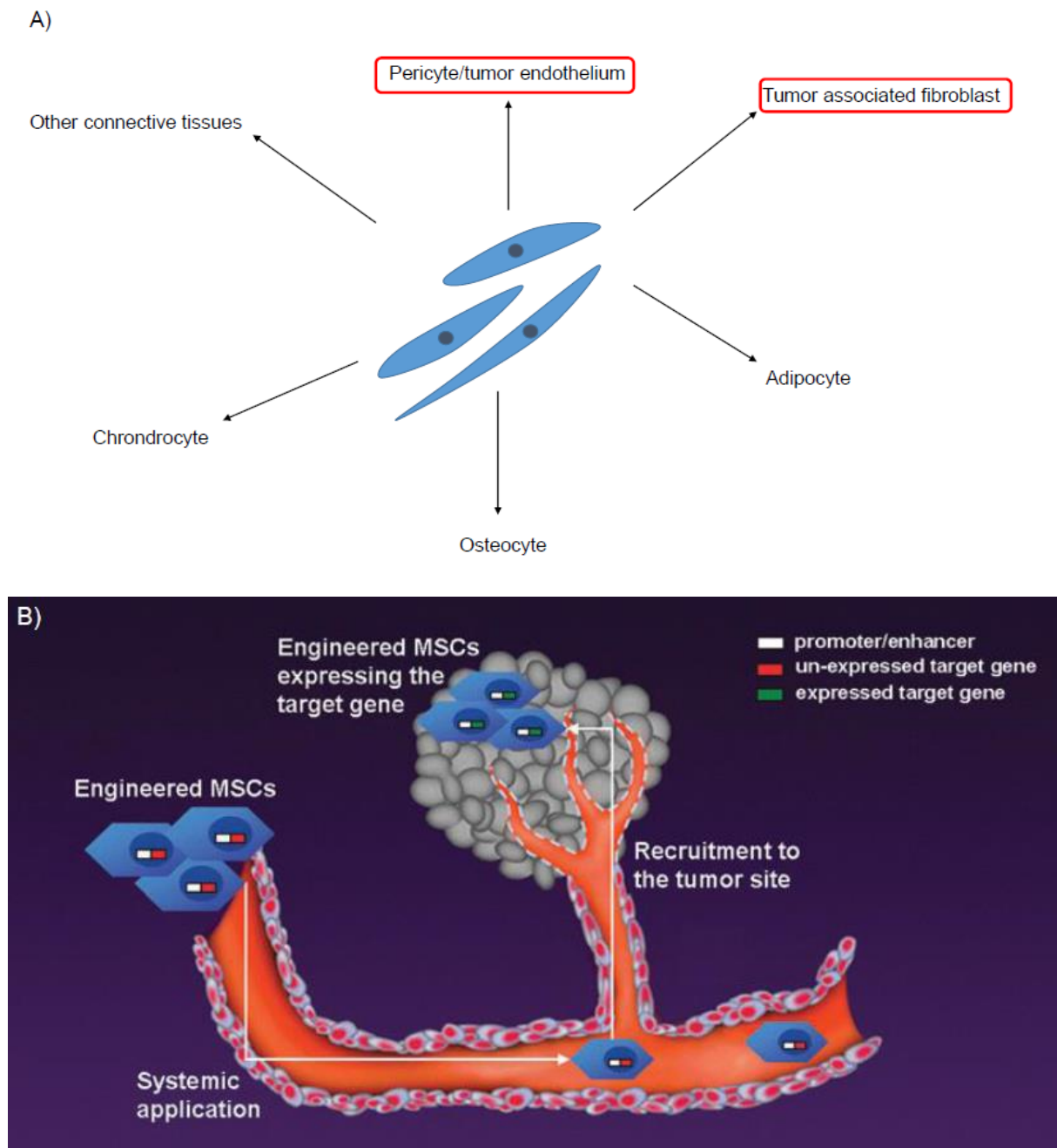


Figure 3: A) Tissue specific MSC differentiation: MSCs are able to differentiate in response to tissue-specific cytokine-, chemokine- and growth factor-signals in tissues. For example, tumor-derived signals initiate the differentiation into pericytes or fibroblasts. **B) Tumor-specific expression of engineered genes in MSCs:** The concept of MSC-based cancer therapy (“Trojan horse” concept) makes use of MSCs’ natural tumor tropism and ability to differentiate. Consecutively, tumor specific promoters drive the activation of target genes and limit effects to cancerous sites. [B) adapted from (Bao et al. 2012)]

The research in our group that preceding this thesis made use of another enzyme, the Herpes Simplex Virus Thymidine Kinase (HSV-TK) in combination with ganciclovir. Various gene promoters were evaluated *in vitro* and *in vivo* (mouse model) in different tumor settings with this suicide gene system. An approach by Conrad et al. targeted tumor angiogenesis selectively by making use of MSC differentiation in response to angiogenic signals. Applying MSCs engineered with the Tie2 enhancer controlling HSV-TK in a syngeneic, orthotopic pancreatic cancer mouse model led to gene activation almost exclusively at sites of neoangiogenesis within the tumor. MSC

therapy combined with ganciclovir treatment significantly decreased primary tumor growth and prolonged life span. (Conrad et al. 2011)

The cytokine CCL5 is induced during the differentiation of MSC into TAF inside the tumor stroma (Rajab et al. 2013). This biology was used in a second approach by Zischek et al. MSCs were engineered with the HSV-TK under control of a RANTES/CCL5 promoter. In an orthotopic pancreatic cancer mouse model, and a spontaneous breast cancer mouse model, effects on tumor growth and tumor metastases were evaluated. Results showed a significant reduction of tumor growth and incidence of metastases as well as prolongation of life span in both models. (Zischek 2011)

The direct comparison of the effectiveness of the Tie2 promoter with the RANTES/CCL5 promoter in an orthotopic HCC mouse model, suggested that the CCL5 targeting was more effective, while effects on tumor growth were equal (Niess et al. 2011). The RANTES/CCL5 protocol has now advanced into phase II of clinical trial (Niess et al. 2015).

In the next generation of experiments, we have sought to enhance the effectiveness of the concept by making use of a combined therapeutic and diagnostic (theranostic) gene, the sodium iodine symporter (NIS). An initial study by Knoop et al. in a HCC xenograft mouse model showed that MSCs engineered with the NIS gene constitutively expressed (CMV promoter) effectively homed to the tumor. Treatment with ^{131}I application significantly delayed tumor growth. (Knoop et al. 2011)

To increase tumor-specificity of the concept Knoop et al. engineered MSCs with NIS gene under control of RANTES/CCL5 promoter. In the same HCC mouse model, tumor growth was significantly reduced and overall survival improved by MSC treatment in combination with ^{131}I or ^{188}Re application. (Knoop et al. 2013) In a metastatic colon cancer mouse model CCL5-NIS engineered MSCs were shown to home to liver metastases and with treatment reduced the level of metastases and tumor load (Knoop et al. 2015).

When using NIS therapy for extra-thyroidal tumors, it becomes necessary to protect the thyroid gland from damage by uptake of radioactive iodine (Knoop et al. 2011). Pretreatment of experimental animals (or human patients) with thyroid hormones reduces the endogenous expression of NIS in the thyroid gland (Knoop et al. 2011) and ensures protection of the vital thyroidal tissue.

1.3. Role of thyroid hormones in tumor microenvironments and MSC biology

Thyroid hormones 3,3',5-triiodo-L-thyronine (T3) and L-thyroxine (T4) help control the growth, differentiation and metabolism of many types of tissues and also play an important role in tumor stroma formation (Yen et al. 2006, Davis et al. 2011).

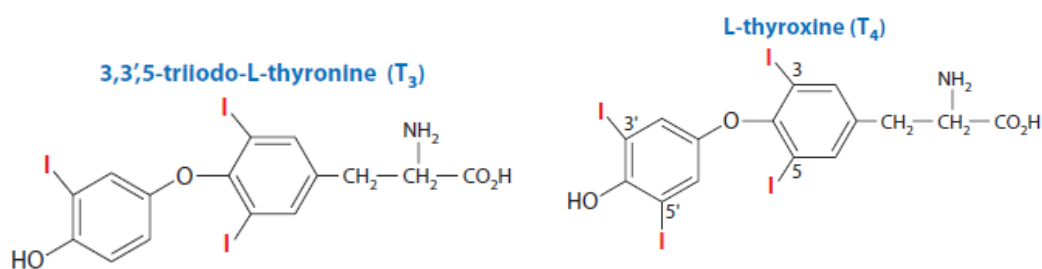


Figure 4: Molecular structure of T3 and T4 (Davis et al. 2011)

Originally, it was thought that T3 and T4 mediate their effects only through nuclear receptors. By binding to a heterodimeric nuclear thyroid hormone receptor (TR), T3

initiates genomic events (Bergh et al. 2005). The receptor trafficks into the nucleus and drives transcription of thyroid hormone responsive genes (Bergh et al. 2005). Circulating T4 has to be deiodinated first in order to become active (Bergh et al. 2005).

Within the last two decades, Davis et al. showed that thyroid hormones can also influence cell proliferation through an immediate mechanism. This “non-genomic” pathway can also alter gene expression (Davis et al. 2014a) and influence proliferative pathways including the growth of tumor stroma via upregulation of angiogenesis and tumor cell proliferation (Davis et al. 2014b, Cayrol et al. 2015). Moreover, it can downregulate apoptosis (Sharma et al. 2014, Straub 2014, Lin et al. 2015).

The effects of this second pathway are mediated by a cell surface receptor identified as integrin $\alpha v \beta 3$ (Davis et al. 2011). Integrin membrane receptors are a family of transmembrane glycoproteins that form noncovalent heterodimers transmitting signals from the extra cellular matrix to the cytosol (Bergh et al. 2005, Cody et al. 2007). The cells expressing integrin $\alpha v \beta 3$ include endothelial cells, vascular smooth muscle cells, osteoclasts and most cancer cells (Davis et al. 2009). The receptor contains two different binding sites. The first controls mainly cell proliferation, and binds T3 and T4 (Davis et al. 2014b). It activates the mitogen-activated protein kinase (MAPK respectively ERK1/2) pathway downstream, which plays an important role in the induction of angiogenesis (Davis et al. 2014b).

The second site binds T3, and activates phosphatidylinositol 3-kinase (PI3K), which influences angiogenesis, tumor cell division, and drives the transcription of HIF1 α , the main regulator of hypoxia response system (Hiroi et al. 2006, Patiar et al. 2006, Davis et al. 2009, Davis et al. 2014b). In addition, PI3K activation mediates a normoxic upregulation of HIF1 α (Moeller et al. 2005) and promotes cancer cell proliferation, apoptosis, migration and invasion (Kim et al. 2013b). PI3K signaling has also been linked to pluripotency in somatic cells making it possible to cultivate induced pluripotent stem cells (Chen et al. 2012).

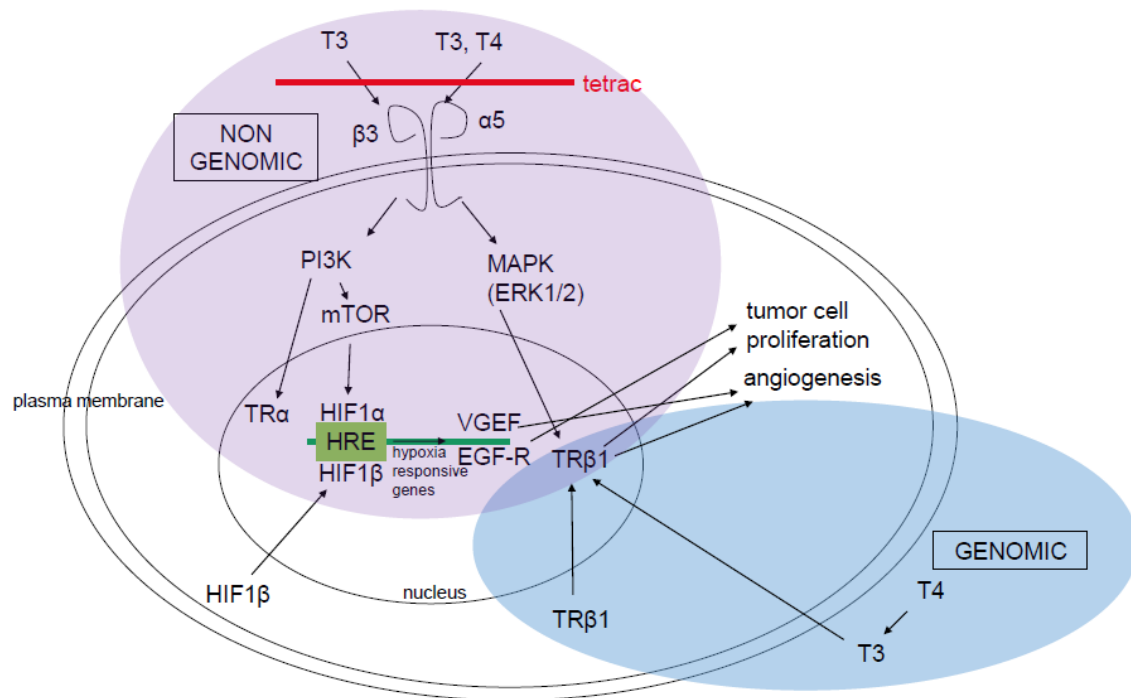


Figure 5: Overlap of non-genomic and genomic thyroid hormone effects. Integrin $\alpha\beta3$ receptor domains and downstream effects including upregulation of HIF1 α : Genomic pathway (*blue*) initiated by T3 (or deiodinased T4) leading to transduction of constitutively expressed TR $\beta1$ into nucleus driving gene expression and protein synthesis e.g. in cell proliferation and angiogenesis. Non-genomic pathway (*purple*) initiated at αv or $\beta3$ integrin receptor domain activating either PI3K or MAPK (ERK1/2). Downstream effects include transduction of TR α into nucleus, upregulation of hypoxia responsive genes including VEGFa and EGF-R, as well as transduction of TR $\beta1$ into nucleus, which lead to activation of angiogenesis and tumor cell proliferation. [adapted from (Fujita et al. 2007, Davis et al. 2011, Hammes et al. 2015)]

Based on these diverse effects integrin $\alpha\beta3$ has become strategically important as a target for anticancer therapies. Tetraiodothyroacetic acid (Tetrac), a deaminated T4 derivative, is an inhibitor of the integrin $\alpha\beta3$ (Davis et al. 2014b). This inhibition alters gene transcription within the cell including VEGFa, EGFR, MMP9 and HIF1 α genes (Davis et al. 2014b). Furthermore, it induces radiosensitization and chemosensitization of cancer cells (Davis et al. 2014b).

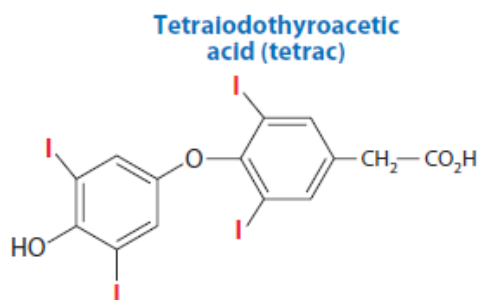


Figure 6: Molecular structure of Tetrac (Davis et al. 2011)

In addition to proliferation and angiogenesis, thyroid hormones also influence the invasiveness and migratory capacities of tumor cells by signaling via integrin $\alpha\beta3$ (Cohen et al. 2014). In general, integrin receptors play an important role in the adhesion and migration of many cells e.g. leucocytes (Fox et al. 2007). MSCs and fibroblasts use these cell surface molecules likewise (De Wever et al. 2003, Fox et al. 2007, Salem et al. 2010).

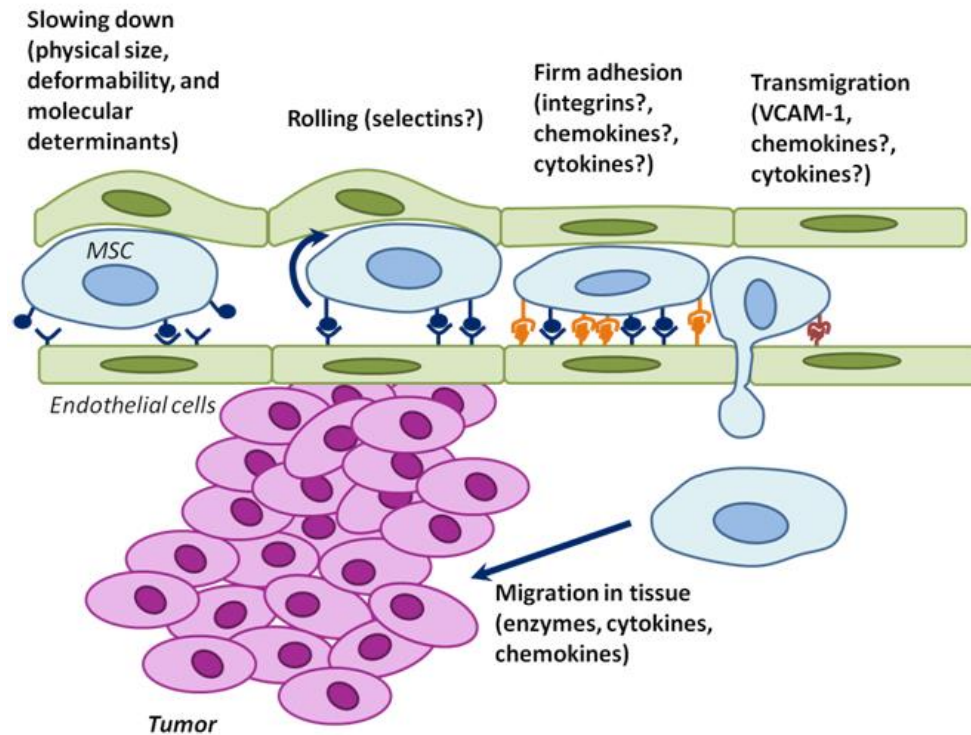


Figure 7: Role of integrin receptors in MSC recruitment and tumor homing: Although the mechanisms of MSC homing are poorly understood, they likely involve partially overlapping steps of deceleration in the blood flow, rolling, adhesion, transmigration through the endothelium, and migration into surrounding tissues. The possible molecular determinants are indicated. Integrin receptors play an important role in MSC adhesion. [adaped from (Droujinine et al. 2013)]

1.4. MSCs as vehicles for cancer therapy: Hypoxia as possible new mechanism for selective transgene induction

Aggressive and rapidly growing solid tumors like HCC contain a hypoxic microenvironment due to their fast growth outpacing simultaneous growth of vascularization. Hypoxia fuels treatment resistance to conventional cancer therapy as well as upregulation of epithelial mesenchymal transition (EMT) markers, which is associated with a poor prognosis (Gammon et al. 2013, Casazza et al. 2014, Liu et al. 2014). In addition, tumor hypoxia strongly induces expression of the hypoxia induced transcription factors (HIFs), which leads to downregulation of adhesion molecules potentially promoting metastases (Chaturvedi et al. 2013). Hypoxia also leads to increased angiogenesis and contributes to a metabolic shift from aerobic to anaerobic metabolism by glycolysis (Vaupel 2004). Summing up, hypoxia promotes transcription of genes that are crucial to cancer development (Figure 4). Affected are angio-genesis, cell survival, glucose metabolism and invasion (Semenza 2003).

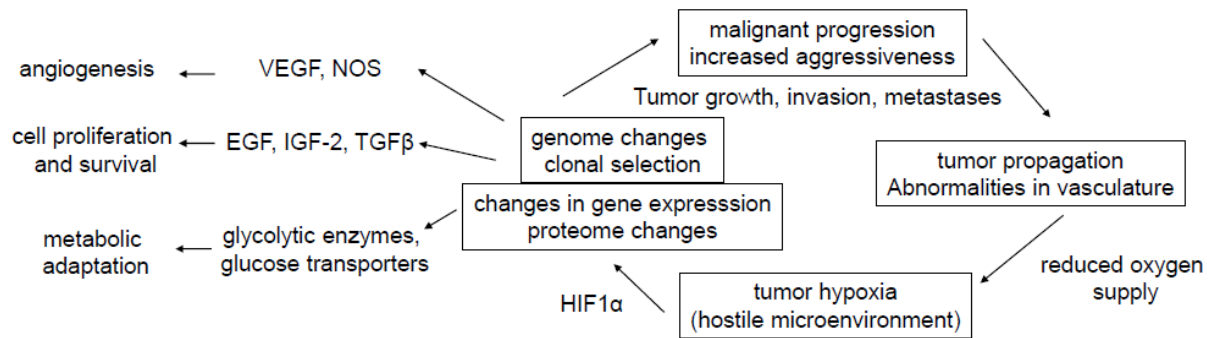


Figure 8: Circle of tumor hypoxia: Promotion of tumor growth, invasion and metastases [adapted from (Vaupel 2004)]

These observations led to the idea of selectively directing MSC-based gene therapy into hypoxic areas within the tumor.

A key player in adaptation to changing oxygen levels is expression of the transcription factor HIF1 (Liu et al. 2012), a heterodimeric protein composed of the constitutively expressed β subunit, also named aryl-hydrocarbon receptor nuclear transporter (ARNT), and the α subunit, whose expression is regulated by intracellular oxygen levels (Figure 5). Both are basic helix-loop-helix transcription factors that bind to hypoxia responsive elements (HRE) within the promoters of hypoxia-regulated genes (Liu et al. 2012). The α subunit contains an oxygen-dependent degradation domain as well as two transactivation domains, which allow the hypoxia-dependent stabilization or oxygen-dependent degradation by hydroxylation and ubiquitination via the proteasome pathway under normoxic conditions (Liu et al. 2012). In addition to effects that occur after several hours, more rapid responses occur on the posttranslational level, or through membrane depolarization (Bruick 2003).

Approximately 90% of all known cancers are solid tumors (Vaupel 2004). The hypoxic microenvironment represents an important therapeutic target. For example, HIF1 α inhibitors (Patiar et al. 2006), HIF1 α stability suppressors (Kim et al. 2013a) or hypoxia activated prodrugs such as Q6 are currently being used. Q6 significantly reduces proliferation under hypoxic conditions, and induces caspase-dependent apoptosis in HCC cell lines (Liu et al. 2014).

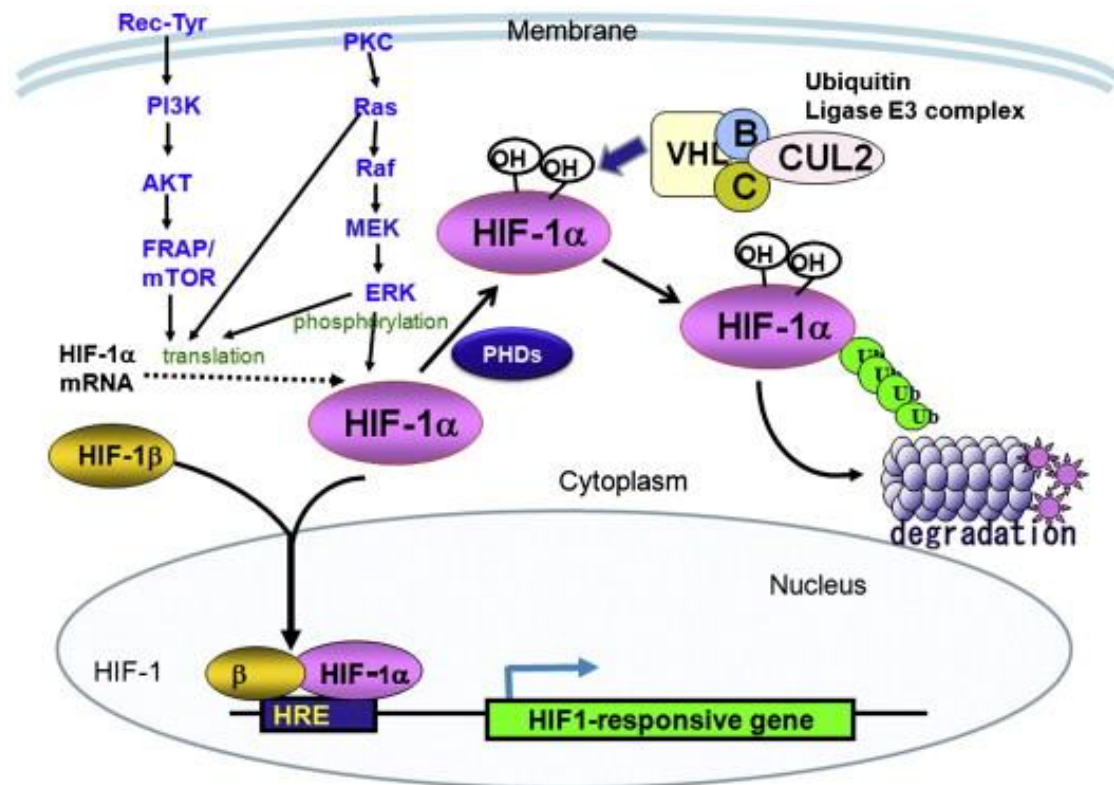


Figure 9: Hypoxia response system: HIF1 α is the central regulator of the hypoxia response. It forms heterodimers with constitutively expressed HIF1 β subunit and subsequently activates hypoxia responsive elements (HREs) of HIF1-responsive genes. HIF1 α expression is regulated by intracellular oxygen level. Dependent on oxygen supply HIF1 α undergoes hydroxylation by prolyl hydroxylases (PHDs). This allows binding of von Hippel-Lindau tumor suppressor protein (VHL) and subsequent targeting for ubiquitination and proteasomal degradation. [adapted from (Kizaka-Kondoh et al. 2009)]

Oxygen levels play an important role in the life cycle of MSCs. These cells reside in hypoxic perivascular niches, mainly located in the bone marrow, and are reported to show a normoxic stabilization of HIF1 α , which allows them to have an alternate energy metabolism (Palomaki et al. 2013). Additionally, it has been reported that hypoxia contributes to MSC tumor tropism as it promotes the inflammatory signals emitted by the tumor (Spaeth et al. 2008) as well as MSC adhesion and transmigration (Hagenhoff et al. 2016). Consequently, the circulating pool of MSCs increases under hypoxic conditions (Salem et al. 2010). Hypoxia also leads to the upregulation of CXCL12 within the tumor (Hagenhoff et al. 2016). Activated MSCs can express the receptor for this chemokine (CXCR4). This ligand-receptor interaction is thought to be one of the most important factors influencing MSC migration (Hagenhoff et al. 2016).

Thyroid hormones have been proposed to enhance the hypoxia response of MSCs by the upregulation of HIF1 α (Figure 5), leading to an enhancement of the effectiveness of hypoxia targeted MSC-based NIS-therapy.

1.5. Rationale of this study

This study focused on ways to maximize the therapeutic efficiency of MSC cancer therapy based on use of the theranostic NIS gene product.

The use of NIS-based therapy for non-thyroidal tumors requires the establishment of a hyperthyroid status to protect the thyroid gland from damage. Non-genomic thyroid hormone effects caused by this metabolic state including upregulation of hypoxia

response can alter effectiveness of MSC-based cancer therapy, as the thyroid hormone receptor integrin $\alpha\beta3$ is expressed by MSCs.

As described above, the choice of gene promoter used to drive the therapy transgene can make MSC-based gene therapy more tumor-specific. With the goal of identifying new tumor-specific promoters, we focused on making use of the biology driving hypoxic areas within aggressive, therapy resistant and rapidly growing solid tumors like HCC. To this end, we sought to evaluate a synthetic hypoxia responsive promoter with regards to effectiveness of gene activation inside the tumor milieu, as well as the applicability to target hypoxic areas in tumors. Secondly, the potential non-genomic influence of thyroid hormones on MSC biology in the context of tumor stroma, and the effectiveness of the new targeting approach, was assessed *in vitro*. The effects of these factors on MSC proliferation, differentiation, gene activation, chemotaxis and hypoxia response system were examined.

1.6. Specific aims and scope

To study in detail a hypoxia-based protocol for MSC gene therapy and to compare its general efficiency with the current RANTES/CCL5 protocol, the potential tumor-specificity of gene activation was evaluated, and potential influences of thyroid hormone treatment on MSC biology that might alter the efficiency of the therapy were assessed. The scope of this study was directed toward the following specific aims:

- *Evaluation of synthetic HIF1 α -responsive promoter as tumor-specific promoter:*
 - *Evaluation of HIF1 α protein levels in MSCs under different oxygen conditions.*
 - *Comparison of HIF1 α - and RANTES/CCL5-driven reporter gene activation in hypoxia and normoxia. Evaluation of potential tumor tropism and gene activation within tumor stroma.*
- *Evaluation of non-genomic, integrin $\alpha\beta3$ -mediated thyroid hormone effects on MSC biology: (Tetrac, integrin $\alpha\beta3$ -inhibitor, was used to confirm pathway)*
 - *Evaluation of non-genomic thyroid hormone effects on MSC hypoxia response.*
 - *Influence on HIF1 α protein levels in MSCs under different oxygen conditions.*
 - *Influence on reporter gene activation of HIF1 α - and CCL5-driven reporter genes.*
 - *Influence on mRNA levels of HIF1 α regulated genes in MSCs.*
 - *Examining effects of thyroid hormones on MSC chemotaxis and chemokinesis.*
 - *Examining potential thyroid hormone effects on MSC proliferation.*

2. Materials and Methods

2.1. Materials

2.1.1. Cell culture

2.1.1.1. Media and supplements, dyes and other reagents

Media

Dulbecco's Modified Eagle Medium (DMEM), 10x (#D2429)	Sigma-Aldrich, St. Louis
Dulbecco's Modified Eagle Medium (DMEM), 1g glucose, GlutaMAX™ supplement, pyruvate (# 21885-025)	GIBCO™, Thermo Fisher Scientific Inc., Waltham
F12 Nut Mix Ham , L-Glutamine (# 21765-029)	GIBCO™, Thermo Fisher Scientific Inc., Waltham
MEM α-medium , GlutaMAX™ supplement, no nucleosides (#32561-029)	GIBCO™, Thermo Fisher Scientific Inc., Waltham
RPMI 1640 , GlutaMAX™ supplement (#61870-150)	GIBCO™, Thermo Fisher Scientific Inc., Waltham
RPMI, 10x (#R1145)	Sigma-Aldrich, St. Louis
RPMI 1640 without phenol red (#11835-063)	GIBCO™, Thermo Fisher Scientific Inc., Waltham

Supplements

2-Mercaptoethanol (2-ME) 99% p.a.	Carl Roth GmbH, Karlsruhe
3,3',5-triiodo-L-thyronine (T3) sodium salt	Sigma-Aldrich, St. Louis
Blasticidin (#ant-bl-1), 10mg/ml	Invitrogen, Toulouse
Bovine serum albumin (BSA) Fraction V	GIBCO™, Thermo Fisher Scientific Inc., Waltham
β-GP-glycerophosphate disodium salt hydrate (in house solution 5g/l in aqua dest.) (#G9891)	Sigma-Aldrich, St. Louis
BSA fraction V	GIBCO™, Thermo Fisher Scientific Inc., Waltham
Cobalt(II)chloridehexahydrate (CoCl ₂)	Sigma-Aldrich, St. Louis
Dexamethasone powder (#D4902)	Sigma-Aldrich, St. Louis
Fetal calf serum (FCS)	Biochrom AG, Berlin
Heparin	Ratiopharm, Ulm
HEPES 1M (4-(2-hydroxyethyl)-1-piperazineethanesulfonic acid)	GIBCO™, Thermo Fisher Scientific Inc., Waltham
G418-BC 50mg/ml	Biochrom AG, Berlin
Indomethacin (#I7378)	Sigma-Aldrich, St. Louis
Insulin solution, human (#I9278)	Sigma-Aldrich, St. Louis
3-isobutyl-1-methylxanthine (IBMX) (#I7018)	Sigma-Aldrich, St. Louis
L-Ascorbic acid -2-phosphate	Sigma-Aldrich, St. Louis
L-Glutamine	Biochrom AG, Berlin
L-Thyroxine sodium salt pentahydrate (T4)	Sigma-Aldrich, St. Louis
NaOH 1M	Merck, Grafing
Penicillin/Streptomycin (P/S), 100x	PAA-Laboratories, Pasching
Sodiumhydrogencarbonat (NaHCO ₃)	GIBCO™, Thermo Fisher Scientific Inc., Waltham
Stripped fetal calf serum (sFCS)	produced in house
Tetrac 100μM	Provided by Prof. Spitzweg, Med. Klinik und Poliklinik II, Klinikum Großhadern, München

Platelet concentrate	Blood bank of Städtisches Krankenhaus Schwabing, München
Trypsin 0.05%/EDTA 0.02% in PBS	Pan Biotech, Aidenbach
2-Mercaptoethanol (2-ME) 99% p.a.	Carl Roth GmbH, Karlsruhe

Dyes

Alizarin-Red	Sigma-Aldrich, St. Louis
Nuclear fast red	Carl Roth GmbH, Karlsruhe
Oil-Red-O	Sigma-Aldrich, St. Louis
Trypan blue	Sigma-Aldrich, St. Louis
Bromphenol blue	Carl Roth GmbH, Karlsruhe
Rox Reference dye (RNA) (12223-012)	Thermo Fisher Scientific, Waltham

Other chemicals

Collagen I 5mg/ml Bovine Protein	GIBCO™, Thermo Fisher Scientific Inc., Waltham
Dimethylsulfoxide (DMSO)	Merck, Darmstadt
Dulbecco's Phosphate buffered salt solution (PBS) without Ca ²⁺ or Mg ²⁺ , 1x/10x	Pan Biotech, Aidenbach
Lipofectamine 2000 DNA transfection reagent	Invitrogen, Carlsbad
MTT powder (Thiazolyl Blue Tetrazolium Bromide)	Sigma-Aldrich, St. Louis
Poly HEMA	Sigma-Aldrich, St. Louis

2.1.1.2. Cell lines and primary cells

Cell line	Description	Source	Medium	Supplements
<i>L87, adherent</i>	Clonal, human bone marrow derived MSC cell line	In house	RPMI 1640 with GlutaMAX™	10% sFCS, 1% P/S
<i>MSC09, adherent</i>	Polyclonal, human bone marrow derived, immortalized with pIRES EGFP-SV40	Extracted from bone marrow donations of healthy donors provided by AKB Gauting	DMEM with GlutaMAX™	10% sFCS, 1% P/S
<i>hBMSC120809/1 20503/140826/120814, adherent</i>	Primary, polyclonal, human bone marrow derived MSC	Extracted from bone marrow donations of healthy donors provided by AKB Gauting	DMEM with GlutaMAX™	10% sFCS, 1% P/S 5% platelet concentrate (~5x10 ⁷ thrombocytes/ml), 1000 IE Heparin
<i>Ap00172_1, adherent</i>	Primary, polyclonal, human bone marrow derived MSC	Extracted by Apceth GmbH, München from bone marrow donations of healthy donors provided by AKB Gauting	DMEM with GlutaMAX™	10% sFCS, 1% P/S 5% platelet concentrate (~5x10 ⁷ thrombocytes/ml), 1000 IE Heparin

<i>HUH7, adherent</i>	Human hepatocellular carcinoma cell line	Provided by Prof. Spitzweg, Medizinische Klinik und Poliklinik II, Klinikum Großhadern, München (from JRCB Cell bank, Osaka, Japan)	DMEM with GlutaMAX™ and HAM F12, ratio 1+1	10% FCS/sFCS, 1% P/S
<i>HT29, adherent</i>	Human colorectal adenocarcinoma cell line	Present by Prof. Griffeon, Maastricht, Netherlands	DMEM with GlutaMAX™	10% FCS, 1% P/S

All primary bone marrow derived MSCs used within the scope of this thesis were isolated from human bone marrow donations by healthy male volunteers obtained at the Stiftung Aktion Knochenmarksspende Bayern Gauting (Robert-Koch-Allee 7, 82131 Gauting). The contact and consent by the ethics committee was obtained by PD Dr. Dr. med. Irene Teichert von Lüttichau (Kinderklinik München Schwabing).

All specimens were obtained by informed consent and according to protocols approved by institutional ethics committees.

Information about donors:

Name of cell line	Isolation date	Donor	Health status
<i>Ap00172_1</i>	28.08.2014	Male, 37 yrs	Healthy
<i>hBMSC140826</i>	26.08.2014	Male, 24 yrs	Healthy
<i>hBMSC120809</i>	09.08.2012	Male, 42 yrs	Healthy
<i>hBMSC120503</i>	03.05.2012	No information	Healthy
<i>hBMSC120814</i>	14.08.2012	Male, 25 yrs	Healthy

After isolation in house, or by Apceth GmbH (Munich, Germany) modified after the Tübinger method (2.2.1.4.), primary human bone marrow derived CD34 negative MSCs were characterized with standard laboratory procedures according to the minimal criteria for MSCs released by the international society for cellular therapy in passage three to five (Dominici et al. 2006). (for methods used, see 2.2.1.5.)

All isolated primary human mesenchymal stem cells used within the scope of this thesis met the following minimum criteria:

- Plastic adherence (Figure 10A)
- FACS-profile: (data not shown)
 - negative for: CD14, CD19, CD34, CD45, HLA-DR
 - positive for: CD73, CD90, CD105
- Adipogenic and osteogenic differentiation

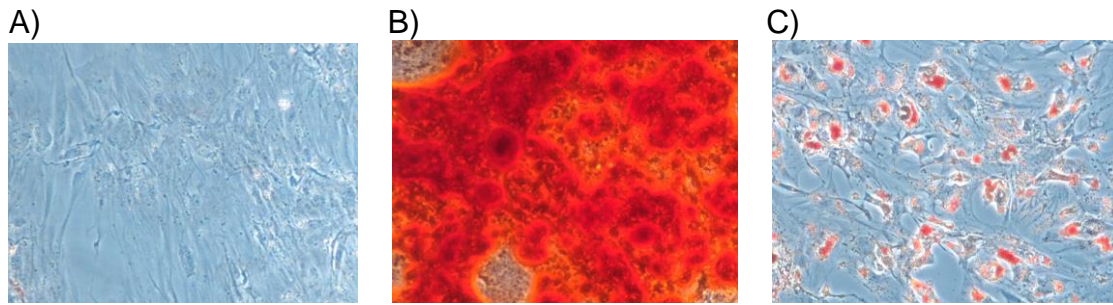


Figure 10: MSCs showing adipogenic (after 20 days) and osteogenic (after 12 days) differentiation: A) Undifferentiated MSCs showing plastic adherent growth pattern. B) Osteogenic differentiated MSCs stained with Alizarin Red. C) Adipogenic differentiated MSCs stained with Red Oil.

After isolation, cells were sometimes immortalized by transfection with plasmid pIRES-EGFP-SV40 in passage three or four (2.2.1.10.). Immortalized MSCs appeared to retain characteristics of primary MSCs (FACS profile, differentiation, plastic adherence; data not shown). For all experiments immortalized MSCs passaged five to ten times, and primary MSCs passaged two to seven times were used.

The MSC cell line L87 is a SV40 immortalized human bone marrow derived MSC cell lines that retains important characteristics of MSCs (Thalmeier et al. 1994, Conrad et al. 2008). This cell line was used to establish experimental conditions before performing experiments with primary MSCs. Immortalized MSCs were used only for Luciferase reporter gene assays as the experimental setup was too challenging for primary MSCs. Chemotaxis, invasion, western blot, qPCR, MTT-Assay experiments were performed using primary MSCs from different bone marrow donations.

Integrin $\alpha v \beta 3$ characterization (Schmohl et al. 2015)

The MSCs used in this thesis were shown to express integrin $\alpha v \beta 3$. This expression was not altered by thyroid hormone or Tetrac treatment. The HCC cell line HUH7 did not express integrin $\alpha v \beta 3$.

2.1.2. Bacteria/Microbiology

E.coli DH5 α ; Genotype: supE44, Δ lacU169 (Φ 80 lacZ Δ M15) hsdR17 recA1 endA1 gyrA96 thi-1 relA1

E.coli XL1-blue supercompetent cells for site-directed mutagenesis kit: Fermentas, St. Leon-Rot

2.1.3. Buffers and solutions

If not stated otherwise, all buffers were prepared in ultra-pure H₂O.

2.1.3.1. SDS-PAGE and western blot**Buffers and solutions produced in house:**

Ammoniumpersulfate (APS)	10% APS (w/v)
Blocking solution	5% skimmed milk powder (w/v) in TBST
Dual Extraction buffer A (Kumar 2009)	20mM HEPES (pH 7.9) 20% glycerol 10mM NaCl 1.5mM MgCl ₂ 0.2mM EDTA (pH 8.0) 1mM DTT 0.1 % Triton X100 1mM CoCl ₂ Protease inhibitor (1 tablet/50ml)
Dual Extraction buffer B (Kumar 2009)	Like A 500mM NaCl instead of 10mM NaCl
Electrophoresis buffer	1.9M Glycine 0.25M Tris 1% SDS (w/v)
HIF1 α extraction buffer (Srinivasan et al. 2011)	20mM HEPES 1.5mM MgCl ₂ 0.2mM EDTA 450nM NaCl 1mM CoCl ₂
Laemmli buffer 3x	150mM Tris/HCl, pH 6.8 (rt) 30% Glycine (v/v) 6% SDS (w/v) 0.3% Bromphenol blue (w/v) 7.5% β -mercaptoethanol (v/v)
RIPA lysis buffer	Tris/HCl 50mM, pH 7.4 NaCl 150mM EDTA 1mM Triton X100 1% sodium orthovanadate 1% SDS 0.1% CoCl ₂ 1mM Protease inhibitors (Roche complete #04693116001) 1 tablet per 50ml
Sodiumdodecylsulfate (SDS), 10%	10% SDS (w/v)
Tris, 1M, pH 6.8	Dissolved in ultrapure H ₂ O, pH adjusted with HCl at room temperature
Tris, 1.5M, pH 8.8	Dissolved in ultrapure H ₂ O, pH adjusted with HCl at room temperature
Tris-buffered saline (TBS), 10x	1.5M NaCl 100mM Tris 10mM NaN ₃
Tris-buffered saline with Tween (TBST)	0.05% Tween 20 (v/v) in 1x TBS

Commercially available buffers and solutions:

Acrylamide/Bisacrylamide solution, 30%	Carl Roth GmbH, Karlsruhe
ECL plus detection reagents (Cat. Nr. RPN2132)	GE Healthcare, München
NuPAGE LDS sample buffer, 4x	Invitrogen, Carlsbad
NuPAGE transfer buffer, 20x, #NP0006-1	Invitrogen, Carlsbad
WesternBreeze® Blocking solution	Invitrogen, Carlsbad

2.1.3.2. Molecular biologyBuffers and solutions produced in house:

Agarose gel 0.6/2%	300ml TBE buffer 0.6/2% agarose powder (w/v)
Agarose-gel-electrophoresis buffer	1l 5x TBE buffer 1 drop ethidium bromide
Agarose-gel-electrophoresis loading buffer	0.25% bromophenol blue (w/v) 0.25% xylen-cyanol FF (w/v) 30% glycerin (w/v)
Hexanucleotide mix, 10x, solution (#11 277 081 001)	Roche, Mannheim
SYBRgreen master mix (500µl volume)	10x Taq buffer 100µl without detergent dNTPs (25mM) 7.5µl Rox 20µl PCR optimizer 200µl BSA PCR grade 10µl SYBRgreen1(stock 2µl 1:100 in 20% DMSO) MgCl ₂ 25mM 120µl H ₂ O 40.5µl
Tris-borate-EDTA (TBE) buffer, 1x	90mM Tris 2mM boric acid 0.01M EDTA pH 8.0 (rt)

Commercially available buffers and solutions:

Buffers for DNA restriction enzymes	NEB, Frankfurt
First strand buffer, 5x	Invitrogen, Carlsbad
Linear Acrylamid, 5mg/ml (#9520)	Ambion®, Thermo Fisher Scientific, Waltham
PCR assays	Applied Biosystems, Thermo Fisher Scientific, Waltham
Platinum Quantitative PCR SuperMix-UDG with ROX, 1x (#11743-100)	Invitrogen, Carlsbad
SpeedAmp PCR buffer, 10x	Analytik Jena, Jena
Taq buffer without detergent, liquid, 10x (#B55)	Thermo Fisher Scientific, Waltham
ThermoPol buffer for Taq polymerase, 10x	NEB, Frankfurt
T4 DNA Ligase buffer, 10x	NEB, Frankfurt

2.1.3.3. MicrobiologyBuffers and solutions produced in house:

Agar 2x	3% Agar-Agar (w/v), autoclaved
Ampicillin solution	50mg/ml Ampicillin in 70% ethanol (w/v)
CaCl ₂ solution (for preparation of competent bacteria)	60mM CaCl ₂ 15% Glycerol (v/v) 10mM PIPES, pH7 (rt) Sterile filtered (0.2 µm)
Freezing solution for bacteria 10x (autoclaved)	132.3 mM KH ₂ PO ₄ 21mM Sodiumcitrate 3.7mM MgSO ₄ *3H ₂ O 68.1mM (NH) ₂ SO ₄ 459.3mM K ₂ HPO ₄ *3H ₂ O 35.2% Glycerin (w/v)

LB-Medium 1x	2% bacto tryptone (w/v) 10g 342 mM NaCl 10g 1% yeast extract (w/v) 5g Ad 1l pH 7.2-7.3 (rt) through 1M NaOH, autoclaved
LB-Medium 2x (for agar plates)	5g bacto tryptone 5g NaCl 2.5g yeast extract Ad 250ml

Commercially available materials:

Ampicillin sodium salt (#K029)	Carl Roth GmbH, Karlsruhe
Bacto tryptone (#211705)	BD Biosciences, Heidelberg
Yeast extract (#212750)	BD Biosciences, Heidelberg

2.1.3.4. Histological and immunohistological staining

Alexa Fluor® 594 AffiniPure Donkey Anti-Mouse IgG (H+L) (a-mIgG)	Jackson Immunoresearch, West Grove
Cell Tracker™ green CMFDA (5-Chloromethylfluorescein Diacetate)	Molecular probes®, Life technologies, Carlsbad
DAPI (4',6-Diamidino-2-Phenylindole, Dihydrochloride)	Molecular probes®, Life technologies, Carlsbad
donkey serum	Jackson Immunoresearch, West Grove
Eosin Y solution, alcoholic	Sigma-Aldrich, St. Louis
Hematoxylin solution, Harris modified	Sigma-Aldrich, St. Louis
Hoechst 33342	Invitrogen, Carlsbad
Hypoxyprobe™-1 Kit	Hpi, Burlington
PI (P4864)	Sigma-Aldrich, St. Louis
TritonX100	Sigma-Aldrich, St. Louis
Tween 20	Carl Roth GmbH, Karlsruhe
Xylol	Sigma-Aldrich, St. Louis
Vectamount mounting medium	Vector laboratories, Burlingame

2.1.3.5. Cell culture

Buffers and solutions produced in house:

Acidified isopropyl	0.4ml 1N HCl 9.6ml Isopropyl
Erythrocyte lysis buffer	8.29g Ammonium chloride NH ₄ Cl 1g Potassiumhydrogencarbonate KHCO ₃ 0.037g Triplex III Na ₂ -EDTA Dissolved in 1l ultra-pure H ₂ O Sterile filtered (0.2 µm)
PolyHEMA solution	2% polyHEMA 95% ethanol

2.1.3.6. Other buffers and solutions

FACS-buffer	1x PBS (cell culture grade)
-------------	-----------------------------

2.1.4. Antibodies for FACS and WB

Primary antibodies (target species: human):

Immuno- gen	Host species/ isotype	Appli- cation	Label	Source	Concentration	Incubation
HIF-1 α	Mouse/ IgG1	WB	none	BD Biosciences Heidelberg	1:1000	overnight at 4°C
α -tubulin	Rabbit/ polyclo- nal	WB	none	Cell signaling, Danvers (#2144)	1:1000	overnight at 4°C
Integrin $\alpha\beta$ 3	Mouse/ IgG1	FACS	none	abcam®, Cambridge (#ab78289)	2 μ g/10 ⁶ cells	45 min on ice
CD14	Mouse/ IgG2	FACS	APC	BD Biosciences Heidelberg (#345787)	1:50; 0.1 μ g/10 ⁶ cells	30 min on ice
CD19	Mouse/ IgG1	FACS	FITC	BD Biosciences Heidelberg (#555412)	1:50	30 min on ice
CD34	Mouse/ IgG1	FACS	FITC	BD Biosciences Heidelberg (#345801)	1:50; 0.05 μ g/10 ⁶ cells	30 min on ice
CD45	Mouse/ IgG1	FACS	PE-CY5	BD Biosciences Heidelberg (#555484)	1:50	30 min on ice
CD73	Mouse/ IgG1	FACS	APC	BD Biosciences Heidelberg (#560847)	1:50	30 min on ice
CD90	Mouse/ IgG1	FACS	PE-CY5	BD Biosciences Heidelberg (#555597)	1:300; 66ng/10 ⁶ cells	30 min on ice
CD105	Mouse/ IgG1	FACS	PE	BD Biosciences Heidelberg (#560839)	1:50	30 min on ice
HLA-DR	Mouse/ IgG2	FACS	PE	BD Biosciences Heidelberg (#555812)	1:50	30 min on ice

Secondary antibodies (target species: mouse):

Immuno-gen	Host species/ Isotype	Appli- cation	Label	Source	Concen- tration	Incubation
IgG (H+L)	Donkey Polyclonal IgG (H+L)	FACS	Cyanine Cy™3	Jackson Immuno Research Europe Ltd., Suffolk (#715-165- 151)	2µg/10 ⁶ cells	30 min on ice
Polyclonal Rabbit Anti- Mouse Immuno- globulins/ HRP	Rabbit/Polyclonal	WB, HIF1α	none	Dako, Glostrup (#P0260)	1:5000	1 hr at RT
Amersham ECL Rabbit IgG, HRP- linked	Donkey/ IgG	WB, α- tubulin	none	GE Healthcare Life Sciences, Freiburg (#NA934- 100UL)	1:5000	1 hr at RT

2.1.5. Enzymes

Alkaline phosphatase	Roche, Mannheim
Phusion DNA polymerase	NEB, Frankfurt
Restriction enzymes	NEB, Frankfurt
Super script II reverse transcriptase	Invitrogen, Carlsbad
T4 DNA ligase	NEB, Frankfurt
Taq DNA polymerase	NEB, Frankfurt

2.1.6. Size standards for electrophoresis

1kb DNA ladder	Invitrogen, Carlsbad
MagicMark™ XP western protein standard	Invitrogen, Carlsbad
Molecular weight marker (Cat. Nr. 27-2111)	PeQLab, Erlangen

2.1.7. Primers/Oligonucleotides

Application	Gene	Sequence/melting point	Source
qPCR, SYBRgreen	hCCL5 fw	TACACCAGTGGCAAGTGCTC 58.3°C	AG Spitzweg, Großhadern
	hCCL5 rv	TGTACTCCCGAACCCATTTC 58.3°C	
qPCR, SYBRgreen	hCTGF fw	CCAATGACAACGCCTCCTG 61°C	Invitrogen, Carlsbad
	hCTGF rv	TGGTGCAGCCAGAAAGCTC 61°C	
qPCR, SYBRgreen	hCXCL12 fw	AGAGCCAACGTCAAGCATCT 58.5°C	Invitrogen, Carlsbad
	hCXCL12 rv	CTTTAGCTTCGGGTCAATGC 58.4°C	
qPCR, SYBRgreen	hFGF2 fw	GGAGAAGAGCGACCCTCAC 61°C	Invitrogen, Carlsbad
	hFGF2 rv	AGCCAGGTAACGGTTAGCAC 59.4°C	
qPCR, SYBRgreen	hHGF fw	CTGGTTCCCTTCAATAGCA 60.1°C	AG Spitzweg Großhadern
	hHGF rv	CTCCAGGGCTGACATTTGAT 60°C	
qPCR, SYBRgreen	hHIF1α fw	GCTTTAACTTTGCTGGCCCC 60°C	AG Spitzweg, Großhadern
	hHIF1α rv	TTCAGCGGTGGGTAATGGAG 60°C	
qPCR, SYBRgreen	hID1 fw	GTCTGTCTGAGCAGAGCGTG 51°C	Self-designed (Invitrogen, Carlsbad)
	hID1 rv	CGTTCATGTCTGAGAGCAGC 49°C	

qPCR, SYBRgreen	hIL6 fw hIL6 rv	TACCCCCAGGAGAAGATTCC TTTTCTGCCAGTGCCTCTTT	60.3°C 60°C	AG Spitzweg, Großhadern
qPCR, taqman	hMMP2 fw hMMP2 rv	ATGCCGCCTTTAACTGGAG GGAAAGCCAGGATCCATTTT	56.7°C 55.3°C	Entelechon, Bad Abbach
qPCR, SYBRgreen	hMMP9 fw hMMP9 rv	ACGACGTCTTCCAGTACCGA TTGGTCCACCTGGTTCAACT	59.4°C 57.3°C	Entelechon, Bad Abbach
qPCR, SYBRgreen	hTGFβ1 fw hTGFβ1 rv	CAGCACGTGGAGCTGTACC AAGATAACCACTCTGGCGAGTC	62°C 62°C	QuantiTect, Hilden
qPCR, SYBRgreen	hTIMP1 fw hTIMP1 rv	CTGTTGTTGCTGTGGCTGAT ACTTGGCCCTGATGACGAG	47°C 48°C	Self-designed (Invitrogen, Carlsbad)
qPCR, SYBRgreen	hVEGFa fw hVEGFa rv	CTACCTCCACCATGCCAAGT ATGATTCTGCCCTCCTCCTT	60°C 60°C	AG Spitzweg Großhadern
qPCR, Control taqman assay	Eukaryotic 18S rRNA (VIC/TAMRA Probe)			Thermo Fisher Scientific, Waltham (#4310893E)
qPCR, SYBRgreen	18SRNA fw 18SRNA rv	GCAATTATTCCCATGAACG AGGGCCTCACTAAACCATCC	58.6°C 58.8°C	Entelechon, Bad Abbach

2.1.8. Plasmids and vectors

For plasmid maps, see cloning strategies (2.2.5.)

Plasmid	Description	Source	Selection	Application
pIR-EGFP-SV40	CMV promoter, SV40 Large T antigen, internal ribosomal entry site, green fluorescent protein	In house (Anke Fischer)	Kana- mycin	Immortalization of MSCs (success can be evaluated by expression of GFP)
pRL-TK/CMV	CMV promoter, Renilla luciferase, constitutive expression of luciferase	Promega, Madison	Ampicillin	Control plasmid for dual luciferase assays
pGL3-RFL	RANTES promoter, firefly luciferase, promoter dependent expression of luciferase	In house (Fessele 2001)	Ampicillin	RANTES dependent luciferase expression
pGL3-6xHRE-luc-blasti_clockwise	HIF1α-responsive promoter, firefly luciferase, promoter dependent expression of luciferase	In house (Anna Hagenhoff)	Blasticidin, Ampicillin	Reporter gene activity under different oxygen conditions

2.1.9. Kits

BioLux® Gaussia Luciferase Flex Assay Kit	NEB, Frankfurt
ECL-Kit	Perkin Elmer, Waltham
QIAquick Gel Extraction Kit	Qiagen, Hombrechtikon
Dual-Luciferase® Reporter Assay	Promega, Fitchburg
Endofree Plasmid Maxi Kit	Qiagen, Hilden
Innuprep Plasmid Mini kit	Analytik Jena, Jena
Pierce™ BCA Protein Assay Kit	Thermo Fisher Scientific, Waltham
PureLink RNA Mini Kit	Life technologies, Carlsbad
Quant-iT RNA assay	Life technologies, Carlsbad

Quant-IT dsDNA high sensitivity Assay Kit	Invitrogen, Carlsbad
Quant-IT dsDNA broad range Assay Kit	Invitrogen, Carlsbad
Quickchange Site-directed mutagenesis it	Stratagene, Santa Clara
MykoAlert Mycoplasma Detection Kit	Lonza, Basel
RNase-free DNase set	Qiagen, Hilden

2.1.10. Chemicals

Active charcoal (#C9157)	Sigma-Aldrich, St. Louis
Agar (# 214010)	BD Biosciences, Heidelberg
agarose powder (# 15510-500)	Invitrogen, Carlsbad
ammonium chloride (NH ₄ Cl) (#101145)	Merck, Darmstadt
Ammoniumperulfate (APS) 10g	Carl Roth GmbH, Karlsruhe
Boric acid	Carl Roth GmbH, Karlsruhe
β-Mercaptoethanol	Sigma-Aldrich, St. Louis
BSA (molecular biology grade), 20mg/ml	Thermo Fisher Scientific, Waltham
CaCl ₂	Merck, Darmstadt
Dextran	Carl Roth GmbH, Karlsruhe
EDTA	Merck (Calbiochem), Darmstadt
Ethanol 70%	Pharmacy Klinikum Großhadern, München
Ethanol 95%	Pharmacy Klinikum Großhadern, München
Ethanol 96%	Pharmacy Klinikum Großhadern, München
Ethanol 99%	Sigma-Aldrich, St. Louis
Ethanol 100%	Sigma-Aldrich, St. Louis
Ethidium bromide, 0,5% solution (#HP46)	Carl Roth GmbH, Karlsruhe
Formalin 4%	Sigma-Aldrich, St. Louis
dNTP Set (100mM aqueous solution of each of dATP, dCTP, dGTP, dTTP) (#R0182)	Thermo Fisher Scientific, Waltham
DTT	Serva, Heidelberg
Glycine	Carl Roth GmbH, Karlsruhe
Glycerol	Carl Roth GmbH, Karlsruhe
HCl	Merck, Darmstadt
Isopropyl	Carl Roth GmbH, Karlsruhe
K ₂ HPO ₄	Carl Roth GmbH, Karlsruhe
Methanol	Merck, Darmstadt
MgCl ₂	Carl Roth GmbH, Karlsruhe
MgSO ₄	Sigma-Aldrich, St. Louis
MTT	Sigma-Aldrich, St. Louis
NaCl 5M	Sigma-Aldrich, St. Louis
(NH) ₂ SO ₄	Sigma-Aldrich, St. Louis
PCR optimizer Bio Stab (LC120-0001)	Bitop, Witten
PIPES	Sigma-Aldrich, St. Louis
Potassiumhydrogencarbonate (KHCO ₃) (#104854)	Merck, Darmstadt
n-propyl gallate	Sigma-Aldrich, St. Louis
Protease Inhibitor cocktail tablets Complete	Roche, Mannheim
RNasin Rnase inhibitor	Promega, Madison
Rnase free water	Thermo Fisher Scientific, Waltham
SDS	Carl Roth GmbH, Karlsruhe
Skimmed milk powder	Carl Roth GmbH, Karlsruhe
Sodium Azide NaN ₃	Merck, Darmstadt
Sodium citrate	Merck, Darmstadt
Sodium orthovanadate	Sigma-Aldrich, St. Louis

SYBR® Green I nucleic acid gel stain, 10000x, in DMSO (#86205)	Fluka, Sigma-Aldrich, St. Louis
Tissue Tek® O.C.T.™ Compound	Sakura Finetek Europe B.V.
Titriplex III Na ₂ -EDTA (#108418)	Merck, Darmstadt
Tris-borate-EDTA	Carl Roth GmbH, Karlsruhe
Triton X100 hydrogenated (Triton X100h)	Calbiochem./Merck, Darmstadt
Tween 20	Carl Roth GmbH, Karlsruhe
Vectashield® Mounting Medium	Vectorlaboratories, Burlingame
Water injection grade (Aqua ad iniectabilia)	Braun Melsungen AG, Melsungen
Xylen-cyanol FF	Carl Roth GmbH, Karlsruhe

2.1.11. Disposables and other materials

μ-slide Chemotaxis 3D, ibiTreat, tissue culture treated, sterile	Ibidi, Martinsried
0.22μm filter (for seringue)	BD Biosciences, Heidelberg
4mm cuvettes	PeqLab Biotechnologie GmbH, Erlangen
96 well tissue culture plates round/flat bottom	TPP Techno plastic products, Trasadingen
48/24/6 well plate	TPP Techno plastic products, Trasadingen
6/10/15cm ² cell culture vessels	TPP Techno plastic products, Trasadingen
Amersham Hyperfilm ECL autoradiography film	GE Healthcare, Uppsala
Al ₂ O ₃ notched plate (for WB)	GE Healthcare, Uppsala
Beveled pipette tips (20μl pipette)	Greiner Bio-One GmbH, Frickenhausen
Centrifuge tubes 15/50ml	TPP Techno Plastic Products, Trasadingen
Combitipps migration	Greiner Bio-One GmbH, Frickenhausen
Counting chamber	Hecht-Assistant, Sondheim
Cryomold embedding cassettes	Sakura Finetek Inc., St. Torrence
Cryovials 2ml	Alpha laboratories, Hampshire
FACS tubes	BD Biosciences, Heidelberg
Humid chamber for chemotaxis assay: 15cm ² cell culture dish, facial tissues, deionized water	TPP Techno Plastic Products, Trasadingen; Wepa Mainz
Luminometer tubes	Sarstedt, Kleinstadt
Microlance 3	BD Biosciences, Heidelberg
Microtubes 1.5/2ml	Böttger, Bodenmais
Microtubes 5ml	Eppendorf Research, Hamburg
Millipore Immobilon-P PDVF membrane	Merck Millipore, Darmstadt
Pasteur pipettes	Peske
Pipette tips 1250/200/20/10 μl	Greiner bio-one, Frickenhausen
Scraper	TPP Techno Plastic Products, Trasadingen
Seringue 2ml Discardit II	BD Biosciences, Heidelberg
Serological pipettes 50ml with reservoir	TPP Techno Plastic Products, Trasadingen
Serological pipettes cellstar 5/10/25ml	Greiner bio-one, Frickenhausen
Serological pipettes 1/2ml	TPP Techno Plastic Products, Trasadingen
Superfrost™ plus microscope slides	Thermo Fisher Scientific, Waltham
Transofix	Braun Melsungen AG, Melsungen
Tissue culture dishes 6/10/15 cm	TPP Techno Plastic Products, Trasadingen

Tweezer	Merck Millipore, Darmstadt
Vacuum filter system	TPP Techno Plastic Products, Trasadingen

2.1.12. Other laboratory equipment (devices)

Assistent Rollenmischer RM5, Nr. 348	Karl Hecht KG, Sondheim/Rhön
Autoclave	WEBECO GmbH, Selmsdorf
Binocular stereomicroscope SZX90	Olympus, Shinjuku
Biofuge pico	Heraeus Instruments GmbH, Hanau
BioRad 3000 Xi	Bio-Rad, München
BioRad power Pac300	Bio-Rad, München
Capacitance Extender	Bio-Rad, München
Centrifuge 5402	Eppendorf Research, Hamburg
Centrifuge Rotanta 460R	Hettich Zentrifugen, Ebersberg
Cold light source KL1500	Schott AG, Mainz
Cryostat Jung CM 3000	Leica, Wetzlar
Curix60 (Developer for autoradiography films)	Agfa, Mortsel
Dispenser pipette	Eppendorf Research, Hamburg
Eppendorf Easypet® 3	Eppendorf Research, Hamburg
Fluorescence activated cell scanner FACSCalibur	Becton, Dickinson
Fluorometer Qubit	Invitrogen, Carlsbad
Gene Pulser (Electroporation cell culture)	Bio-Rad, Hercules
Incubator Galaxy 48 R	Eppendorf Research, Hamburg
Incubator	Thermo Fisher Scientific, Waltham
Incubator	Memmert, Schwabach
Inverted fluorescence microscope DMIL	Leica, Wetzlar
CCD Camera ProgRes® CF	Jenoptik, Jena
Heated, incubation chamber	Ibidi, Martinsried
Motorstage	Prior Scientific Instr. Ltd., Fulbourn
Light Cycler® 480 II	Roche, Mannheim
Lumat LB9507	EG&G Berthold
Megafuge 1.0R	Thermo Fisher Scientific, Waltham
Microtome HM-340-E	Microm, Walldorf
Multiwell plate reader GFNios Plus	Tecan, Crailsheim
PCR machine Mastercycler®pro	Eppendorf Research, Hamburg
Pipetman Pipettes 1000/200/20/2µl	Gilson, Middleton
Power Pac 300	Bio-Rad, Hercules
RCT basic	IKA® Labortechnik, Staufen
Rotilabo®-mini-centrifuge	Carl Roth GmbH, Karlsruhe
Scale BP1109	Sartorius, Bradford
Scale Excellence E2000 D	Sartorius, Bradford
Scale P1200N	Mettler-Toledo LLC, Columbus
Scale PJ3000	Mettler-Toledo LLC, Columbus
Sorvall RC 5B plus centrifuge	Thermo Fisher Scientific, Waltham
Sterile Hood Class II Type A/B3	The Baker Company inc., Sanford, Maine
Thermomixer comfort	Eppendorf Research, Hamburg-
UV Transilluminator	UVP, LLC, Upland
Vortex-Genie 2	Scientific industries Inc., Bohemia
Water bath	GFL, Burgwedel
Water jet vacuum pump	In house

2.1.13. Software

Name	Application	Source
CellQuest	Acquisition of FACS data	BD Biosciences, Bedford
Clone manager	Planning of cloning strategies, generation of plasmid maps	Sci-Ed Software, Morrisville
Endnote X 7.3.1.	Organization of literature resources	License from Ludwig Maximilians University Munich
Fiji 1.48q	Analysis of MSC distribution in invasion experiments	National Institute of Health, Bethesda
FlowJo	Evaluation of FACS data	TreeStar Inc., Ashland
Graph Pad Prism 6	Statistical analysis, generation of diagrams	GraphPad Software, La Jolla
Image J and plugins manual tracking, chemotaxis tool	Image editing, Evaluation of migration data	National Institutes of Health, USA
Light Cycler® 480 Software release 1.5.0. SP4	Analysis of q-PCR data	Roche, Mannheim
Micro-Manager	Picture acquisition video microscopy (open source microscopy software)	Open Imaging Inc., San Francisco
Mircosoft office	Generation of diagrams, analysis of q-PCR data	License from Ludwig Maximilians University Munich
ProgRes Capture	Leica fluorescence microscope image acquisition	Jenoptik, Jena
SnapGene	Plasmid maps	GSL Biotech LLC, Chicago
XFluor	Control of ELISA plate reader	Tecan, Crailsheim

2.2. Methods

2.2.1. Cell culture

2.2.1.1. General cell culture

The culture of living cells was performed in a laminar flow hood. Penicillin and Streptomycin were added to the culture media. All reagents and supplements were preheated to 37°C using a water bath except for those used for the chemotaxis assay. These solutions were incubated in a cell culture incubator set to 37°C and 5% CO₂ to allow pH adjustment as well as preheating. Incubation of cells was performed in humidified atmosphere at 37°C, 21% O₂ and 5% CO₂ unless stated otherwise for experiments using hypoxic conditions (see 2.2.1.8.). When splitting cells, they were first rinsed with PBS and then detached using Trypsin-EDTA at room temperature. The reaction was stopped by adding an equal volume of medium containing 10% sFCS (or twice the volume if the medium contained less sFCS), and the cells were pelleted by centrifugation for 3 min at 200rcf (at room temperature). After carefully suspending the cell pellet in fresh culture medium cells were seeded into an appropriate cell culture vessel.

2.2.1.2. Freezing and thawing of cells

For long-term storage, cells were detached after rinsing with PBS and after the centrifugation step, suspended in respective culture medium. In order to prevent water crystallization, the cell suspension was subsequently mixed with freezing medium in a 1+1 ratio. Freezing medium consisted of 60% sFCS, 20% respective culture medium and 20% DMSO. Due to the toxicity of the DMSO, the procedure was performed as rapid as possible and the cryotubes were placed into isopropanol containers at -80°C for 24 hrs allowing slow decrease of the temperature to -80°C. The cells were stored in a liquid nitrogen container at -196°C.

For thawing cells, cell culture vessels containing preheated culture medium were prepared and the frozen cell suspension was thawed quickly in a 37°C water bath. When almost completely thawed the cell suspension was transferred into the culture vessel rapidly to ensure quick dilution of the DMSO. After cells were adherent (4-6 hrs) the culture medium was exchanged and transgene selection medium was added.

2.2.1.3. Cell quantification

To quantify the cell numbers, a defined volume of cell suspension was diluted with trypan blue solution (0.4%) and subsequently pipetted into a Neubauer counting chamber. Cells in four of the big squares were counted and cell concentration calculated after the following formula:

$$\text{concentration (cells/ml)} = \frac{\text{number of cells} \times 10000}{\text{number of squares} \times \text{dilution}}$$

Figure 11: Formula for cell counting with Neubauer Chamber

2.2.1.4. Isolation of primary MSCs

Primary MSCs were isolated from bone marrow donations preserved in EDTA after the Tübinger method (Muller et al. 2006) with slight modifications of the culture medium used for isolated MSCs (see 2.1.1.1.) The whole procedure was performed at room temperature. Samples were incubated with approximately the same volume of erythrocyte lysis buffer (see 2.1.3.5.). From time to time mixture was stirred and

after 10 min centrifuged at 500 rcf for 5 min and the sediment transferred into PBS, lysated and centrifuged again until lysis was completed. Lysate was rinsed with PBS and plated with 2ml respective culture medium (see 2.1.1.1) per 1ml bone marrow sample into a 75cm² culture flask (max. 10ml) and then cultured in 21% O₂. Every two days medium was changed and cells were subcultured according to their density.

2.2.1.5. Characterization of MSCs and HUH7 (FACS, differentiation, immortalization)

As detailed in 2.1.1.2., MSCs had to meet certain minimum criteria. To ensure this, differentiation ability and surface markers were examined in house. Moreover, all cells used for this thesis were examined for integrin $\alpha\beta$ 3 expression in house and at the cooperating laboratory of Prof. Spitzweg at Großhadern.

2.2.1.5.1. FACS analysis of characteristic surface markers

Surface marker analysis cells was performed using fluorescence activated cell sorting (FACS). This method uses fluorescence labeled antibodies for the detection of surface molecules. Size, granularity and fluorescence signal were detected and subsequently expression of targeted molecules was evaluated.

Cells were detached using trypsin-EDTA and suspended in PBS. Cell number, antibody concentration and incubation period can be found in 2.1.4. Antibodies without fluorescence tag were incubated with a secondary fluorescence marked antibody for 30 min on ice. After washing twice with PBS, cells were analyzed on a FACS Calibur with Cell Quest Software. Cell debris was excluded by appropriate gating. MSCs were analyzed between passages three and five. HUH7 cells in passages ten to fifteen.

MSCs met the minimum criteria of surface markers. Moreover, MSCs used for this thesis expressed integrin $\alpha\beta$ 3 while tumor cell line HUH7 was negative for integrin $\alpha\beta$ 3. The integrin $\alpha\beta$ 3 expression on MSCs was not influenced by thyroid hormone or Tetrac treatment (Schmohl et al. 2015).

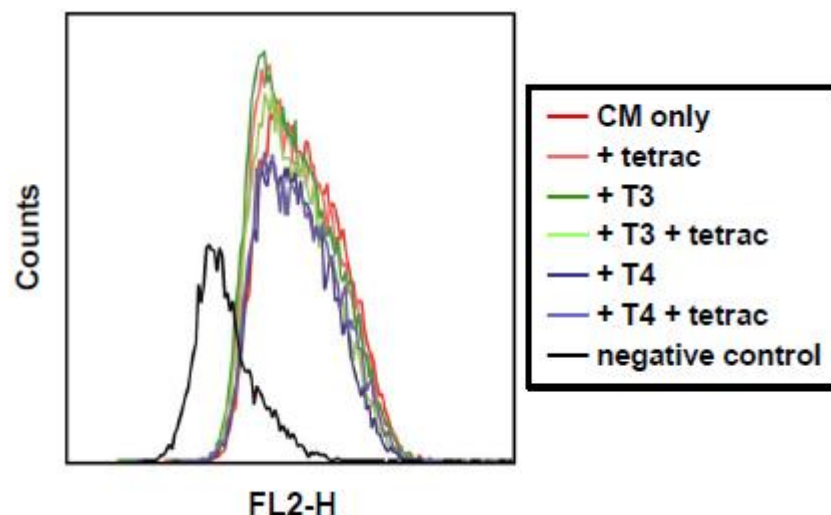


Figure 12: Integrin $\alpha\beta$ 3 expression on MSCs is not influenced by T3/T4/Tetrac treatment: MSCs were treated with HUH7 conditioned medium and 1nM T3 or 1 μ M T4 with or without 100nM Tetrac for 24 hrs, harvested and analyzed for integrin $\alpha\beta$ 3 expression by flow cytometry with an integrin $\alpha\beta$ 3-specific antibody and Cy3-conjugated secondary antibody. Cells incubated with secondary antibody alone served as negative control. (Schmohl et al. 2015)

2.2.1.5.2. Differentiation and histochemical staining

To demonstrate sustained adipogenic and osteogenic differentiation capability, MSCs were plated into three wells on two six well plates. After reaching 80% confluency, differentiation was initiated by changing the respective culture medium into differentiation medium.

Osteogenic differentiation was conducted for twelve days, adipogenic differentiation for nineteen days with medium changes every two to three days. After this period, cells were fixed in 4% Formalin for 20 min at room temperature.

Osteogenic differentiated cells were rinsed with NaCl after fixation and incubated with alizarin red for 10 min, staining Ca^{2+} deposits. After another three rinses in NaCl, to remove excess stain, cells were characterized under the microscope.

Adipogenic differentiated cells were rinsed with PBS and then incubated with freshly prepared 0.03% Oil Red O solution for 20 min at room temperature, staining accumulated lipid droplets. After rinsing three times to remove excess stain cells were characterized under the microscope.

Two controls were included per differentiation: One incubated with normal culture medium and one incubated with the differentiation medium for osteocytes/adipocytes. Both were stained as described above with the non-corresponding dye (Figure 13). These controls ensured proper experimental quality and excluded spontaneous differentiation. All controls were negative in the experiments performed.

Differentiation	Medium	Specific supplements
<i>Osteogenic</i>	DMEM+10%FCS+1% P/S	10nM dexamethasone 10mM β -GP-glycerophosphate 50 μ g/ml Ascorbic acid
<i>Adipogenic</i>		10 μ M dexamethasone 0.5mM isobutyl methyl xanthine (IBMX) 50 μ M indomethacin 1 μ g/ml insulin

Table 1: Media for osteogenic and adipogenic differentiation of MSCs [modified after (Pittenger et al. 1999, Liu et al. 2009)]

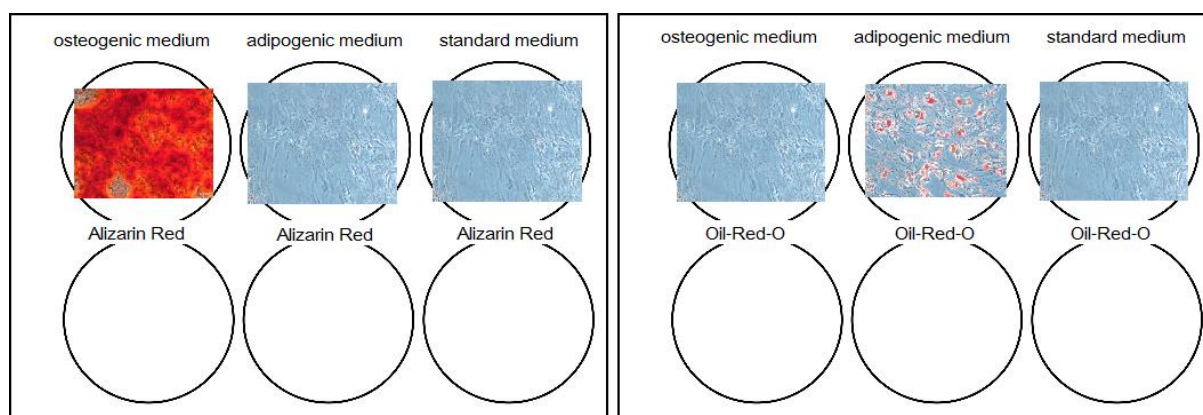


Figure 13: Plating plan for osteogenic (left) and adipogenic (right) differentiation: MSCs were seeded onto a 6-well-plate and differentiation performed as described above. For each differentiation, two controls were included, to exclude spontaneous differentiation. Alizarin red stain (for osteocytes) was performed after 12 days on the left plate, Oil-Red-O stain (for adipocytes) after 19 days on the right plate.

All primary MSCs isolated and immortalized within the scope of this thesis met the minimum differentiation criteria as stated in 2.1.1.2. The established MSC cell line L87 retained limited features of primary isolated MSCs (Thalmeier et al. 1994, Conrad et al. 2008). L87 cells showed osteogenic differentiation after 28 days but no

adipogenic differentiation. In addition, migratory capacities were reduced. However, *in vitro* handling was easier due to less vulnerability of cells. Therefore, the cell lines promoted a stable *in vitro* model of MSC biology for preliminary experiments to establish experimental routines.

2.2.1.5.3. Immortalization

In order to establish a uniform pool of MSCs out of the heterogenic isolated population, cells were stably transfected with an in house established pIR-EGFP-SV40-plasmid, a plasmid expressing EGFP for transfection efficiency control and Simian virus 40 (SV40) large T antigen. SV40 inactivates certain tumor suppressor genes and enhances telomerase activity, when incorporated into the genome. This transgene engineering leaves migration and invasion capacities as well as differentiation capacities unaffected but allows the establishment of clonal uniformity not given in isolated primary MSC populations. These experiments were performed in collaboration with Anke Fischer (MTA, AG Klinische Biochemie, Prof. Peter Nelson). Primary MSCs were transfected in passage three. Transfection did not yield the expected effect of persisting immortalization but an expansion of the life span from five to ten passages and made cells more robust. Starting in passage ten cells grew slower and started to die or differentiate spontaneously. Consequently, only immortalized cells up to passage ten were used for experiments. For method of stable transfection, see 2.2.1.10.

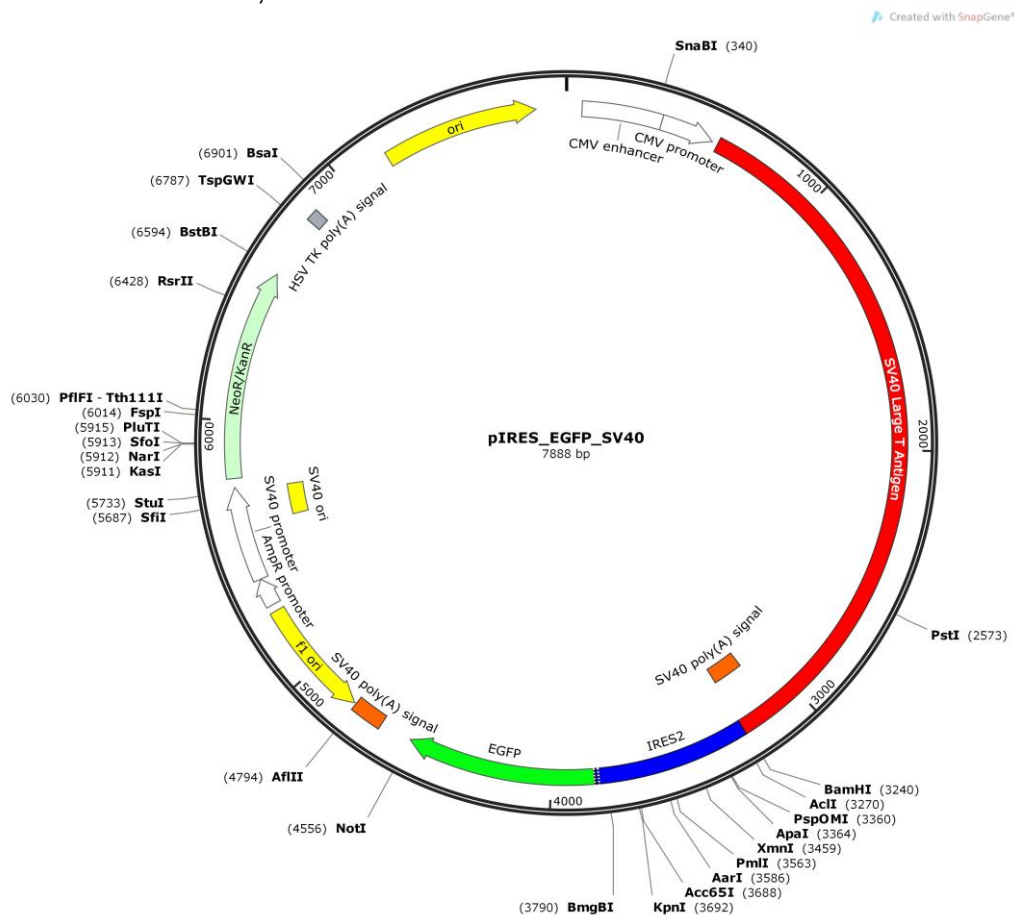


Figure 14: Plasmid map of pIRES-EGFP-SV40 used to immortalize primary MSCs: The plasmid contains a CMV promoter driving SV40 Large T Antigen, IRES2 sequence (allowing initiation of translation in the middle of mRNA) and green fluorescent protein (EGFP).

2.2.1.6. Stripping of fetal calf serum

As fetal calf serum (FCS) normally contains varying concentrations of thyroid hormones thus, possibly confounding experiments of this thesis, it had to be depleted of thyroid hormones. This was performed by stripping the FCS with dextran coated active charcoal after a protocol adapted from the procedure developed by Prof. Spitzweg's research group at Großhadern: 25g active charcoal was coated with 2.5g Dextran by adding both ingredients to 1l PBS in a 1l measuring cylinder under a fume cupboard. Mixture was stirred at 4°C. Simultaneously, two bottles of FCS were thawed at 4°C. After 12hrs, the mixture was filtrated with a sterile 500ml-TPP vacuum filtration-system into a sterile 1l glass bottle. The coated charcoal was transferred into a second sterile glass bottle and autoclaved. Then 800ml sterile FCS were added to the autoclaved charcoal under a laminar flow hood and the mixture was stirred 24 hrs at 4°C. Afterwards mixture was centrifuged twice for 15 min at 10000 rcf and 4°C. Sub-sequently the mixture was filtrated with a sterile 500ml-TPP vacuum filtration-system. Then the whole procedure was repeated using the stripped FCS (sFCS) from round one instead of fresh FCS. Afterwards sterile sFCS was aliquoted and stored at -20°C. Depletion success was confirmed at the clinical chemistry laboratory at university hospital Großhadern. The hormone content for different batches was for T3 between non-detectable and a maximum of 0.13pg/ml (=0.19pM) and for T4 between 0.81ng/dl (=1nM) and 1.01ng/dl (=1.3nM). These concentrations were at least tenfold below the lowest concentrations of thyroid hormone (1nM T3, 10nM T4) used to stimulate the cells.

2.2.1.7. Production of HUH7 conditioned medium (CM)

HUH7 conditioned medium, used to stimulate MSCs, was produced by plating 2.5 Mio HUH7 cells [in DMEM+hamF12 (ratio 1:1) medium with 10%sFCS and 1%P/S] into 15cm² culture vessels. After reaching 80% density medium was changed and cells were incubated for 48 hrs. Afterwards supernatant was removed, centrifuged at 330 rcf for 5 min to remove cell debris and then stored at -20°C.

The supernatant used to stimulate cells in the chemotaxis assay was produced slightly different. 2.5 Mio HUH7 cells were cultured in respective culture medium like above. When cells reached 100% confluence medium was changed to chemotaxis assay medium (RPMI or DMEM + 1%BSA+15mM HEPES) and cells were incubated for 48 hrs. Then supernatant was removed and processed as described above.

2.2.1.8. Stimulation of MSCs with hypoxia, thyroid hormones and HUH7 conditioned medium (CM)

Hypoxic stimulation of MSCs was either performed in a hypoxic incubator using a culture atmosphere of 5% CO₂, 1%O₂ and 94% N₂ (for L87 and HUH7 cell lines a culture atmosphere of 5% CO₂, 2.5%O₂ and 92.5% N₂), or mimicked by using 50-100µM of CoCl₂. CoCl₂ mimics hypoxia by stabilizing HIF1α, the main mediator of hypoxia (Shweta et al. 2015).

To stimulate cells with thyroid hormones and/or Tetrac for migration, invasion, western blot and qPCR experiments cells were subcultured 1:2 into 6cm² plates with respective culture medium. After 24 hrs the medium was renewed and the hormone and/or Tetrac was added in various concentrations (T3: 1nM, 10nM, 100nM; T4: 10nM, 100nM, 1000nM; Tetrac: 100nM). Primary MSCs were also subcultured 1:2 into 6cm² plates with respective culture medium. After 24 hrs culture medium was changed to medium without thrombocytes and after another 24 hrs stimulation was performed as described above.

Stimulation with CM produced in house was performed by replacing 20% of the respective culture medium with CM. Thyroid hormones, Tetrac and various oxygen conditions were applied in addition as described above.

For western blot experiments, protein was extracted after 14 hrs of culture with stimulants.

For qPCR experiments the cells were incubated 36 hrs with stimulants and then lysated following the PureLink RNA Mini Kit instructions.

For migration or invasion experiments, cells were incubated with stimulants for 24 hrs and then transferred into the migration slides or cocultured with tumor spheroids.

Transiently transfected cells were stimulated 24 hrs after the transfection in a 24-well or 96-well plate without medium change. First various oxygen conditions were added for 24 hrs. The following 24 hrs other stimulants were added in addition as described above.

2.2.1.9. Transient transfection and luciferase reporter assay

To examine function of promoter elements in HUH7 cells and MSCs, the cells were transfected with pGL3-luciferase-reporter constructs carrying a hypoxia responsive promoter or the RANTES/CCL5 promoter (2.1.8.). Renilla reniformis luciferase encoding plasmid (pRL-TK/CMV, Promega) was cotransfected to normalize reporter gene activity with the number of viable cells. Consequently, activity of photinus pyralis luciferase could be related with the activity of renilla luciferase. Both enzyme activities could be determined in the same sample as the enzymes used different substrates. Given account to the fact that transfection experiments can yield differing results all samples were performed in triplets and all experiments were at least repeated three times.

2.2.1.9.1. Transient transfection using electroporation and lipofectamine[®] reagent

For transient transfection by electroporation, L87 and HUH7 cells in the exponential growth phase (70-80% confluency) were detached using Trypsin-EDTA. Subsequently 1.8 Mio cells were suspended in 200µl respective culture medium without any supplements. DNA (4µg reporter, 0.04µg control; ratio 1:100) was added and the mixture was incubated on ice for 10min in a precooled 4mm cuvette. The ratio of reporter plasmid to control plasmid was determined previously in house. Depending how many stimuli were tested more cuvettes were needed. All cuvettes were prepared in one sample. Cells were electroporated at respective voltage (experimentally tested: L87 230V, HUH7 200V) and seeded into cell culture vessels at a density of 32,000 cells/cm². After 4 hrs in normoxic culture, the cells were exposed to desired oxygen conditions or CoCl₂ for 20 hrs. Subsequently, hormone stimulation and/or stimulation with HUH7 conditioned medium was applied for 24 hrs. Experiment was terminated by lysating the cells and performing a luciferase assay.

Lipofectamine[®] transfection was used for in house isolated and immortalized primary MSCs. Cells were seeded into 96-well plates so that on the day of transfection 70-80% confluency (exponential growth phase) was reached. Transfection was performed after manufacturer's protocol on 96 well plates. Final DNA amount per well was 500ng (ratio of reporter to control plasmid 500:1). Final amount of lipofectamine[®] reagent per well was 0.5µl. Transfection was incubated in the normoxic incubator for 4-6 hrs. It was terminated by a medium change to normal respective culture medium. Now cells were incubated either in the hypoxic or normoxic incubator for 14 hrs and then stimulated with thyroid hormones and tumor supernatant as described above in 2.2.1.8. and incubated for another 24 hrs. Then cells were lysated and a luciferase assay was performed.

2.2.1.9.2. Dual Luciferase assay

For analysis of reporter gene activity, the Dual-Luciferase® Reporter Assay was used according to the manufacturer's protocol. After removing the medium and rinsing the cells with 1xPBS, they were lysated with passive lysis buffer (PLB) for 15 min at 350rpm and room temperature on a thermoshaker. While shaking, assay reagents were prepared according to the instructions. Afterwards 20µl of the lysate were analyzed in the luminometer. 20µl PLB were used as empty control.

2.2.1.10. Stable transfection of MSCs

The plasmid of interest was first linearized with appropriate restriction enzymes and then purified with the QIAquick Gel Extraction Kit from QIAGEN after the QIAquick PCR purification protocol.

Cells were subcultured to reach 90% confluency on the day of transfection (ca. 10 Mio cells in a 10cm² plate). For transfection, they were detached as usual and rinsed with PBS twice. Then cells were suspended in 300µl PBS and 30µg linearized plasmid/10 Mio cells were added and the mixture incubated on ice for 10 min. Afterwards cells were transferred into a precooled 4mm cuvette and then electroporated at 960µF and 230V. After another 10 min on ice, cells were transferred into a 6cm² plate with respective culture medium. After 24-48 hrs medium was changed and dead cells were removed. Selection medium was added after cells had recovered from transfection (for pIR-EGFP-SV40: kanamycin 100µg/ml). After one to two weeks, transfection success was evaluated. The SV40 transfected cells were tested under the fluorescence microscope and by FACS analysis for EGFP expression.

2.2.1.11. Mycoplasma test

Mycoplasma are small prokaryotes that need hosts because of their limited biosynthesis capabilities. Frequently they are the reason for cell culture contaminations that can lead to reduced cell proliferation and abnormal gene expression. In order to exclude the possibility of this contamination before experiments cells were tested for mycoplasma on a regular basis with the MykoAlert Mycoplasma Detection Kit. In this assay mycoplasma from cell supernatant incubated for at least 24 hrs were lysated. Released enzymes initiated a bioluminescence reaction including the conversion of ADP to ATP, which could be detected using a luminometer. The ATP ratio allowed conclusions regarding the mycoplasma amount.

2.2.2. Microscopy of cells

Regular cell microscopy was performed with a binocular stereomicroscope SZX90. Fluorescence imaging was performed with an inverted fluorescence microscope at 10-40x magnification.

2.2.3. Microbiology

2.2.3.1. Preparation of agar plates

Agar plates were prepared by heating 3% Agar and mixing it with an equal volume of 2xLB medium. If necessary appropriate antibiotics were added (Ampicillin: 100 µg/ml final concentration; Kanamycin: 50 µg/ml final concentration) and the mixture was dispensed into petri dishes. Finished plates were wrapped in plastic bags and stored at 4°C.

2.2.3.2. Freezing and thawing of bacteria

Bacteria were long-term preserved in glycerol cultures. 900µl of 12 hrs incubated liquid bacteria culture were mixed with 100µl of freezing solution (10x), filled into cryotubes and stored at -80°C. To thaw bacteria a part of the glycerol stock was

scraped off, spread on agar plates and incubated for 24 hrs. Subsequently one colony was picked from the plate and bacteria expanded using liquid culture in LB medium. Plasmid DNA was extracted using the Qiagen MiniPrep as described in 2.2.3.4.

2.2.3.3. Preparation of competent *E.coli* DH5 α

To prepare chemically competent *E. coli* one colony was first picked from an agar plate (see 2.2.3.2.) and incubated in 50ml LB medium over night at 37°C and 250 rpm on a shaker. 4ml of the overnight culture was diluted 1:100 into fresh LB medium and incubated at 37°C and 250 rpm until an OD_{600nm} of 0.375 was reached. After aliquoting the culture into 50ml aliquots that were kept on ice for 5 min, they were centrifuged for 7 min at 1600 rcf (4°C). Bacteria pellet was suspended in 10ml ice cold PBS and the centrifugation step repeated. Subsequently, the pellet was suspended again in 10 ml ice-cold CaCl₂ solution and incubated on ice for 30 min. Following another centrifugation as described, bacteria were suspended in CaCl₂ solution and aliquoted into 250 μ l samples. Subsequently, aliquots were snap frozen in an ethanol/dry ice bath and stored at -80°C. The exposition with calcium ions led to a better transformation capability. Bacteria thus were called “competent”.

For transformation of competent *E. coli* DH5 α bacteria, 1/10 of an entire ligation reaction (ca 50-100ng DNA) were used. After rapidly thawing the bacteria, 50 μ l of suspension were added to the DNA. After incubation on ice for 10 min, bacteria were transformed by heat shock at 42°C for 45 sec and immediately cooled on ice again. The transformed bacteria were suspended in 1 ml LB medium and incubated for 45 min at 37°C and 250 rpm on a thermoshaker. Afterwards the mixture was plated onto agar plates, containing antibiotics for selection of successfully transformed colonies, and incubated over night at 37°C. On the next day, single colonies were picked and transferred into 5ml LB liquid cultures in order to prepare plasmid DNA. They were incubated 12 hrs on a shaker at 37°C.

2.2.3.4. Purification of up to 20 μ g plasmid DNA

DNA was extracted using the Qiagen MiniPrep Kit plasmid according to the manufacturer’s instruction from the cultures prepared in 2.2.3.2. The final elution was performed with 50 μ l injection grade water, which usually yielded a DNA concentration of 300ng/ μ l. A diagnostic restriction digestion followed the purification and preparations were ana-lyzed on a 0.6% or 2% agarose gel. Three successful preparations were chosen to be sequenced and one correctly sequenced sample chosen for further expansion.

2.2.3.5. Purification of up to 10mg plasmid DNA

After validation of the DNA sequence, plasmid DNA was expanded further by picking respective colonies again and incubation a liquid culture of 100ml LB medium for 12hrs on a shaker at 37°C. DNA was isolated and processed using the endofree plasmid maxi kit from Qiagen after the manufacturer’s manual. The elution step was performed with 100-300 μ l injection grade water depending on DNA pellet size. Thus, the process yielded about 200-500 μ g DNA. Preparations were analyzed again on 0.6% or 2% gels and sequenced.

2.2.4. Molecular biology

2.2.4.1. Restriction digestion of DNA

For restricted digestion of DNA using restriction enzymes, one unit of enzyme per μ g DNA was used in combination with the enzyme’s respective buffer. The enzyme

solution did not exceed 1/10 of the mixture based on water. Digests were incubated at appropriate temperature and time on a thermoshaker (37°C, 1 hr).

2.2.4.2. Separation of DNA fragments by agarose gel electrophoresis

Agarose gels, containing between 0.6 and 2% agarose, were used to analyze DNA fragments. Electrophoresis was performed in 0.5xTBE buffer. DNA samples were mixed with 6x agarose gel electrophoresis loading buffer prior to loading into the gel. Additionally, 200-400ng of the size standard were loaded into the gel electrophoresis was performed at approx. 120V (depending on band size and room temperature) until optimal separation (approx. 1 hr). Photos of the gels were taken under UV light for documentation. When separating DNA fragments, desired bands were cut out under UV light. Extraction out of the gel was performed with the QIAquick gel extraction kit from Qiagen after the manufacturer's protocol. The elution step was performed with injection grade water instead of included buffer.

2.2.4.3. Determination of DNA and RNA concentrations

DNA concentrations were measured fluorometrically with the „Qbit Fluorometer” from Invitrogen. The concept of „Quant-IT Technology” is based on a weak fluorescent intercalating color, which was added to a standardized volume of DNA or RNA. When binding to nuclear acids a fluorescent signal was emitted. It was linearly dependent on the amount of DNA or RNA. Through comparison with two standards, DNA concentration could be determined. For DNA concentrations between 0.2 and 100 ng/ml the „Quant-IT dsDNA HS Assay Kit” from Invitrogen was used. For higher concentrations between 2ng/ml to 1000ng/ml the „Quant-IT dsDNA BR Assay Kit” from Invitrogen was used. All steps were performed according to manufacturer's instructions. Measuring of RNA concentrations was performed similarly with the „Quant-iT RNA” assay.

2.2.4.4. Ligation of DNA fragments

Three different reactions were prepared when ligating vector and insert DNA. Two reactions used a molar ratio of 3:1 and 10:1 (insert vector). As control a third reaction only contained vector. The total volume of each reaction was 20µl containing 400 U (~1µl) T4 DNA ligase and 2µl 10x T4 DNA ligase buffer. Ligation was incubated for 1 hr at room temperature.

2.2.4.5. DNA sequencing

Sequencing of plasmid DNA was performed by Entelechon, Bad Abbach through cycle sequencing after the described termination of chain reaction (Sanger et al. 1992). All plasmids used within the scope of this thesis proved to contain the correct sequence.

2.2.4.6. Analysis of gene expression

2.2.4.6.1. Isolation of RNA

Cells cultured and stimulated (2.2.1.8.) in 6cm² plates were lysated using the “PureLink RNA Mini Kit” after the manufacturer's instructions including the optional DNase digestion step. The homogenization step was performed when necessary. RNA was eluted from the columns using 35µl RNase free water and the RNA concentration was determined (2.2.4.3.).

2.2.4.6.2. Reverse transcription

The following mixture (RT_{plus}) was prepared for reverse transcription of RNA into cDNA:

Component	Amount (concentration)
RNA	2µg (0.05µg/µl)
First strand buffer (5x)	8µl (1x)
DTT (0.1M)	2µl (0.5mM)
RNAasin (40U/µl)	1µl (1U/µl)
Acrylamide (15µg/µl)	0.5µl (0.1875µg/µl)
Hexanucleotide (dNTPs, 2µg/µl)	0.43µl (0.0215µg/µl)
Superscript II reverse transcriptase (200U/µl)	0.86µl (4.3U/µl)
RNase free water	Ad 40µl

Table 2: Reaction mixture for reverse transcription of 2µg RNA

As control for contaminations with genomic DNA, a second reaction containing 0.2µg RNA was prepared in which the reverse transcriptase was replaced by RNase free water (RT_{minus} control). The reaction mixtures were incubated for 90 min at 42°C and 350 rpm and subsequently stored at -20°C or used immediately for qPCR.

2.2.4.6.3. Quantitative real-time-PCR (qRT-PCR)

The qRT-PCR determines the amount of amplification products of a specific PCR-reaction. The method is based on fluorescent signals that are caused by amplification of the sample and their detection with laser technology. There are two main concepts; the Taqman method and SYBRgreen assay. For this thesis, both methods were used as explained below.

All assay reagents were designed not to amplify genomic DNA (e.g. intervening introns). All controls, containing H₂O instead of RNA, were negative in the performed experiments as expected.

Taqman method

Taqman assays use primers and a double marked probe that hybridizes to the cDNA. The probe is marked with a fluorescent dye [FAM (6-Carboxyfluorescein) or VIC] and a quencher. Only when primer and probe attached to the cDNA and the Taq polymerase amplified the strand, fluorescent dye and quencher were separated by the 5'-3'-exonucleaseactivity of the polymerase producing a fluorescence signal. This signal could be detected. Sequences of assay primers are listed in 2.1.7. (qPCR, taqman).

Component	Amount (concentration)
cDNA	2µl (1:10 diluted RT _{plus} -sample and undiluted RT _{minus} sample)
Taqman Universal PCR Mastermix	10µl (1x)
Taqman Assay (primer probe mix)	1µl
RNase free water	Ad 20µl

Table 3: Reaction mixture used for qRT-PCR using premixed Taqman assay

A variant of this experiment included separate forward and reverse primers instead of one complete assay. The mixture was prepared as outlined below:

Component	Amount (concentration)
cDNA	2 μ l (1:10 diluted RT _{plus} -sample and undiluted RT _{minus} sample)
SYBRgreen mastermix	10 μ l (1x)
Target	0.4 μ l (100nM)
FW-primer	0.6 μ l (300nM)
RV-primer	0.6 μ l (300nM)
RNase free water	Ad 20 μ l

Table 4: Reaction mixture used for qRT-PCR with separate forward and reverse primers

The components were plated onto 96 well plates with a total volume of 20 μ l per well. For qRT-PCR ABIPrism7000 Sequence detection system and a heat activated Taq-polymerase were used. After an initial incubation for 2 min at 50°C and for 10 min at 95°C samples were cycled 40 times for 15 sec at 95°C and for 60 sec at 60°C. For each sample RT_{plus}, RT_{minus} and NTC (no template control, no cDNA, primer control) in duplicates were examined. Due to the genes of interest being involved in the HIF1 α biology, no GAPDH- or HIF1 α -driven genes were used as reference genes. Therefore, expression of target genes was normalized to ubiquitously expressed reference genes rRNA. For quantification of the PCR product kinetics of the reaction have to be taken into consideration. To do so the threshold cycle was determined for each sample (CT-value). Low CT-value stands for a signal detection in an early cycle and thus for a higher amount of mRNA in the sample, opposite is true for high CT-values. Quality criteria for good PCR reaction were negative NTC controls a difference of 5 cycles in between RT_{plus} and RT_{minus} samples. Amount of the target PCR product was calculated using the reference gene after the following formula: $\Delta CT = CT(\text{target gene}) - CT(\text{reference gene})$. As cDNA doubles each cycle of the exponential phase, values were expressed as $2^{\Delta CT}$. Negative samples were given the value 40, as this was the maximum number of cycles.

SYBRgreen method

SYBRgreen-based detection works if a gene-specific amplicon is generated during the PCR. SYBRgreen causes green fluorescence after intercalation in double stranded DNA at low temperatures. Fluorescence is linearly dependent on the amplification of template DNA. Melting temperatures were analyzed to check the specificity of the amplicons. Increasing of assay temperature from 50 to 95°C lead to dissociation of double stranded DNA and decrease of fluorescence at a specific temperature. This temperature is characteristic for each amplicon as it depends on length and base content. Only wells with a single melting point (fluorescence drop off) at expected temperature were included. Primers are listed in 2.1.7. (qPCR, SYBRgreen).

The components were plated onto 96 well plates with a total volume of 20 μ l per well. After an initial incubation for 10 min at 95°C, samples were cycled 40 times for 15 sec at 95°C and 1 min at 60°C.

For each sample RT_{plus}, RT_{minus} and NTC (no template control, no cDNA, primer control) in duplicates were examined. Due to the genes of interest being involved in the HIF1 α biology no GAPDH- or HIF1 α -driven genes were used as reference genes. Therefore, expression of target genes was normalized to reference gene 18S rRNA. Quantification using CT values was performed as described above. In addition, a one peaked melting curve ensured a specific amplicon product.

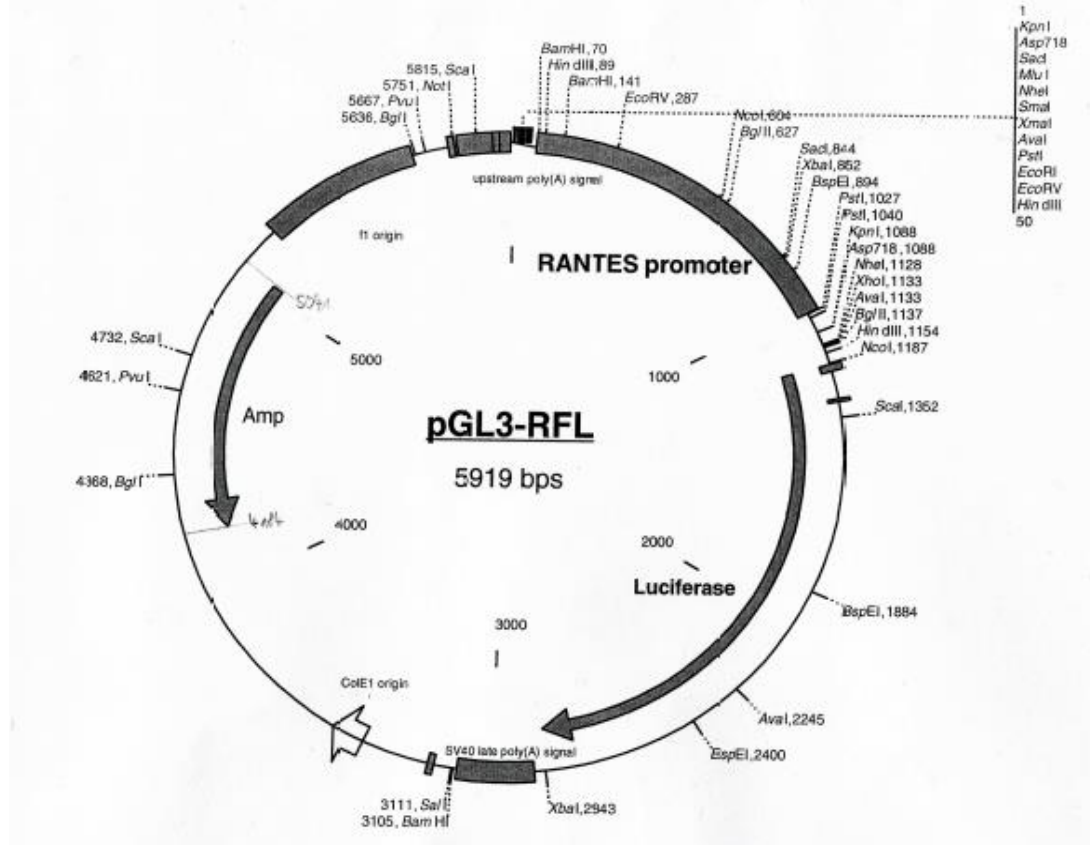
Component	Amount (concentration)
cDNA	2 μ l (1:10 diluted RT _{plus} -sample, undiluted RT _{minus} -sample)
SYBRgreen mastermix	10 μ l (1x)
SYBRgreen FW-primer	0.6 μ l (300nM)
SYBRgreen RV-Primer	0.6 μ l (300nM)
Taq DNA polymerase	0.12 μ l (U/ μ l)
RNase free water	Ad 20 μ l

Table 5: Reaction mixture used for qRT-PCR using SYBRgreen method

2.2.5. Cloning strategies for luciferase reporter constructs

The constructs used to evaluate reporter gene activity were based on the basic pGL3 luciferase reporter vector [by Promega (USA)]. The pGL3 basic vector does not contain eukaryotic promoters or enhancer elements, while the pGL3-SV40 promoter vector contains a minimal SV40 promoter. The pGL3-SV40 vector is used to study enhancer-like activity of cloned sequences. For selection in bacteria, the plasmid contains an ampicillin resistance gene. The RANTES/CCL5 construct was cloned in house by Sabine Fessele (AG Klinische Biochemie, Prof. Nelson) (Fessele 2001). It contains 971 nucleotides of the human RANTES/CCL5 immediate upstream region driving firefly luciferase (Figure 15A). To characterize MSC hypoxia response HIF1 α - responsive elements were inserted in front of the SV40 minimal promoter as well as a blasticidin selection controlled by a CMV promoter downstream from the firefly luciferase to allow stable cell transfection [modification in house by Anna Hagenhoff (AG Klinische Biochemie, Prof. Nelson)]. (Figure 15B)

A)



B)

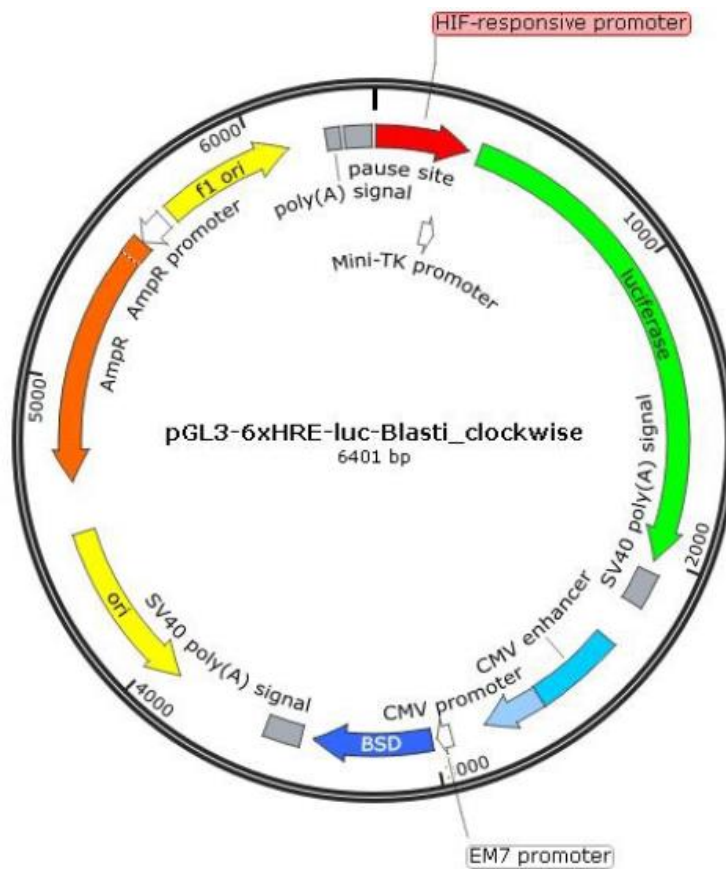


Figure 15: pGL3-based luciferase reporter vectors: A) RANTES/CCL5 promoter (pGL3-RFL) driving firefly luciferase reporter versus B) HIF1 α -responsive promoter (pGL3-6xHRE-luc-Blasti_clockwise) driving firefly luciferase reporter.

2.2.6. Protein biochemical methods

Western blotting was used to determine the intracellular level of HIF1 α protein in MSCs and HUH7 cells under different conditions. As first step, a protocol was established to reach an optimal protein yield. Therefore, different extraction buffers and a time course of different extraction time points were evaluated. Primary cells did not yield enough protein for large-scale analyses. Therefore, preliminary experiments were performed using immortalized MSCs.

2.2.6.1. Protein extraction

Cells were plated into 6cm² culture vessels and incubated with stimulants for 12 hrs as described in 2.2.1.8. Afterwards cells were rinsed with ice-cold PBS and protein extraction was performed using RIPA lysis buffer (2.1.3.1.) to gain a whole cell lysate. For hypoxic samples PBS and RIPA were equilibrated in a hypoxic incubator. Cells were scraped off the plate and the lysate was transferred into 1.5ml tubes on ice where the lysate was incubated for 1 hr and stirred lightly from time to time. Afterwards lysate was centrifuged for 15 min at 16000rpm and 4°C in a refrigerated centrifuge. The supernatant was aliquoted and frozen at -20°C immediately.

In addition to the RIPA lysis buffer, we also tested a buffer separating nuclear from cytosolic proteins (Kumar 2009) and a self-designed buffer based on buffers for HIF protein extraction in different publications (Srinivasan et al. 2011). For separating nuclear and cytosolic proteins cells were washed with ice-cold PBS, collected in buffer A and incubated on ice for 15min. Suspension was centrifuged for 15 min at 2000 rcf and 4°C. The supernatant contained the cytosolic protein fraction. The pellet was suspended in 200 μ l buffer B, incubated on ice for 1 hr and centrifuged at 16000 rcf and 4°C for 15min. Supernatant was aliquoted and immediately frozen at -20°C. The buffer based on Srinivasan et al. served for cell collection as well. Suspension was rotated upside down for 1 hr at 4°C, centrifuged for 10 min at 10000 rcf and the supernatant frozen at -20°C.

After a preliminary experiment comparing all three buffers we decided to carry out all further experiments with the RIPA buffer as described above.

After evaluating different protein extraction buffers a time course from 12 to 72 hrs was performed in order to optimize the best time point for extraction and maximum expression. 12 hrs proved to yield sufficient protein concentrations for analysis. Thus, RIPA buffer and 12 hrs incubation time were used for all further experiments. For normoxic conditions, the cells were incubated in 21% O₂, whereas for hypoxic conditions either incubation in 1% O₂ atmosphere or treatment with 100 μ M CoCl₂ was used for stabilization of HIF1 α .

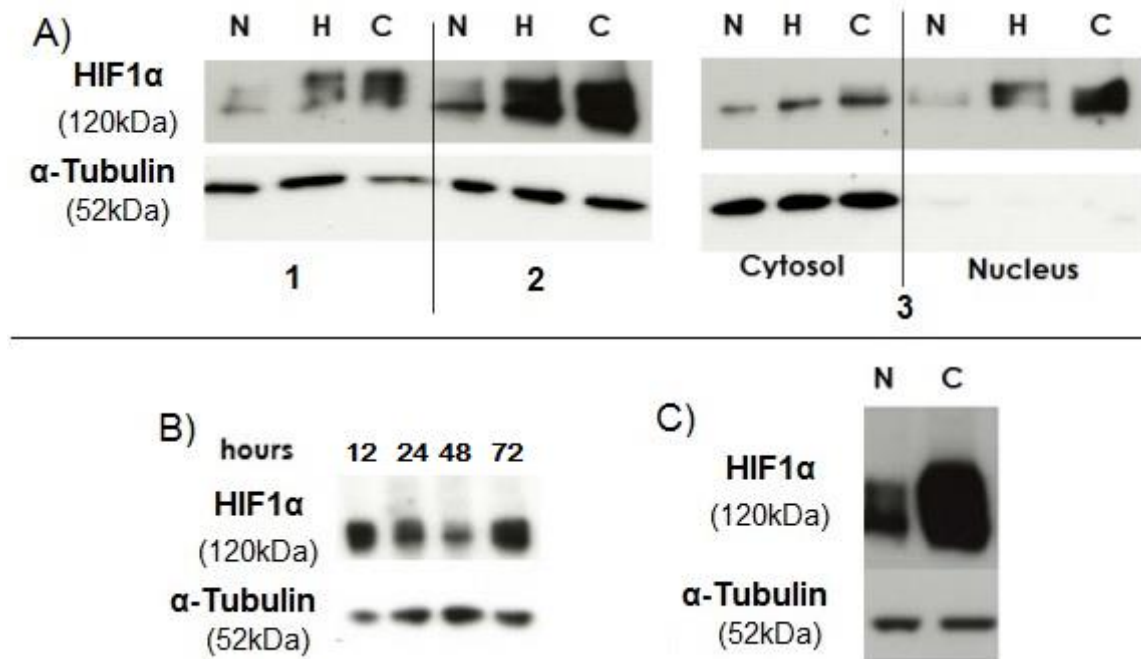


Figure 16: Establishment of western blot conditions for analysis of MSC hypoxia response: N=21%O₂, H=1%O₂, C=100μM CoCl₂. Extracts were run on 6-8% gradient gels under non-denaturing conditions. α-tubulin antibody was used as internal control to ensure equal protein amount in samples. **A) Evaluation of different protein extraction buffers for HIF1α protein:** 1. Self-designed buffer, whole cell lysate 2. RIPA buffer, whole cell lysate 3."Dual buffer", cytosolic and nuclear fraction. Results show increase of HIF1α protein after 12 hrs exposure with 1%O₂ and 100μM CoCl₂ in comparison to normoxic exposure (21%O₂); RIPA buffer proves to be most effective. Extraction with "Dual buffer" shows that HIF1α protein is located in the cytosol as well as the nucleus. **B) Extraction at different time points to find maximum expression of HIF1α:** Protein was extracted using RIPA buffer from cells treated with 100μM CoCl₂ at four different time points: 12, 24, 48 and 72 hrs. 12 hrs proved to be optimal. **C) Optimal assay conditions: HIF1α protein level increases under hypoxic conditions after 12 hrs in MSCs.**

2.2.6.2. BCA-Assay Protein quantification

The measurement of protein content in samples was performed with Pierce™ BCA Protein Assay Kit. This assay from Thermo Scientific™ is a detergent-compatible formulation based on bicinchoninic acid (BCA) for the colorimetric detection and quantification of total protein. This method combines the well-known reduction of Cu²⁺ to Cu⁺ by protein in an alkaline medium (the biuret reaction) with the highly sensitive and selective colorimetric detection of the cuprous cation (Cu⁺) using a unique reagent containing bicinchoninic acid. The purple-coloured reaction product is formed by the chelation of two molecules of BCA with one cuprous ion. This water-soluble complex exhibits a strong absorbance at 562nm that is nearly linearly dependent on increasing protein concentrations over a broad working range (20-2000μg/ml). The BCA method is not a true end-point method; that is, the final colour continues to develop. However, following incubation, the rate of continued colour development is sufficiently slow to allow large numbers of samples to be assayed together.

Protein concentrations generally are determined and reported with reference to standards of a common protein such as bovine serum albumin (BSA). A series of dilutions of known concentration are prepared from the protein and assayed along side the unknown before the concentration of each unknown is determined based on the standard curve. If precise quantification of an unknown protein is required, it is advisable to select a protein standard that is similar in quality to the unknown.

Measurements were performed according to manufacturer's instructions in the Microplate Procedure. This protocol affords the sample handling ease of a microplate and requires a smaller volume (10-25 μ L) of protein sample; however, because the sample to working reagent ratio is 1:8 (v/v), it offers less flexibility in overcoming interfering substance concentrations and obtaining low levels of detection.

2.2.6.3. SDS-Page and western blot

Western blotting was performed as previously described (Towbin et al. 1979).

Reagent	Gel 6%	Gel 8%
H ₂ O	10.6 ml	9.3 ml
30% Acrylamide	4 ml	5.3 ml
Tris-HCl (1.5 M, PH 8.8)	5 ml	5 ml
10% SDS	200 μ l	200 μ l
10% APS (Ammoniumpersulfate)	200 μ l	200 μ l
TEMED (Tetramethylethylenediamine)	20 μ l	20 μ l

Table 6: Recipe for 6-8% resolving gel.

For each sample, an appropriate amount of protein was determined. For normoxic samples 40 μ g, samples from primary MSCs 60 μ g, samples from HUH7 and hypoxic samples 20 μ g. As antibodies typically recognize a small portion of the protein of interest (epitope) and this domain may reside within the 3D conformation of the protein access needs to be enabled by denaturing the protein. To denature, a loading buffer with the anionic denaturing detergent sodium dodecyl sulfate (SDS) was used as described by Laemmli (Laemmli 1970). It was added to corresponding amounts of the different samples and the mixture incubated for 5 min at 95°C in order to reduce and denature samples. For resolving the proteins, a SDS-polyacrylamide gel electrophoresis was performed on a 6% and 8% resolving gel according to the expected sizes of HIF1 α (120kDa) and α -tubulin (52kDa). Resolving gels with a final volume of 20ml were prepared as summarized in Table 6.

Following polymerization, a 5% stacking gel was placed above two layers of resolving gels (6% and 8 %). Gels were stored in humidified atmosphere at 4°C for no longer than one week. Samples were mixed with Laemmli buffer. 0.5-1.5 μ l MagicMark size standard for molecular weight estimation was loaded into one well and subsequently samples were loaded into separate wells. Electrophoresis was performed in electrophoresis buffer at 80V until samples had entered the stacking gel and subsequently at 120V.

Proteins were electro-blotted onto PDVF-membranes in a wet blot with NuPage transfer buffer for 1 hr at 30V. Then the membranes were blocked at least for 1 hr at room temperature or overnight at 4°C with 5% skim milk powder in TBST [0,5 g skim milk powder added to 10 ml TBST (1x TBS + 0,05% (v/v) Tween 20)]. Then membranes were washed three times with water and incubated over night at 4°C on a roller with the Anti-Human HIF-1 α antibody diluted (ratio 1: 1000) in TBST.

On the next day, membranes were washed four times with TBST at room temperature for 10 min. Subsequently membranes were incubated for 1 hr with the second antibody (Polyclonal Rabbit Anti-Mouse Immunoglobulin HRP) diluted (ratio 1:5000) in 5 % skim milk powder in TBST on a roller. Finally, membranes were washed four times with TBST at room temperature for 10 min and then rinsed two times for 5 min with PBS before evaluation using the ECL Kit from Perkin Elmer according to manufacturer's instructions. For developing membranes were trans-

ferred into dark chamber in TBS and immersed in 4ml ECL substrate solution for 1 min. Excess substrate was wiped off and an autoradiography film (Amersham Hyperfilm ECL) was exposed to the membrane. Film was incubated 1 hr for detection of HIF1 α and 10 sec to 5 min for α -Tubulin expression. The film was developed using a developing machine.

2.2.7. Chemotaxis assay

Chemotaxis experiments were performed with the 3D chemotaxis assay from Ibidi using their μ -slide chemotaxis 3D. These slides are a tool used to observe the active movement of cells (chemokinesis) and directed movement towards a chemo attractant (chemotaxis) of cells embedded in 3D gel matrix. The general principle of this experiment is a slide with two large-volume (60 μ l) reservoirs connected by a small gap (=observation area=1000x2000 μ m²). If the two reservoirs contain different chemo attractants or different concentrations of the same chemo attractant, then there is a linear concentration drop inside the gap. Cells placed in the gap are exposed to this gradient.

For 3D experiments as conducted for this thesis, cells were embedded in a collagen gel matrix. The cell number inside the channel was chosen according to the cell's size so that each cell could move freely without touching other cells.

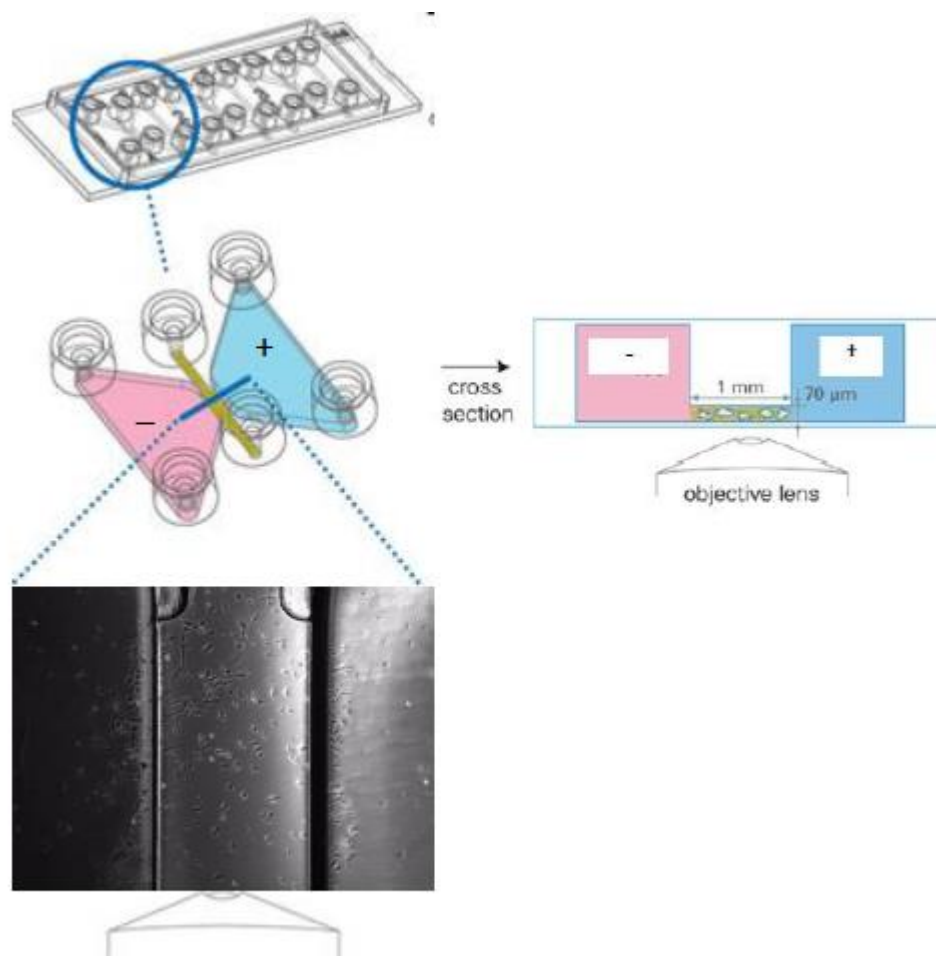


Figure 17: Principle of μ -slide chemotaxis 3D: After stimulation, MSCs in collagen I gel solution were seeded into the observation channel and reservoirs were filled on the left side (*red*) with assay medium and on the right side (*blue*) with HUH7 conditioned medium as chemo attractant. (ibidi GmbH 2012)

2.2.7.1. Chemotaxis assay preparation

The chemotaxis assay was used to examine the MSC response to HUH7 conditioned medium as chemoattractant with or without prior thyroid hormone/Tetrac treatment. In addition, the influence of continuous stimulation with the hormones during the assay was examined. At first, optimal assay conditions were evaluated with the help of Alexandra Wechselberger (MTA, AG Klinische Biochemie, Prof. Peter Nelson). The final choice was a 3D assay with a gel concentration of 1mg/ml and tumor conditioned medium (HUH7 cell line) as chemo attractant. Primary MSCs showed the highest migratory capacities in comparison to immortalized primary or L87 MSCs.

Cells were prestimulated in 6cm² cell culture dishes for 24 hrs as described in 2.2.1.8. For all cell lines, this was conducted in respective growth medium, except for primary MSCs. Here thrombocytes and heparin were removed 24 hrs prior to stimulation. Continuous hormone treatment was performed inside the chemotaxis slide. The μ -slide Chemotaxis 3D was prepared according to manufacturer's instructions (see application note 17+23+26, Ibidi) with the modification that all reagents had to be buffered with 15mM HEPES as recommended alternative for CO₂ fumigation that was not possible while performing the assay. Three different conditions could be examined per slide and four slides could be run at the same time. Assay medium was prepared by adding 1%BSA and 15mM HEPES to DMEM or RPMI medium depending what medium had been used as gel medium. Chemotaxis slide was unpacked, reservoir ports were closed using the plugs provided and afterwards placed inside a wet chamber (15cm cell culture dish with wet tissues). Subsequently, wet chamber, tumor conditioned medium and freshly prepared gel medium were transferred into the cell culture incubator for at least 30 min to ensure gas equilibration to culture atmosphere. For primary MSCs 1mg/ml DMEM gels, for L87 cells 1mg/ml RPMI gels were used:

reagents	manufacturer	final concentration in gel	ingredients
RPMI 10x or DMEM 10x	Sigma R1145 Sigma D2429	1x	} gelmedium
200mM L-Glutamine (30g/l)	Biochrom K0283	RPMI-Gel 0,3g/l DMEM-Gel 0,584g/l	
7,5% NaHCO₃ (75g/l)	GIBCO 25080	RPMI-Gel 2g/l DMEM-Gel 3,7g/l	
1M NaOH	Roth 6771	For pH7,3 $\text{Volume}_{\text{NaOH}} = \text{Volume}_{\text{Collagen}} \times 0.025$	
HEPES	GIBCO 15630	15mM	
Collagen I 5mg/ml	GIBCO A10644-01	1 mg/ml	Collagen

Table 7: Basic recipe for collagen I gel matrix

Stimulated cells were detached and suspended in assay medium at a concentration of 0.6 Mio primary MSCs /ml and for L87 at 0.9 Mio cells/ml.

To prepare a suspension of cells in collagen I gel three parts of gel medium and two parts of collagen were mixed thoroughly by pipetting on ice followed by adding five parts of cell suspension. After thoroughly mixing by pipetting, 6 μ l were put on one side of the observation channel. By aspiration on the other side, the channel was filled. In order to obtain a regular fiber structure the pipetting had to be performed on ice and terminated within 2-3 min, as the formation of collagen fibers is pH- and tem-

perature-dependent. Subsequently, channel ports were closed and reservoir ports opened. After checking the observation channels for air bubbles, cell number and cell distribution the slide was incubated vibration-free for 30min inside the wet chamber in the cell culture incubator in order to let the gel matrix get firm. After channels were checked for homogeneous fiber structure, reservoirs were filled with 65 μ l assay medium on the left and 65 μ l HUH7 conditioned medium on the right. After closing all ports slide was checked again and put into the heated incubation chamber for time-lapse microscopy.

2.2.7.2. Video microscopy

The slide was placed inside a four channel chamber heated to 37°C, under an inverted Leica DMIL microscope with CCD Camera ProgRes®CF. With the ImageJ based MicroManger program, pictures were taken every 12 min over 24 hrs at 50x magnification.

2.2.7.3. Chemotaxis analysis using Image J (plugins: Manual tracking, Chemotaxis tool)

Cells were tracked with the “Manual tracking” plug in from ImageJ. The pixel size (X/Y calibration) was 2.0901 μ m and was determined with a known distance in a Neubauer counting chamber. 20-30 randomly distributed living cells were tracked manually in all 120 pictures. The tracks were analyzed with the ImageJ plug in “Chemotaxis tool” for distance, directionality, velocity. FMI (forward migration index) and distribution (Rayleigh test for vector data) were calculated. Tracks were visualized in a vector plot. Values for each track were exported to Microsoft excel as well as GraphPad Prism and visualized graphically.

2.2.7.4. Chemotactic and chemokinetic parameters

Chemotaxis is the directed movement of cells toward a certain stimulus, whereas chemokinesis is characterized by distance traveled and velocity. I analyzed the chemotactic and chemokinetic response of MSCs to thyroid hormone treatment. MSC migration can be characterized by the following parameters:

- *Chemokinesis:*
 - *Accumulated and Euclidean distance:* The accumulated distance displays the length of the cell's actual path in μ m and considers all direction changes. Opposed to that, the euclidean distance (in μ m) only displays the net distance between the cell's starting and end point.
 - *Velocity* is the quotient of time and travelled distance in μ m/min.
 - *Directionality* describes the directness of the cell trajectories. It is however not taking into account the direction of the cell's movement. It can be calculated by dividing euclidean through accumulated distance. A directionality of $D = 1$ equals a straight-line migration from start to endpoint regardless of the direction.
- *Chemotaxis:*
 - *Forward migration index (FMI)* represents the efficiency of the forward migration of the cells in relation to the chemical gradient (x or y-axis depending on experimental set up). The larger the index on one axis the stronger the chemotactic effect on this axis. In some experiments, the x-axis lies perpendicular to the chemotactic gradient; whereas the y-axis lies parallel to the gradient for other experiments so that the distribution is vice versa. Therefore, the ratio of the cell's net distance travelled along the x/y-axis to the cell's accumulated distance is of interest. A positive FMI means a movement toward higher concentrations of chemo attractant; a negative FMI

means a movement toward lower concentrations of chemo attractant. This means the shorter the accumulated distance in relation to the axis endpoint the more straight forward the cell's pathway and the higher the FMI value.

- *Center of mass (CoM)* describes the averaged movement of all cells from the starting point. It is also a general indicator if the movement tends to be toward higher chemo attractant concentrations, lower or neutral.
- *Rayleigh test for vector data* can be performed with the Image J plugin Chemotaxis and Migration. It is a statistical test of the uniformity of a circular distribution of points. The null hypothesis (uniformity) is rejected with p-values smaller than $p=0.05$. The test for vector data also takes into account the distance from origin, when creating an analysis. (2.2.10.1.)

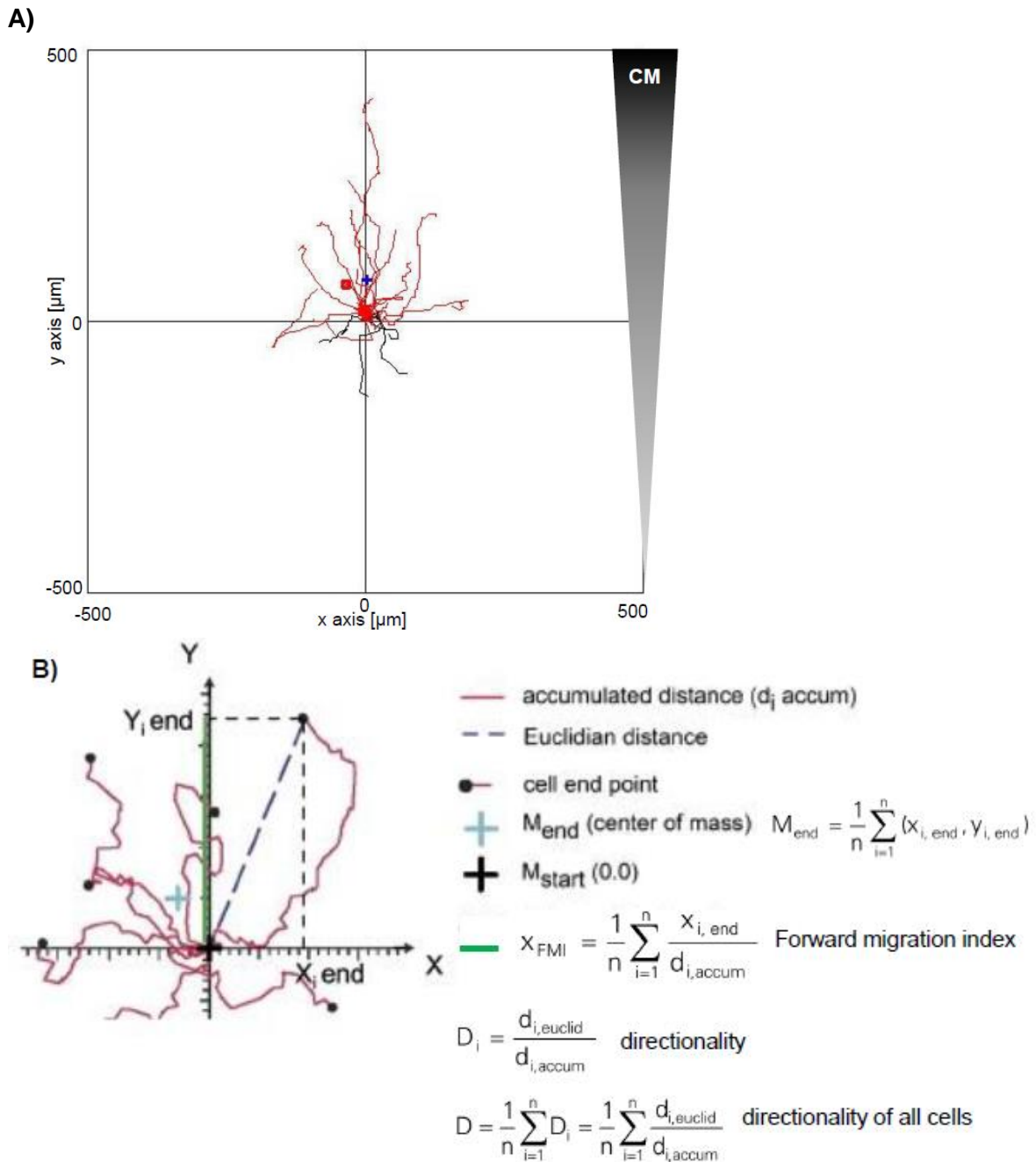


Figure 18: Parameters for evaluation of MSC migration: A) Trajectory plot example: Chemoattractant gradient from lower to upper reservoir (CM). Red lines indicate movement toward the chemoattractant; black lines indicate movements away from chemoattractant. Blue cross indicates the center of mass (CoM). **B) Chemotactic and chemokinetic parameters:** *Accumulated distance* represents the cell's complete pathway, while *euclidean distance* represents the distance between cell's starting point and destination. *Directionality* is the ratio of euclidean distance to accumulated distance. The *forward migration index in y-direction* (y-FMI) indicates movement along the chemical gradient. It is the quotient of the cells net distance travelled in y-direction and the accumulated distance summarized for all cells. *The displacement of center of mass* (M_{end}) calculates the averaged end point of all cell endpoints by subtracting the starting from the end coordinates. Not shown: *Velocity* is the distance travelled over time.

2.2.8. Tumor spheroid model

The tumor spheroid model was established in collaboration with Alexandra Wechselberger (MTA, AG Klinische Biochemie, Prof. Nelson), Anna Hagenhoff (AG Klinische Biochemie, Prof. Nelson) and Svenja Rühlend (bioimaging Zentrum, Prof. Dr. Uhl and AG Klinische Biochemie, Prof. Nelson). After preliminary experiments, shown in this thesis, the method was developed further to a quantifiable MSC invasion assay (Ruhland et al. 2015). Tumor spheroid models are a sufficient means to mimic *in vivo* tumor biology *in vitro*. Especially aspects of intervascular tumor microenvironments as well as tumor growth and physiology can be easily examined in this well manageable model.

2.2.8.1. Spheroid formation

Many tumor cells tend to attach to each other when lacking the possibility to grow in monolayers. Cell attachment was inhibited by coating the culture flasks and dishes with polyHEMA (poly-2-hydroxyethyl methacrylate). They were covered with 2% polyHEMA in 95% Ethanol and allowed to dry completely. This step was repeated once to create an even layer. To obtain hepatocellular carcinoma (HCC) spheroids, HUH7 cells were cultivated in polyHEMA-coated dishes at 37°C and 5% CO₂. After seven to ten days, spheroids had grown to an appropriate size of 200 to 500µm. At this size, spheroids began to show central necrosis. To ensure uniform size spheroids were filtered through a nylon filter with 300µm and 400µm pores. The experiment was conducted likewise for HT29 cells.

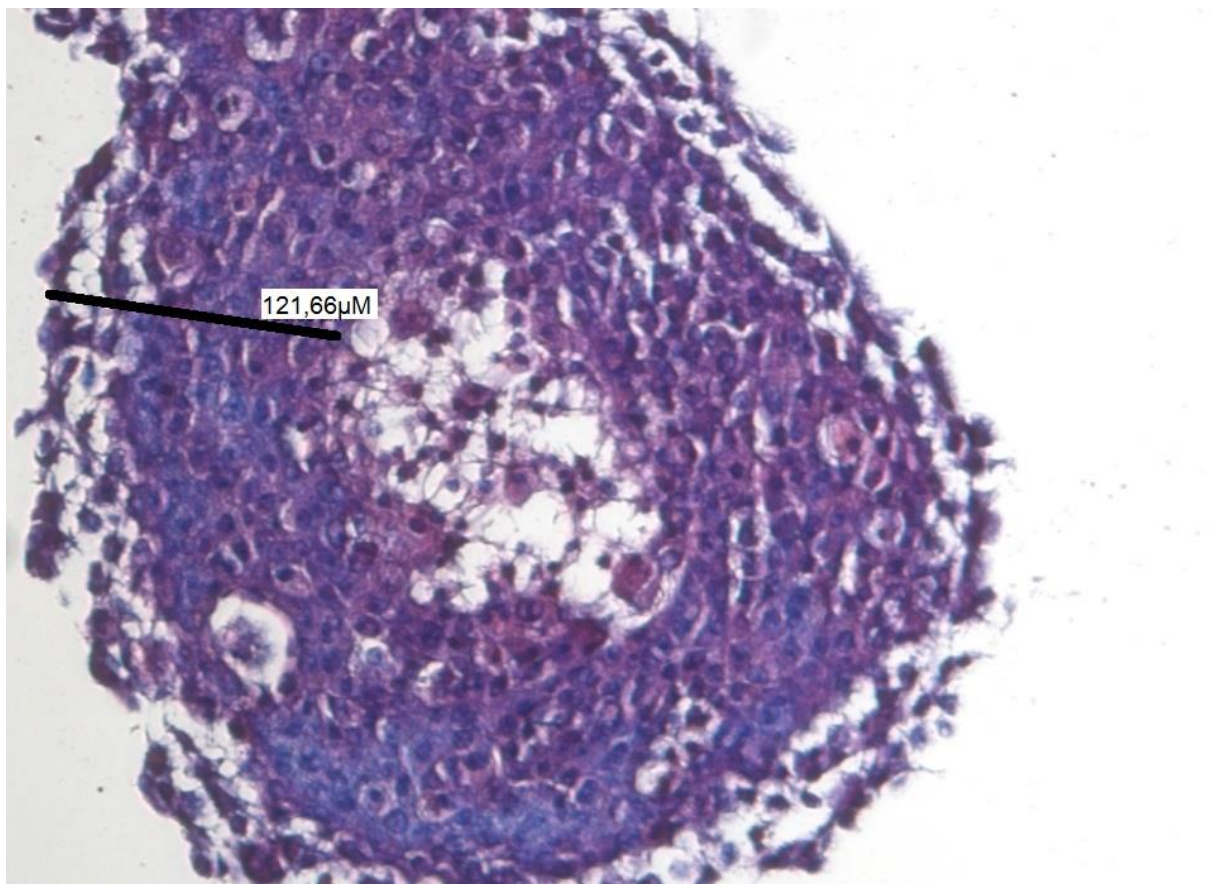


Figure 19: Example of 5-day-old HUH7 tumor spheroid *in vitro*: HE stained, formalin fixed 16µm frozen section of one HUH7 tumor spheroid measuring approximately 300µm in diameter. The spheroid center shows fewer, condensed nuclei that lie further apart depicting necrosis whereas highly proliferating outer layers show tightly packed nuclei.

2.2.8.2. Frozen section of HUH7 tumor spheroids

Spheroids were transferred to cryomoulds and embedded in TissueTek OCT mounting medium (Sakura). They were shock-frozen on dry ice and stored at -20°C. Frozen section was performed with refrigerated microtome Cryostat Jung CM 3000 at -20°C. Serial section into 16µm layers was performed on each spheroid. Complete samples were placed on Superfrost™ Plus microscope slides and were allowed to dry for app. 1 min at room temperature.

2.2.8.3. HE staining of HUH7 tumor spheroids

Before HE staining, sections were fixed in formalin for 10 min and afterwards rinsed with PBS. Haematoxylin stains acidic structures e.g. nuclei with DNA blue. Eosin stains acidophil structures in cytoplasm red. Sections were placed in hematoxylin solution for 3 min and afterwards rinsed with tap water for 5 min. The slide was placed in eosin solution for 20 sec and then dehydrated using ethanol baths with increasing alcohol concentration (70%, 96%, 100%) and xylol. Mounting medium was applied and cover glass placed on top. Samples were examined with inverted fluorescence microscope DMIL.

2.2.8.4. Staining of necrotic and hypoxic areas in HUH7 and HT29 tumor spheroids

To visualize hypoxic and necrotic areas of *in vitro* tumor spheroids, further stainings were performed. Hoechst 33342 is a cell permeable nucleic acid stain, which binds especially to adenine-thymine-rich regions of DNA in living cells. Thus, living cells show blue color in fluorescence microscopy. PI is a membrane impermeant, intercalator dye suitable for fluorescence microscopy. It can only penetrate the cell membrane of dead cells, which appear red in fluorescence microscopy.

For visualization of necrosis a live/dead staining with both chemicals was performed. 19-day-old HUH7 spheroids were cultured for 24 hrs with 1µg/ml Hoechst 33342 and 10µg/ml PI in the cell culture incubator in respective culture medium 2. Afterwards spheroids were examined with inverted fluorescence microscope DMIL.

The stain for hypoxia was performed using the Hypoxyprobe™-1 Kit. The chemical pimonidazole is activated in hypoxic cells and forms stable adducts with thiol groups in proteins. The antibody MAb1 (mouse IgG1 monoclonal antibody) contained in the kit binds to these adducts allowing their detection by immunochemical means. This method allows accurate measurement of oxygen gradients at the cellular level. DAPI binds especially to AT-rich regions of DNA staining cell nuclei with blue fluorescence. Seven-days-old HUH7 tumor spheroids were cultured with 100µM pimonidazole for 24hrs. Serial section was performed as described in 2.2.8.2. Sections were fixed in formalin for 20 min. After three rinses with PBS they were permeabilized for 10 min with 0.5% Triton X100 and blocked with 5% donkey serum in PBS for 1 hr at RT. Afterwards samples were incubated over night at 4°C with MAb1 (1µg/µl) in 0.1% donkey serum-0.1%Tween20-PBS. After three 5 min-rinses with PBS secondary anti mouse antibody conjugated with AF594 from Jackson Immunoresearch (715-585-151) was applied (7.5µg/µl) in PBS with 0.1% donkey serum. Subsequently, nuclei were stained blue with 200ng/ml DAPI in PBS for 10 min and finally slides rinsed with PBS three times for 5 min. Slides were covered with mounting medium consisting of 0.2% NPG, 50% glycerol and PBS and examined with inverted fluorescence microscope DMIL.

As this stain did not work in HUH7 tumor spheroids, possibly due to inadequate uptake of pimonidazole, it was performed in 20-day-old HT29 tumor spheroids.

2.2.8.5. CMFDA staining of MSCs

MSCs were grown to 70-90% confluency in 6cm² cell culture dishes. After rinsing them once with PBS, they were incubated with DMEM and 1µM CMFDA for 30 min at 37°C and 5% CO₂ for dye uptake. Subsequently, dye was removed and MSCs incubated in DMEM with 10% sFCS for another 30 min to allow conversion of the dye to fluorescence product. Afterwards cells were detached using Trypsin-EDTA.

2.2.8.6. Invasion of CMFDA stained MSCs

A single spheroid was rotated horizontally in 50µl culture medium containing 2.5x10⁴ stained MSCs at 36rpm for 2 hrs. To wash away redundant MSCs the spheroid was rinsed three times with 0.5ml culture medium. For further culture, spheroids were transferred into a polyHEMA coated 96well plate with 100µl culture medium. After 24hrs spheroids were fixed in 4% formalin for 2 hrs at room temperature and subsequently rinsed once with PBS.

Frozen serial section was performed and TissueTek OCT was removed by washing in PBS for 5 min at RT. For nuclei staining 200ng/ml DAPI were added to the mounting medium consisting of PBS with 50% glycerol and 0.2% propyl gallate. Samples were examined with inverted fluorescence microscope DMIL.

2.2.9. MTT-Assay

Cell proliferation was evaluated using the MTT-Assay as previously described (Mosmann 1983). With this assay, thyroid hormones, different oxygen conditions and HUH7 cell supernatant were tested for influence on MSC growth rate. The underlying principle is an indirect approach using a chromogenic indicator in this particular case the conversion of water soluble MTT ((3-(4,5-dimethylthiazol-2yl)-2,5-diphenyl-tetrazolium bromide) to insoluble formazan by living cells. Solubilized formazan can be detected at 570nm. The chromogenic signal is linearly dependent on the cell number allowing exacting evaluation of growth rates.

Cells were subcultured in 96 well plates at a ratio allowing the cells to reach 100% confluence on the last day of the assay. All values were evaluated in triplets. Acidified isopropyl was prepared by adding 1N HCl to Isopropyl at a ratio of 1:24. MTT-solution was prepared by adding 50ml of RPMI without phenol red to 250mg of MTT powder and sterile filtrating the solution through a 0.22µm filter. To start the assay supernatant of adherent cells was removed and 50µl of MTT solution added per well. Cells were incubated for 3 hrs at 37°C and 5% CO₂. Subsequently plates were centrifuged for 5 min at 750rcf (ca 2000 rpm), supernatant was removed and 100µl acidified isopropyl were added per well. After solubilization of the color crystals, emission was measured with an ELISA plate reader at 570nm (reference 690nm). If growth rate was evaluated over several days, different plates for each time point had to be prepared.

2.2.10. Statistical analysis

Statistical analysis was performed with Graph Pad Prim 6. Results were analyzed with two-tailed Student's t-test. Unless stated differently means and standard deviation (SD) are reported for n ≥ 3 independent experiments. For qPCR experiments mean fold change is reported. P-values < 0.05 were considered as significant (p<0.05 *, p<0.01 **, p<0.001***, p<0.0001****).

For the chemotaxis assay, Rayleigh Test for vector data was performed in addition with Image J Plugin chemotaxis tool.

2.2.10.1. Rayleigh test for vector data

The p-value calculated by Rayleigh-test for vector data describes the distribution of all tracked endpoints in the chamber. It is a statistical test for the uniformity of a circular distribution of points (cell endpoints). With p-values above 0.05, the null hypothesis (= uniformity) is rejected. Like all statistical tests, it strongly depends on the number of cells being analyzed. It was originally designed to describe circular distributions of data points. The calculated p-value (significance) describes if the cells are rather homogeneously ($p > 0.05$) or inhomogeneously ($p < 0.05$) distributed in the trajectory plot. This parameter also describes the cell's chemotactic response. After a directed migration, cells are distributed rather inhomogeneously, more toward the side of the chemo attractant. The exact calculation can be found in a publication by Moore from 1980 (Moore 1980).

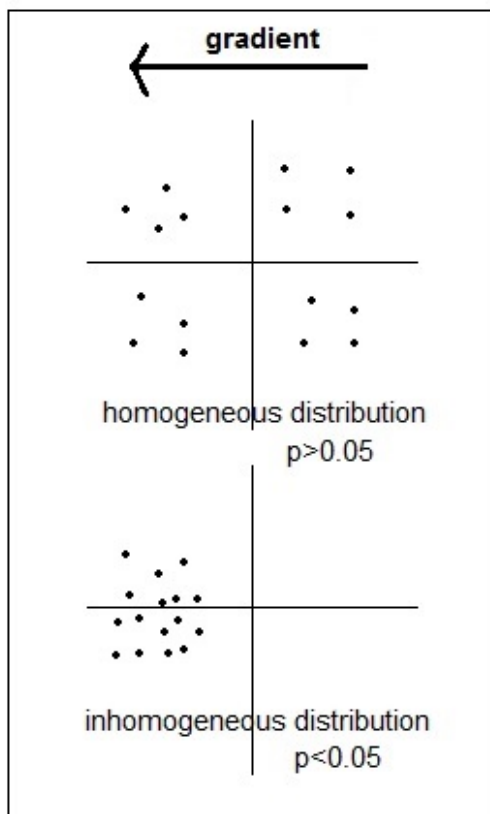


Figure 20: Explanation of p-values in Rayleigh-test: P-value < 0.05 means cells are distributed inhomogeneously, p-value > 0.05 means cells are distributed homogeneously.

3. Results

3.1. Synthetic HIF1 α -responsive promoter in MSC-based gene-therapy of solid cancers

3.1.1. Utilizing the hypoxia response system in MSCs

As detailed in 1.3., the goal of this doctoral thesis was to evaluate a potential new means of targeting transgene MSCs within tumor settings by making use of the hypoxia response system. The first step was to characterize the influence of different oxygen levels on HIF1 α protein expression in MSCs (3.1.2.). Subsequently, HIF1 α -dependent reporter gene activation in MSCs was studied. In parallel, the potential activation of HIF1 α -responsive elements within human RANTES/CCL5 gene promoter, the promoter currently used in the suicide gene system under clinical trial, was assessed. (3.1.3.)

As a next step, cell viability, hypoxia and necrosis were characterized in a HCC tumor spheroid model. The final step was an evaluation of the invasion of engineered MSCs into the spheroid model, and the subsequent activation of HIF1 α -driven reporter genes.

3.1.2. HIF1 α protein level in MSCs increases under hypoxic conditions

Western blot experiments were used to measure HIF1 α protein levels in MSCs under various oxygen conditions. This was performed to characterize the MSC response to hypoxia. As a first step, protein extraction conditions were optimized as described in 2.2.6.1. RIPA buffer was eventually found to work well and was used to extract protein from MSCs after 12 hrs of normoxic (21% O₂) or hypoxic (1% O₂ or 100 μ M CoCl₂) stimulation. Results showed an increase of intracellular HIF1 α protein under hypoxic conditions, in comparison to incubation with 21% O₂ thus providing a baseline for further experiments.

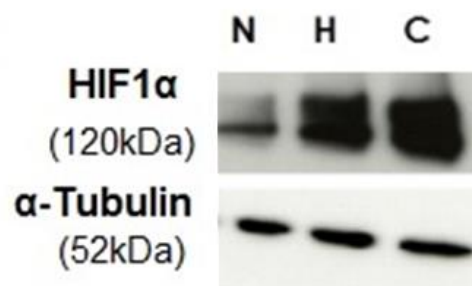


Figure 21: Increased intracellular HIF1 α protein level under hypoxic conditions in MSCs after 12 hrs: Whole cell protein extracts (RIPA extraction buffer) from MSCs, incubated in respective culture medium with 21%O₂ (N), 1%O₂ (H) or 100 μ M CoCl₂ (C) for 12 hrs, were run on 6-8% gradient gels under non denaturing conditions. α -tubulin antibody was used as internal control to ensure equal protein amounts in samples. HIF1 α protein level was significantly increased after 12 hrs incubation in hypoxia in comparison to normoxic incubation. *The results are representative of three independent experiments.*

3.1.3. Hypoxic activation of synthetic HIF1 α -responsive promoter and its comparison to the human RANTES/CCL5 gene promoter

As shown above, MSCs exhibit a stably inducible response to hypoxia. Most solid tumors, such as HCC, contain hypoxic areas of reduced cell viability due to tumor growth outpacing vascularization (Gammon et al. 2013). We sought to determine, if the hypoxic response could potentially be used for tumor-specific transgene MSC-

based therapy by using synthetic HIF1 α -responsive promoters to drive effector gene transcription.

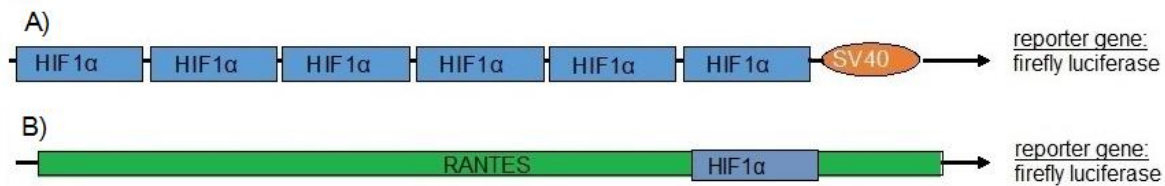


Figure 22: Principle of promoter induced reporter gene activity: A synthetic promoter (A) consisting of six HIF1 α -responsive elements (blue) linked to a SV40 minimal promoter (orange) was used to drive firefly luciferase as reporter gene. Its activation was compared to human RANTES/CCL5 gene promoter [(B), (green)] containing HIF1 α -responsive elements (blue) driving firefly luciferase.

Immortalized primary MSCs were transiently transfected with a reporter construct based on a pGL3 luciferase reporter vector. This plasmid contained a synthetic HIF1 α -responsive promoter driving the firefly luciferase and a blasticidin selection gene [modification in house by Anna Hagenhoff (AG Klinische Biochemie, Prof. Nelson)]. Transfection was performed chemically using lipofectamine transfection reagent. Cells were exposed to 1% O₂ or 100 μ M CoCl₂ for 48 hrs after transfection. Luciferase assays were then used to quantify the potential activation of the transgene. MSCs showed efficient induction of firefly luciferase driven by the HIF1 α -responsive promoter (Figure 23) under hypoxic conditions in comparison to 21% O₂. Repeating the experiment and replacing 20% of the respective culture medium during hypoxic incubation with HUH7 tumor cell conditioned medium (CM) provoked no further induction of reporter gene activity.

Suicide gene therapy using human RANTES/CCL5 gene promoter activated transgene expression has advanced to clinical trials. The potential response of the human RANTES/CCL5 gene promoter to hypoxia was unknown. Human RANTES/CCL5 gene promoter controlled reporter gene constructs were then examined with regards to their activation by hypoxia. This promoter has been reported to contain potential HIF1 α -responsive elements (Yeligar et al. 2009), but to date no data is available showing that these elements are functional under hypoxic conditions. The construct used was based on a pGL3 luciferase reporter vector with 971 nucleotides of the human RANTES/CCL5 immediate upstream region driving firefly luciferase [established in house by Sabine Fessele (AG Klinische Biochemie, Prof. Nelson)]. The plasmid was transiently transfected into immortalized primary MSCs using Lipofectamine transfection reagent, followed by exposure to 1% O₂ for 48 hrs. The results showed that the human RANTES/CCL5 promoter could not be induced by hypoxia-like conditions and thus tumor hypoxia is probably not efficiently targeted by the current RANTES/CCL5-driven gene therapy. For more detailed information about the constructs, please see 2.2.5.

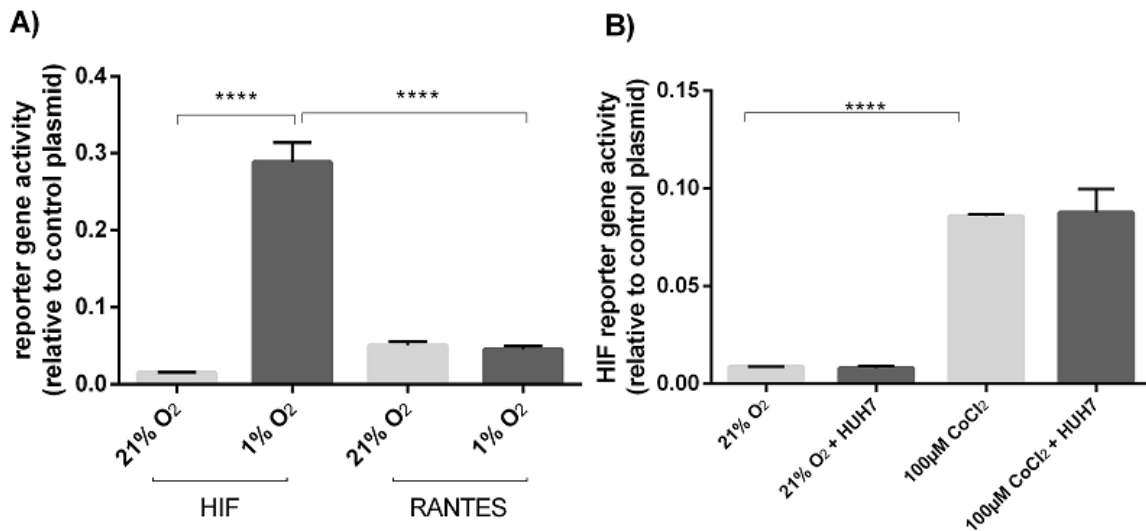


Figure 23: Significant induction of HIF1 α -responsive promoter in MSCs after 48 hrs of hypoxic exposure, with and without additional exposure to HUH7 conditioned medium (CM). No induction of RANTES/CCL5 promoter driven luciferase in hypoxia after 48 hrs: A) Significant ($p < 0.0001$) induction of HIF1 α -responsive promoter driven luciferase activity in transfected MSCs incubated with 1% O₂ for 48 hrs, in comparison to incubation with 21% O₂ for 48 hrs. No induction of RANTES/CCL5-driven luciferase activity under the same conditions. **B)** Significant ($p < 0.001$) induction of HIF1 α -responsive promoter driven luciferase activity in transfected MSCs exposed to 100 μ M CoCl₂ for 48 hrs with and without 20% CM in comparison to MSCs exposed to 21% O₂ for 48hrs. *Experiment performed in triplicates, repeated three times; statistics calculated with two-tailed Student's t-test, reported as mean \pm SD, $p < 0.05$ *, $p < 0.01$ **, $p < 0.001$ ***, $p < 0.0001$ ****.*

3.1.4. Hypoxia in HUH7 and HT29 tumor spheroids

After establishing a reporter gene assay to model the MSC response to hypoxia, the next step was to perform similar assays using experimental tumor spheroids. To this end, a HUH7 (HCC derived) tumor spheroid model was developed. By preventing the adherence of HUH7 cells in polyHEMA coated culture dishes the cells form spheroids of approximately 300-500 μ m diameter after five to seven days of culture. The spheroids were then characterized by fluorescent staining. Necrotic areas were visualized using a live/dead staining. Hoechst 33342 is a cell permeable nucleic acid stain, which stains DNA of living cells with blue fluorescence. PI is a membrane impermeant, intercalator dye, which can only penetrate the cell membrane of dead cells. It exhibits red fluorescence. Results show a red fluorescent center in HUH7 tumor spheroids showing a minimum diameter of 300 μ m. Smaller spheroids contain single dead (red) cells but no necrotic center.

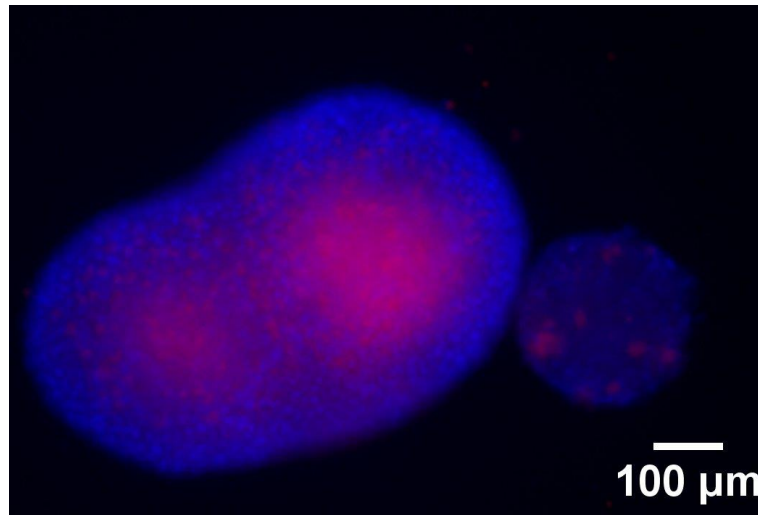


Figure 24: Necrotic center of 19-day-old HUH7 tumor spheroid: Inverted fluorescence microscopy of approximately 500 μ m large HCC tumor spheroid with living cells stained blue (Hoechst 33342) and dead cells stained red (PI). Center of HUH7 spheroid appears necrotic in spheroids at least 300 μ m in diameter.

The second step was to establish an immunochemical method to make hypoxia visible. HydroxyprobeTM-1Kit (red) was used in combination with DAPI (blue) staining of nuclei. Cells take up Pimonidazole, which is added to the culture medium. In hypoxic cells it forms stable adducts with thiol groups in proteins. The antibody MAb1 (mouse IgG1 monoclonal antibody) binds to these adducts allowing their detection by immunofluorescence. This way the oxygen gradient at the cellular level can be made visible. Though several attempts were made, hypoxia staining was problematic in HUH7 cells probably due to cell specific enzymes that metabolized pimonidazole. Therefore, hypoxia was evaluated in another *in vitro* tumor spheroid system established in house showing a similar growth type. Nineteen-day-old, 500 μ m large HT29 cell spheroids (derived from colorectal adenocarcinoma) showed tightly packed proliferating outer layers. Due to reduced proliferation, nuclei were less densely packed deeper into the spheroid. The red fluorescence showed a gradient of hypoxia increasing the closer the center of the spheroid. The center of the spheroid showed no red fluorescence, as the staining process did not work in necrotic cells. DAPI staining confirmed necrosis showing condensed nuclei of dead cells in the spheroid center surrounded by the red, hypoxic belt.

The results correlate with published data about centrifugally spreading necrosis in HCC and HT29 tumor spheroids with simultaneously occurring hypoxia (Waleh et al. 1995, Lee et al. 2015, Pomo et al. 2016). The established visualization of hypoxic and necrotic areas in HUH7 and HT29 tumor spheroids was subsequently used to correlate the distribution and transgene expression of MSCs within these areas.

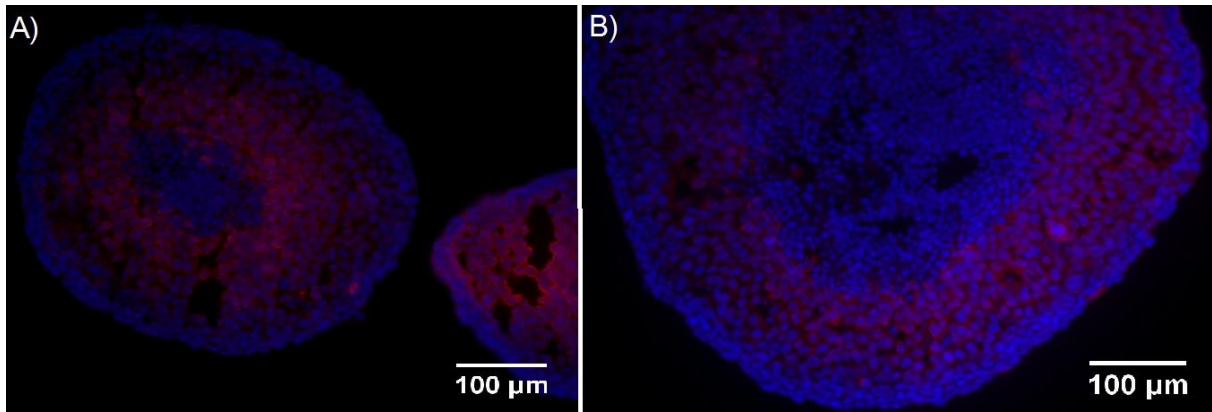


Figure 25: Hypoxic belt around the necrotic center of HT29 tumor spheroids: Inverted fluorescence microscopy of 16µm, formalin fixed frozen sections, of approximately 500µM **(A)** and approximately 700µM **(B)** large colorectal adenocarcinoma tumor spheroids. Nuclei stained blue (DAPI), hypoxic cells stained red (Pimonidazole). Spheroid shows proliferation in outer layers with tightly packed nuclei. When proliferation slows down in inner layers cells start becoming hypoxic. Hypoxia increases centripetally toward the necrotic center. The center consists of necrotic cells (condensed nuclei) due to oxygen lack.

3.1.5. MSCs show a strong tropism for the center of HUH7 tumor spheroids

As a next question, we determined if HIF-engineered MSCs were capable of invading tumor spheroids and if they would then activate the HIF1 α -responsive promoter as they entered the hypoxic core of the experimental tumor. To answer these questions CMFDA stained MSCs were incubated with eight-days-old 300µM large HUH7 tumor spheroids. The results showed MSC invasion into the center of the spheroids matching the area characterized as hypoxic and necrotic.

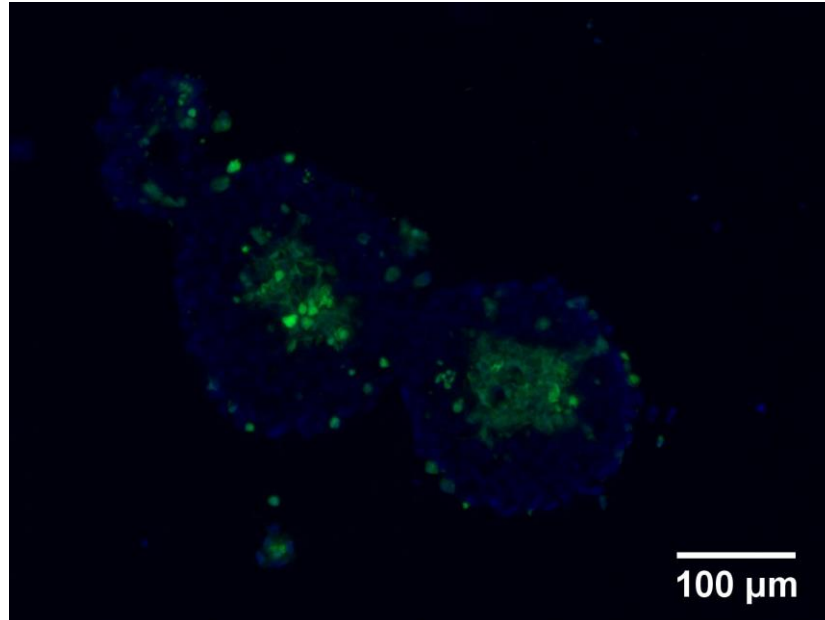


Figure 26: CMFDA stained MSCs show strong tropism for HUH7 tumor spheroid center: Inverted fluorescence microscopy of 16µm frozen sections of eight-days-old HUH7 tumor spheroids (nuclei stained blue with DAPI) incubated with CMFDA-stained MSCs (green). MSCs show invasion into the center of the HUH7 tumor spheroid. This location matches the areas characterized as necrotic and hypoxic in 3.1.4.

In a parallel set of experiments, an additional HIF1 α reporter construct [established in house by Anna Hagenhoff (AG Klinische Biochemie, Prof. Nelson)] was used to examine the activation of the hypoxia responsive promoter inside the experimental tumor microenvironment. The plasmid comprises the HIF1 α -responsive promoter dri-

ving red fluorescent protein. A pilot experiment by Anna Hagenhoff (AG Klinische Biochemie, Prof. Nelson) showed activation of the RFP inside the hypoxic/necrotic center. (data not shown)

In summary, MSCs showed clear tropism for HUH7 spheroid and invasion into its necrotic and hypoxic center. HIF1 α -responsive promoter is activated inside the tumor spheroid setting; however, gene activation within this setting needs to be evaluated further.

3.2. Unresponsiveness of the HUH7 tumor cell line to non-genomic thyroid hormone effects.

The HCC cell line HUH7 does not express integrin $\alpha\beta$ 3 (Schmohl et al. 2015). Therefore, it should be possible to eliminate integrin $\alpha\beta$ 3-mediated effects on the tumor. Using western blots and a luciferase reporter gene activity assay genomic (nuclear) effects of thyroid hormones on HUH7 cells were evaluated.

HIF1 α protein levels were evaluated under different oxygen conditions using western blot. A stable response of HUH7 cells to hypoxia after incubation with 2.5% O₂ or 100 μ M CoCl₂ for 24 hrs was seen. Thyroid hormones (100nM T3, 1000nM T4) did not alter this response.

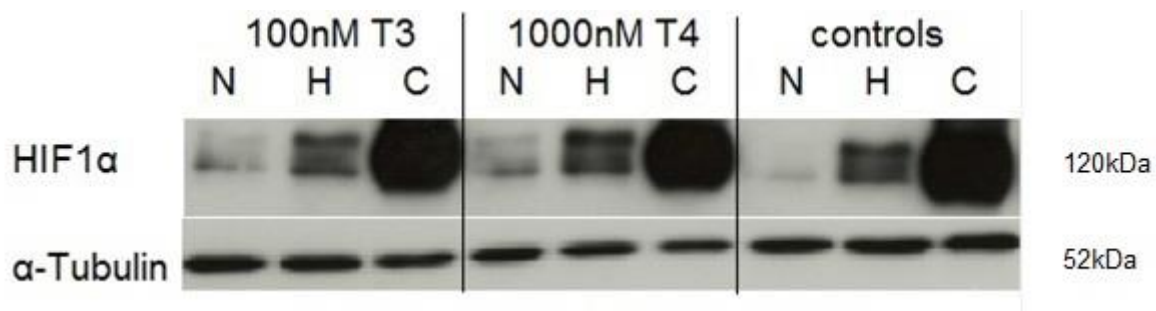


Figure 27: HIF1 α western blot in HUH7 cells shows no effect of thyroid hormone treatment on HIF1 α protein levels under different oxygen conditions: After 24 hrs incubation with 21% O₂ (N), 2.5% O₂ (H) or 100 μ M CoCl₂ (C) with 100nM T3, 1000nM T4 or without thyroid hormone, proteins were extracted using RIPA buffer. Western blots showed a stable response of HUH7 cells to hypoxia after incubation with 2.5% O₂ (H) or 100 μ M CoCl₂ (C) for 24 hrs. Thyroid hormones could not alter this response. *The results are representative of three independent experiments.*

Furthermore, thyroid hormone treatment did not influence HIF1 α -dependent reporter gene activation in HUH7 cells. The reporter construct was transiently transfected by electroporation. After incubation in either 21% or 2.5% O₂ with simultaneous thyroid hormone treatment (1-100nM T3; 10-1000nM T4), reporter gene activity was measured using a luciferase reporter assay. 2.5% O₂ were chosen as this was the lowest oxygen concentration tolerated by HUH7 cells. Hypoxia induced a significant reporter gene activation (p=0.009). Thyroid hormones did not alter reporter gene activity under normoxic or hypoxic conditions. No significant changes in HUH7 biology could be detected.

The results of these experiments show that the HUH7 cell line is unresponsive to integrin $\alpha\beta$ 3-mediated thyroid hormone effects and specifically, the hypoxia response system is not affected. This makes HCC the optimal model cancer for evaluation the hypoxia targeted MSC-based gene therapy and non-genomic thyroid hormone effects on this therapeutic approach.

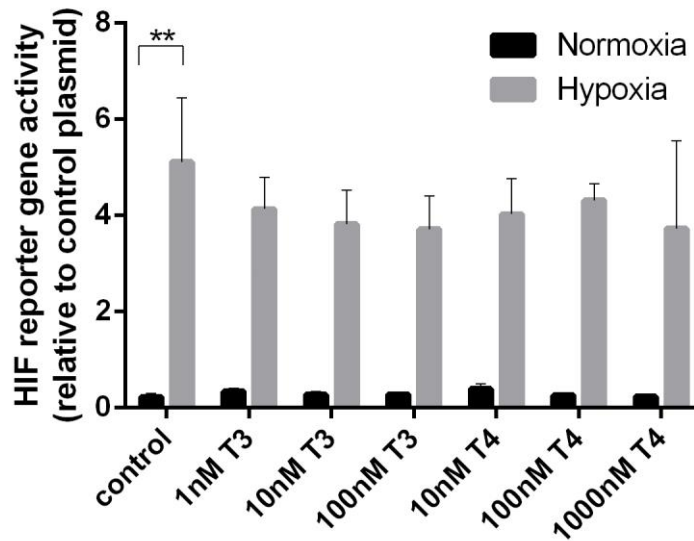


Figure 28: HIF1 α -dependent reporter gene activity in HUH7 cells not influenced by thyroid hormones under hypoxic or normoxic conditions: HUH7 cells were transiently transfected with HIF1 α -responsive promoter driven luciferase reporter construct and incubated in 21% O₂ or 2.5% O₂ for 48 hrs. For the latter 24 hrs additionally 1/10/100nM T3 or 10/100/1000nM T4 were applied. Hypoxia produced a significant ($p=0.009$) increase of reporter gene activity, thyroid hormones did neither alter reporter gene expression in normoxia nor in hypoxia. *Experiment performed in triplicates, repeated three times; statistics calculated with two-tailed Student's t-test, reported as mean \pm SD, $p<0.05$ *, $p<0.01$ **, $p<0.001$ ***, $p<0.0001$ ****.*

3.3. Non-genomic thyroid hormone effects on MSC hypoxia response

As outlined in the introduction, when using the NIS gene to treat non-thyroid tumors, it becomes necessary to pretreat experimental animals (or human patients) with thyroid hormones to reduce the endogenous expression of NIS by the thyroid gland and thereby shield the gland from damage by the administration of radioactive iodine. Importantly, thyroid hormones can influence cells through genomic (nuclear receptor-mediated) or through non-genomic pathways mediated by extracellular receptors found on integrin $\alpha\beta3$. It has been previously reported that thyroid signaling through integrin $\alpha\beta3$ could possibly influence the hypoxia response system by activation of the PI3 kinase. We then sought to test this in our system. To this end, HIF1 α protein expression, HIF1 α -dependent reporter gene activation, and the mRNA expression of known HIF1 α -driven genes were tested under various oxygen conditions with and without thyroid hormone treatment. Thyroid hormone concentrations between 1 and 100nM for T3 and 10 to 1000nM for T4 with and without the presence of 100nM of $\alpha\beta3$ -binding inhibitor Tetrac were applied. To exclude confounding effects of thyroid hormones present in FCS, dextran coated charcoal was used to strip small organic molecules (such as thyroid hormones) from the FCS (sFCS) used in the subsequent *in vitro* experiments.

3.3.1. Thyroid hormones increase normoxic HIF1 α protein level in MSCs in a Tetrac dependent manner

The effects of thyroid hormones on HIF1 α protein expression in MSCs were examined in western blots performed with the experimental conditions established in 3.1.2. After 12 hrs incubation with either normoxia, or hypoxia, as well as T3 and T4, cellular proteins were extracted with RIPA buffer. Tetrac was used to establish if any effects were potentially integrin $\alpha\beta3$ -mediated. The results show that thyroid

hormone treatment increased normoxic HIF1 α protein levels (Figure 29). However, a Tetrac dependency could not be reliably established (data not shown). Under extreme hypoxic activation with 1% O₂ or 100 μ M CoCl₂, thyroid hormones could not increase the level of HIF1 α protein expression (data not shown).

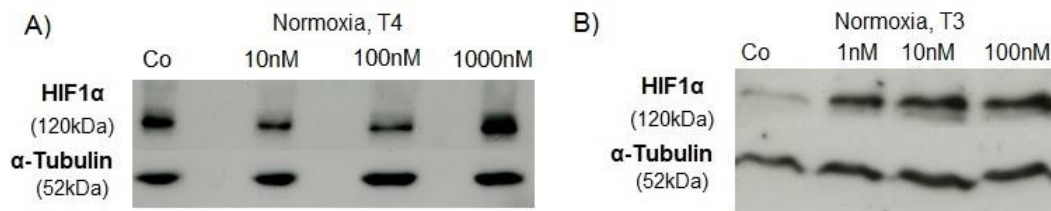


Figure 29: Thyroid hormones increase normoxic HIF1 α protein levels in MSCs after 12 hrs: Western blot analysis of whole cell lysates of MSCs for HIF1 α expression after 12 hrs of normoxic (21%O₂) incubation with different concentrations of T3 and T4 (T3: 1/10/100nM; T4 10/100/1000nM). Co = Control without hormone stimulation. **A)** 12 hrs normoxic exposure with simultaneous application of 1000nM T4 increases HIF1 α protein levels. **B)** 12 hrs normoxic exposure with simultaneous application of 1nM T3 increases HIF1 α expression. Higher hormone concentrations show no further additive effect. The results are representative of three independent experiments.

As a next step, the effect of thyroid hormone treatment on a medium/hypoxic stimulation was examined by using 50 μ M CoCl₂ in combination with HUH7 conditioned medium (CM). These experimental conditions were selected to better mimic potential effects of the tumor environment. 50 μ M CoCl₂ alone and in combination with CM increased HIF1 α protein levels in comparison to the normoxic control. These experimental conditions in combination with physiological concentrations of 10nM T3 led to a Tetrac dependent stable increase of HIF1 α protein stabilization (Figure 30). Physiological concentrations of 100nM T4 did not produce the same effect (data not shown). However, this may be explained in part by a direct T3 activation of the PI3K with downstream effects on HIF1 α .

The influence of thyroid hormones on the hypoxia response of MSCs under tumor milieu conditions was further evaluated on the level of reporter gene expression.

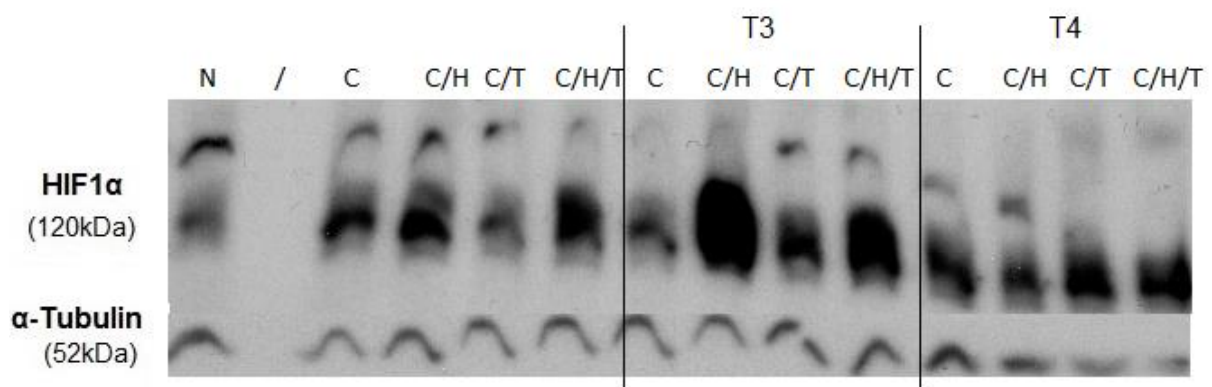


Figure 30: T3 increases HIF1 α protein levels in MSCs in a Tetrac dependent manner under tumor milieu conditions: Incubation with 50 μ M CoCl₂ alone and even more in combination with 20% HUH7 conditioned medium (CM) increases HIF1 α level in MSCs after 12 hrs. 10nMT3 increases HIF1 α protein level further under these conditions in a Tetrac dependent manner. Effect not reproducible with T4 (no direct PI3K activation). Whole cell lysates of MSCs analyzed by western blot for HIF1 α expression after 12 hrs of normoxic (21%O₂) or hypoxic (50 μ M CoCl₂) exposure combined with 20% HUH7 conditioned medium, thyroid hormones (T3: 10nM; T4:100nM) and 100nM Tetrac. N = 21%O₂, C = 50 μ M CoCl₂, T = 100nM Tetrac, H = 20% HUH7 CM. The results are representative of three independent experiments.

3.3.2. Thyroid hormones increase activation of synthetic HIF1 α -responsive promoter in normoxia in a Tetrac dependent manner

The next step in elucidating possible stimulatory effects of thyroid hormones on the hypoxia response system in MSCs, examined potential thyroid hormone effects on HIF1 α -dependent reporter gene expression in MSCs. To this end, promoter-reporter constructs comprised of six HIF1 α -responsive elements were transiently transfected into L87 and primary human MSCs. Reporter gene expression was measured 48 hrs after transfection. This time period included 24 hrs of incubation in normoxia (21% O₂) or hypoxia (1%O₂) and an additional 24 hrs with thyroid hormone stimulation. Tetrac, integrin α v β 3-inhibitor, was used to determine if provoked effects were integrin α v β 3-mediated. In parallel, RANTES/CCL5 promoter-studies were used to determine if agents mentioned could also influence this transgene. Promoter activation after 48 hrs hypoxic/normoxic and 24 hrs thyroid hormone incubation was examined. As detailed in 3.1.3. RANTES/CCL5 promoter was not induced by hypoxic conditions.

Under normoxic conditions (21% O₂) 10 and 100nM T3 ($p=0.04$; $p=0.009$) as well as 10, 100 and 1000nM T4 ($p=0.01$; $p=0.007$; $p=0.01$) significantly increased HIF1 α -dependent reporter gene activity in comparison to normoxic controls. 1nM T3 did show an increase in reporter gene activity as well, however not significant ($p=0.06$). No significant differences could be detected between the different thyroid hormone concentrations. (Figure 31A)

This increase in HIF1 α -driven reporter gene activity was reversible with 100nM Tetrac (Figure 31B).

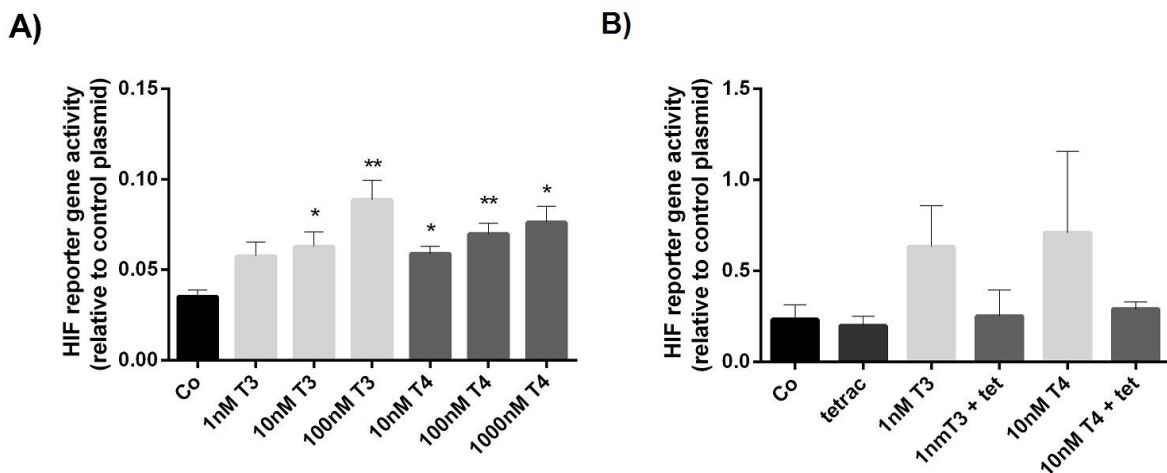


Figure 31: Significant Tetrac dependent increase of HIF1 α -driven reporter gene activation through thyroid hormone treatment in MSCs under normoxic conditions: A) Significant increase of HIF1 α -driven reporter gene activity under normoxic (21% O₂) conditions through 24 hrs thyroid hormone treatment with 10/100nM T3 (*/**) and 10/100/1000nM T4 (*/**/*). **B)** Increase of HIF1 α -driven reporter gene activity is reversed by 24 hrs treatment with 100nM Tetrac. *Experiment performed in triplicates, repeated three times; statistics calculated with two-tailed Student's t-test, reported as mean \pm SD, $p < 0.05$ *, $p < 0.01$ **, $p < 0.001$ ***, $p < 0.0001$ ****.*

Hypoxic incubation (48 hrs; 1% O₂) led to an increase in HIF1 α -dependent reporter gene activity as described in 3.1.3. Additional thyroid hormone treatment (24 hrs) appeared to enhance the HIF1 α -driven reporter gene activity further (Figure 32). However, due to larger variability between single experiments no significant induction or Tetrac dependency could be established (data not shown).

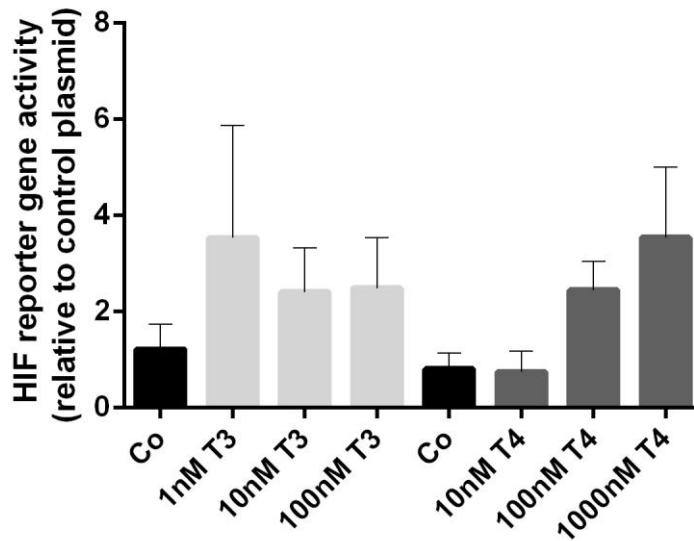


Figure 32: Increase of HIF1 α -driven reporter gene activation through thyroid hormone treatment in MSCs under hypoxic conditions: 24 hrs treatment with 1/10/100nM T3 ($p=0.39$; $p=0.32$; $p=0.34$) and 100/1000nM T4 ($p=0.07$; $p=0.14$) increases of HIF1 α -driven reporter gene activation after 48 hrs hypoxia (1% O₂) in comparison to corresponding hypoxic control (Co). Experiment performed in triplicates, repeated three times; statistics calculated with two-tailed Student's *t*-test, reported as mean \pm SD, $p<0.05$ *, $p<0.01$ **, $p<0.001$ ***, $p<0.0001$ ****.

To examine potential effects of thyroid hormones on the HIF1 α -dependent reporter gene activation in the context of tumor-derived signals, the following experimental setup was used: Normoxic (21% O₂) or hypoxic (1% O₂) stimulation was performed for 48 hrs. At the same time, 20% of the culture medium was replaced with HUH7 conditioned medium (CM). Thyroid hormone was then added during the last 24 hrs. CM in combination with T3 or T4 did not increase the HIF1 α -driven reporter gene activation further under hypoxic or normoxic conditions. (data not shown).

3.3.3. Influence of thyroid hormones and HUH7 tumor cell conditioned medium (CM) on the steady state mRNA expression of known HIF1 α target genes

To assess potential effects of thyroid hormones on MSC hypoxia response further, the effect of thyroid hormone on the steady state mRNA expression of known hypoxia-target genes was examined. The genes tested included the tumor-promoting growth factors FGF2, IL6, TGF β , HGF, TIMP1, CTGF and CXCL12, and the angiogenesis-related markers ID1 and VEGFa. HIF1 α , MMP2, MMP9 and CCL5 expression was also assessed. MMP2 and MMP9 showed almost no steady state expression at all in the experiments performed.

MSCs were incubated with thyroid hormones under normoxic (21% O₂) conditions for 36 hrs. After preliminary experiments, 100nM T3 and 1000nM T4 were found to produce the strongest results and were used in subsequent experiments with Tetrac to determine, if the effects were integrin $\alpha\beta$ 3-mediated. Under normoxic conditions, thyroid hormones (100nM T3, 1000nM T4) led to increased mRNA levels of HIF1 α and CCL5 genes in a Tetrac dependent manner (Figure 33). In the other genes evaluated (IL6, VEGFa, MMP2, MMP9, CTGF, CXCL12, ID1, TGF β , HGF) no stable induction of mRNA levels could be established under normoxia. (data only shown for IL6; Figure 33)

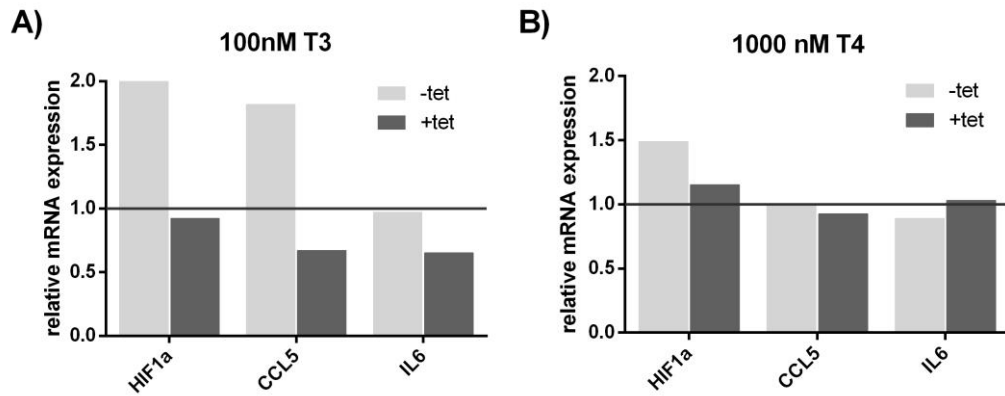


Figure 33: Steady state mRNA level of HIF1 α and CCL5 genes in MSCs increases in a Tetrac dependent manner through thyroid hormone treatment under normoxic conditions: A) MSCs incubated with 100nM T3 with or without 100nM Tetrac in normoxia express increased levels of HIF1 α and CCL5 mRNA compared to untreated MSCs (black line). **B)** MSCs incubated with 1000nM T4 with or without 100nM Tetrac in normoxia express increased levels of mRNA of HIF1 α compared to untreated MSCs (black line). Results are expressed as mean fold change toward untreated MSCs. Experiments were performed in duplets and repeated three times.

As next step, the potential additional effects of tumor-derived signals were evaluated. To this end, hypoxic stimulation was mimicked using 50 μ M CoCl₂ and 20% of the culture medium was replaced with HUH7 conditioned medium (CM). MSCs were also treated with thyroid hormones for 36 hrs with or without Tetrac. Under these experimental conditions, 10nM T3 and 100nM T4 treatment yielded significant and reproducible results.

The trend toward induction of select mRNA species expression by treatment with 50 μ M CoCl₂ and enhanced induction in combination with CM is shown exemplary for the VEGFa gene (Figure 34A).

Treatment with 10nM T3 and 100nM T4 with simultaneous addition of 50 μ M CoCl₂ did lead to a Tetrac dependent increase in HIF1 α and FGF2 mRNA levels (Figure 34B). Adding 20% CM led to enhanced mRNA expression of HIF1 α , CCL5, IL6, VEGFa, FGF2 and CXCL12 (Figure 34C). Other genes (TGF β , HGF, ID1, TIMP1, MMP9) did not show increased mRNA levels. Tetrac dependency can be seen in both set ups (Figure 34B, 34C).

Expanded experiments performed in collaboration with Prof. Spitzweg from Großhadern yielded statistically significant results showing that CM stimulation for 24 hrs in combination with 1nM T3 or 1000nM T4, with or without 100nM Tetrac under normoxic conditions induces the mRNA level of CAF-associated markers in treated MSCs (Schmohl et al. 2015).

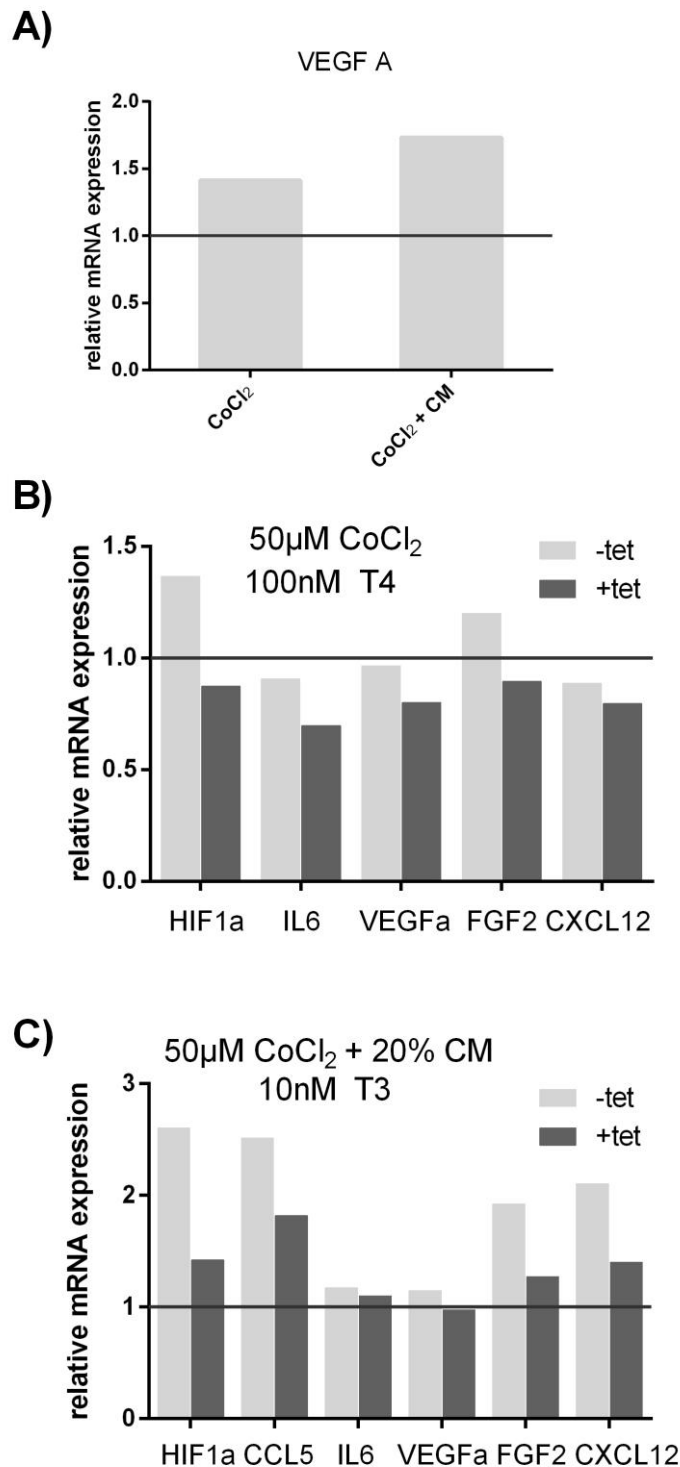


Figure 34: Induction of mRNA expression of HIF1 α , CCL5, IL6, VEGFa, FGF2 and CXCL12 genes in MSCs through thyroid hormone treatment in a Tetrac dependent manner under tumor milieu conditions: A) VEGFa mRNA expression increased after 36 hrs treatment with 50μM CoCl₂ in comparison to untreated cells (black line). Increase is enhanceable through addition of 20% HUH7 conditioned medium (CM). **B)** MSCs treated with 50μM CoCl₂ and 100nM T4 show increased expression of HIF1 α and FGF2 mRNA in comparison to MSCs incubated with 50μM CoCl₂ alone (black line). Tetrac reverses this effect. **C)** MSCs treated with 50μM CoCl₂ in combination with 20% CM and 10nM T3 show increased expression of HIF1 α , CCL5, IL6, VEGFa, FGF2 and CXCL12 mRNA in comparison to MSCs incubated with 50μM CoCl₂ and 20% CM alone (black line). Tetrac reverses this effect. Results are expressed as mean fold change toward A) untreated MSCs B) MSCs treated with 50μM CoCl₂ C) MSCs treated with 50μM CoCl₂ and CM. Experiment performed in duplets, repeated twice.

3.4. Thyroid hormones enhance chemotaxis and chemokinesis of MSCs in a Tetrac dependent manner

Tumor-specific migration is an important component of MSC-based therapy. A chemotaxis chamber assay was developed to study the directed migration of MSCs in collaboration with Alexandra Wechselberger (AG Klinische Biochemie, Prof. Nelson). Prior to this assay, the primary human MSCs were incubated for 24 hrs with thyroid hormones, with and without Tetrac. Subsequently, cell migration was observed for 24 hrs in ibidi assay chambers, which provide easy *in vitro* assessment of travelled distances, velocity and distribution of cells exposed to a gradient of chemoattractant. Furthermore, effect of continuous stimulation 24 hrs before and during the chamber assay was examined.

In a second model, MSC invasion into experimental HCC tumor spheroids was studied (described in 3.1.5.) with support from Alexandra Wechselberger, Anna Hagenhoff and Svenja Rühland (AG Klinische Biochemie, Prof. Nelson). MSCs were incubated the same way as for chemotaxis chamber assay, dyed with CMFDA and then coincubated with HUH7 spheroids. Preliminary results are shown in 3.1.5.

In both assays, MSCs showed a large variability of basic migratory capacities. HUH7 conditioned medium (CM) was used as chemoattractant. The migration of MSCs along a CM gradient was straightforward (Figure 35). This migration was characterized relative to controls representing no gradient (culture medium or CM on both sides).

While MSCs showed slightly elevated levels of basic movement, when adding the chemoattractant to both assay chambers, this effect did not occur when both sides were filled with respective culture medium. When comparing the chemotaxis and chemokinesis of MSCs exposed to the chemical gradient with the two controls the increase of directed migration in gradient exposed MSCs was significantly elevated above the controls for all parameters assessed (Figure 35).

MSCs showed significantly increased FMI ($p=0.0002$), in comparison to non-gradient exposed MSCs. Rayleigh test for vector data proved a significantly inhomogeneous cell distribution of gradient exposed cells in comparison to both controls ($p<0.05$). The displacement of center of mass (CoM) was increased for gradient exposed MSCs in comparison to both controls. All chemokinetic parameters were significantly increased above the culture medium control level in gradient exposed cells (directionality $p<0.0001$, accumulated distance $p=0.0044$, Euclidean distance $p<0.0001$ and velocity $p=0.004$). Only directionality ($p=0.0017$), accumulated distance ($p=0.0071$) and Euclidean distance ($p=0.0241$) reached significance when comparing to the CM control without gradient.

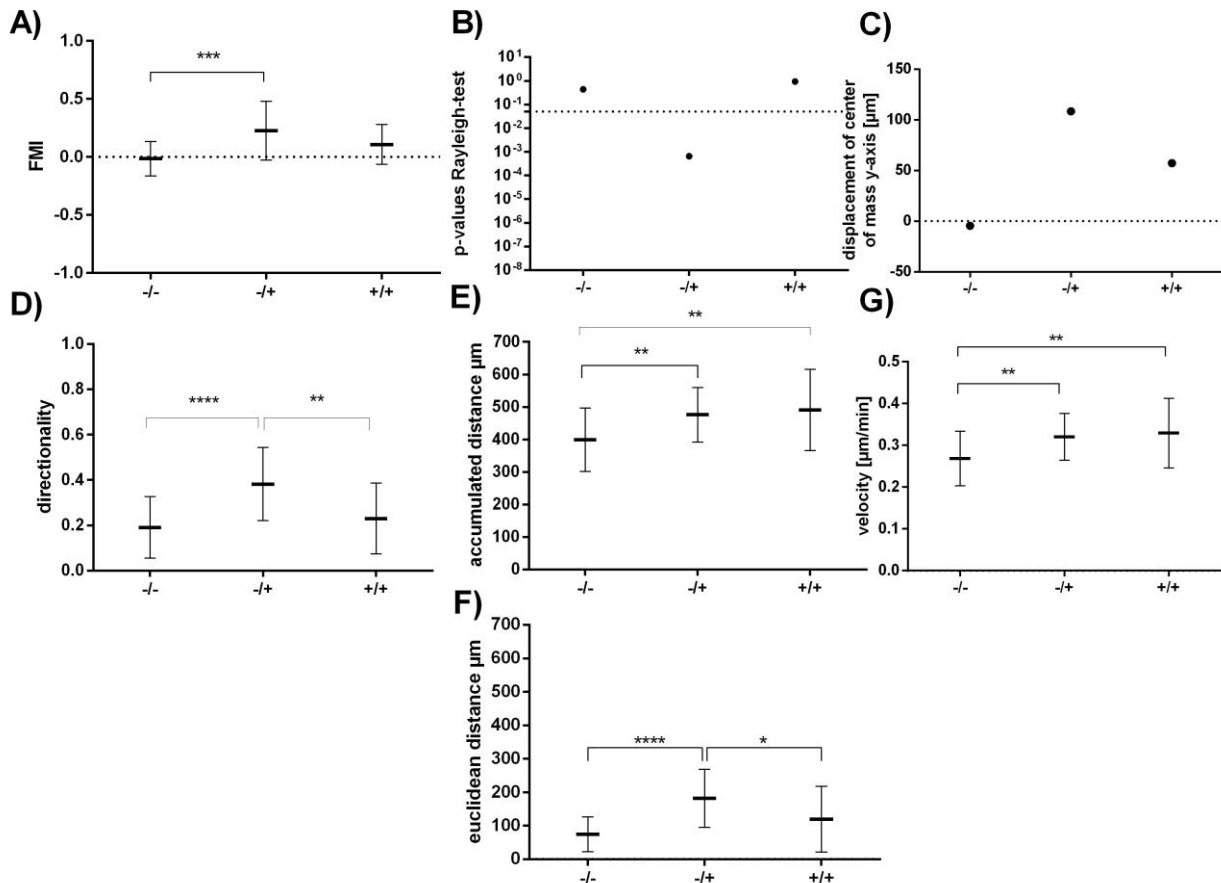


Figure 35: Stable directed migration of MSCs along a gradient of HUH7 conditioned medium (CM): -/- culture medium/culture medium, +/+ CM/CM, -/+ culture medium/CM (gradient) **A)** FMI was significantly ($p=0.0002$ and $p=0.0681$) increased when a CM gradient was applied in comparison to application of culture medium or CM alone. **B)** Rayleigh test for vector data showed a significantly ($p<0.05$) inhomogeneous cell distribution when applying CM gradient. (dotted line represents $p=0.05$) **C)** The center of mass (CoM) was furthestmost away from starting point when applying CM gradient. Application of CM without gradient showed a displaced CoM, too. **D)** Directionality was significantly ($p<0.0001$ and $p=0.0019$) increased when applying CM gradient. **E)** Accumulated distance was significantly ($p=0.0044$) increased when applying CM gradient or applying CM without gradient ($p=0.0071$). **F)** Euclidean distance was significantly ($p<0.0001$ and $p=0.0241$) increased when applying CM gradient. **G)** Velocity was significantly ($p=0.004$) increased when applying CM gradient or applying CM without gradient ($p=0.0066$). The results are representative of three independent experiments. Statistics calculated with two-tailed Student's *t*-test and Rayleigh test for vector data. * $p<0.05$, ** $p<0.01$, *** $p<0.001$, **** $p<0.0001$. Results expressed as mean \pm SD.

MSCs are integrin $\alpha v\beta 3$ -positive. Other cells positive for this integrin have been reported to alter their migration when stimulated via thyroid hormones (Cohen et al. 2014). Therefore, in the next step we sought to determine if thyroid hormones could increase the established tumor directed migration of MSCs. Thyroid hormones (1/100nM T3 and 10/1000nM T4) were added to the cells 24 hrs prior to the assay. The results showed that 1nM T3 and 1000nM T4 increased FMI and displacement of CoM best. Rayleigh test for vector data showed significantly increased chemotaxis for 1nM and 100nM T3 ($p=0.002$; $p=0.008$) as well as 1000nM T4 ($p=0.007$) (Figures 36, 37). Velocity and accumulated distance showed higher values with 100nM T3 or 1000nM T4. Subsequent studies performed in collaboration with Schmohl et al were able to demonstrate statistically significant effects of T3 and T4 prestimulation on the directed migration of primary human MSCs (Schmohl et al. 2015).

Subsequently, the results were validated with Tetrac. Stimulation of chemotaxis (FMI and displacement of CoM) by 1nM T3 and 1000nM T4 could be reversed with 100nM

Tetrac (Figures 38, 39). These results suggest that the mechanism of the stimulation is integrin $\alpha v\beta 3$ -mediated. For chemokinetic parameters no clear Tetrac dependency could be established (data not shown).

As a further step, 24 hrs prestimulation were compared to continuous stimulation lasting throughout the chamber assay (thyroid hormones were included in all assay components) to get an idea of how different thyroidal statuses *in vivo* would influence MSC tumor directed migration. Results showed no conclusive trend that continuous stimulation alters MSC chemotaxis in comparison to prestimulation (data not shown). In the second model, MSC invasion into HCC tumor spheroids preliminary results (described in 3.1.5) show that MSCs are attracted by tumor-derived factors *in vitro*. The set-up was evaluated with thyroid hormone treatment by Svenja Rühland (AG Klinische Biochemie, Prof. Nelson) in collaboration with Prof. Spitzweg at Großhadern. The published results substantiated findings of this thesis as well as further *in vivo* experiments in a mouse model (Schmohl et al. 2015).

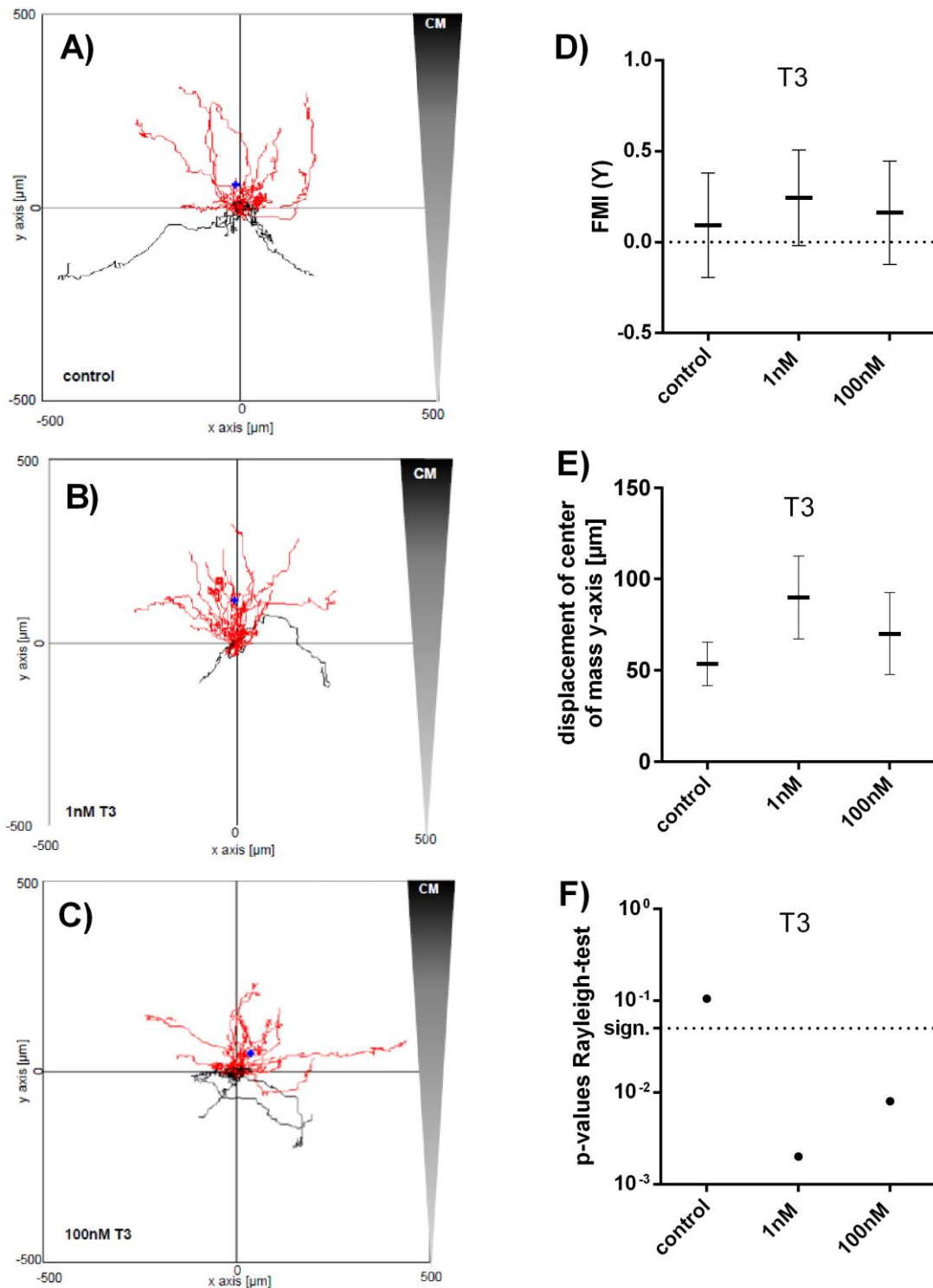


Figure 36: T3 increases tumor directed chemotaxis of MSC: **A)** Exemplary trajectory plot of untreated MSCs showing moderate tumor directed migration. **B)** and **C)** Exemplary trajectory plots of MSCs treated with 1nM or 100nM T3 for 24 hrs showing increased chemotaxis compared to unstimulated MSCs. **D-F)** Quantification of chemotaxis parameters: Rayleigh Test for vector data (**F**) proved significant chemotaxis for 1nM and 100nM T3 treated MSCs ($p=0.002$, $p=0.008$). FMI (**D**) and displacement of CoM (**E**) showed no significant but consistent trends substantiating the Rayleigh test. Red pathways along the chemical gradient, black pathways against the chemical gradient; blue cross represents the CoM. CM stands for HUH7 conditioned medium. The results are representative of three independent experiments. Statistics calculated with two-tailed Student's *t*-test and Rayleigh test for vector data. * $p<0.05$, ** $p<0.01$, *** $p<0.001$, **** $p<0.000$. Results expressed as mean \pm SD.

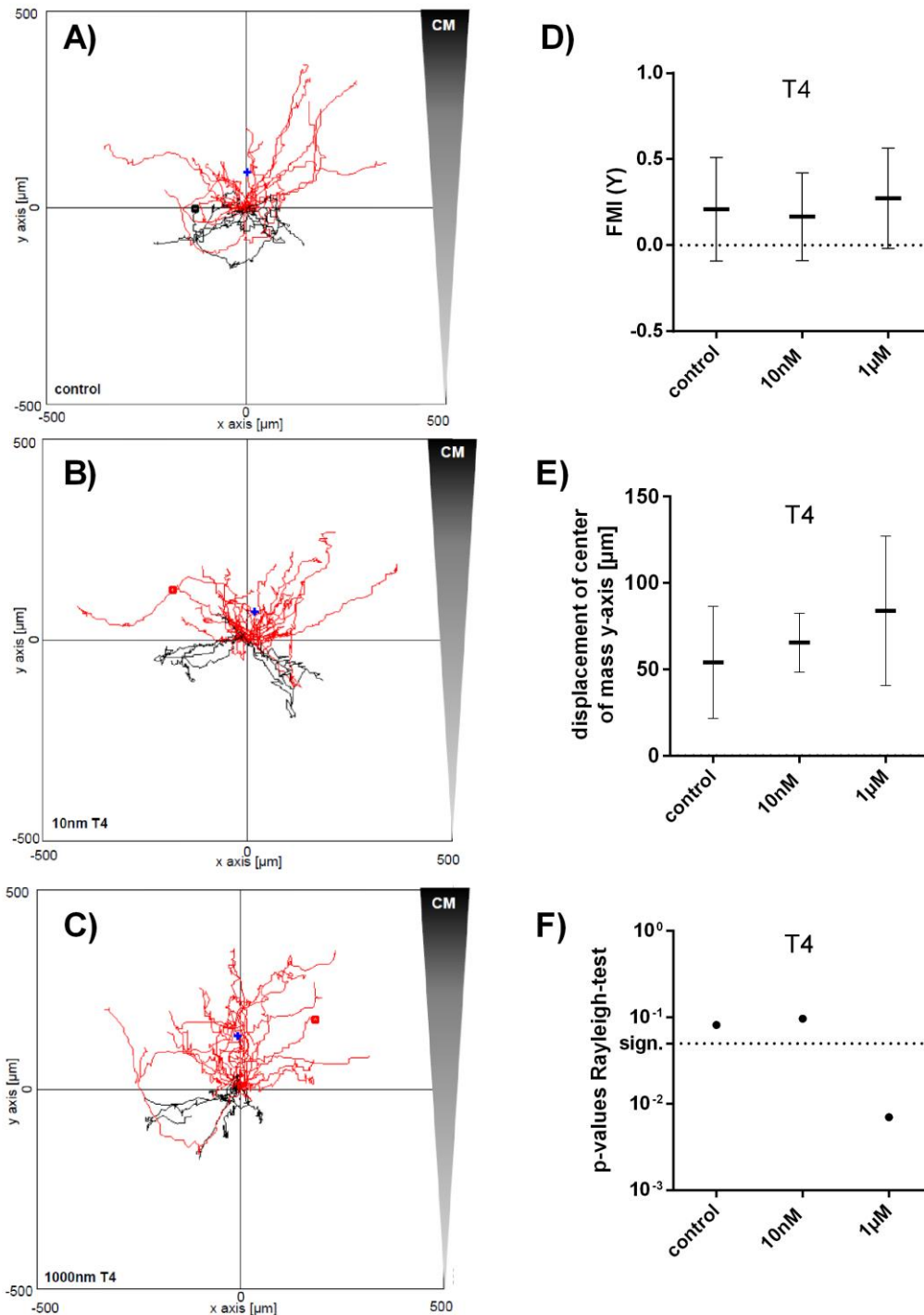


Figure 37: T4 increases tumor directed chemotaxis of MSCs: **A)** Exemplary trajectory plot of untreated MSCs showing moderate tumor directed migration. **B)** and **C)** Exemplary trajectory plots of MSCs treated with 10nM or 1 μM T4 for 24 hrs showing increased chemotaxis for 1 μM T4 compared to unstimulated MSCs. **D-F)** Quantification of chemotaxis parameters: Rayleigh Test for vector data (**F)** proved significant chemotaxis for 1 μM T4 treated MSCs ($p=0.007$). FMI (**D)** and displacement of CoM (**E)** showed no significant but consistent trends indicating most effective chemotaxis for 1 μM T4 treated MSCs. Red pathways along the chemical gradient, black pathways against the chemical gradient; blue cross represents the center of mass. CM stands for HUH7 conditioned medium. The results are representative of three independent experiments. Statistics calculated with two-tailed Student's *t*-test and Rayleigh test for vector data. * $p<0.05$, ** $p<0.01$, *** $p<0.001$, **** $p<0.000$. Results expressed as mean \pm SD.

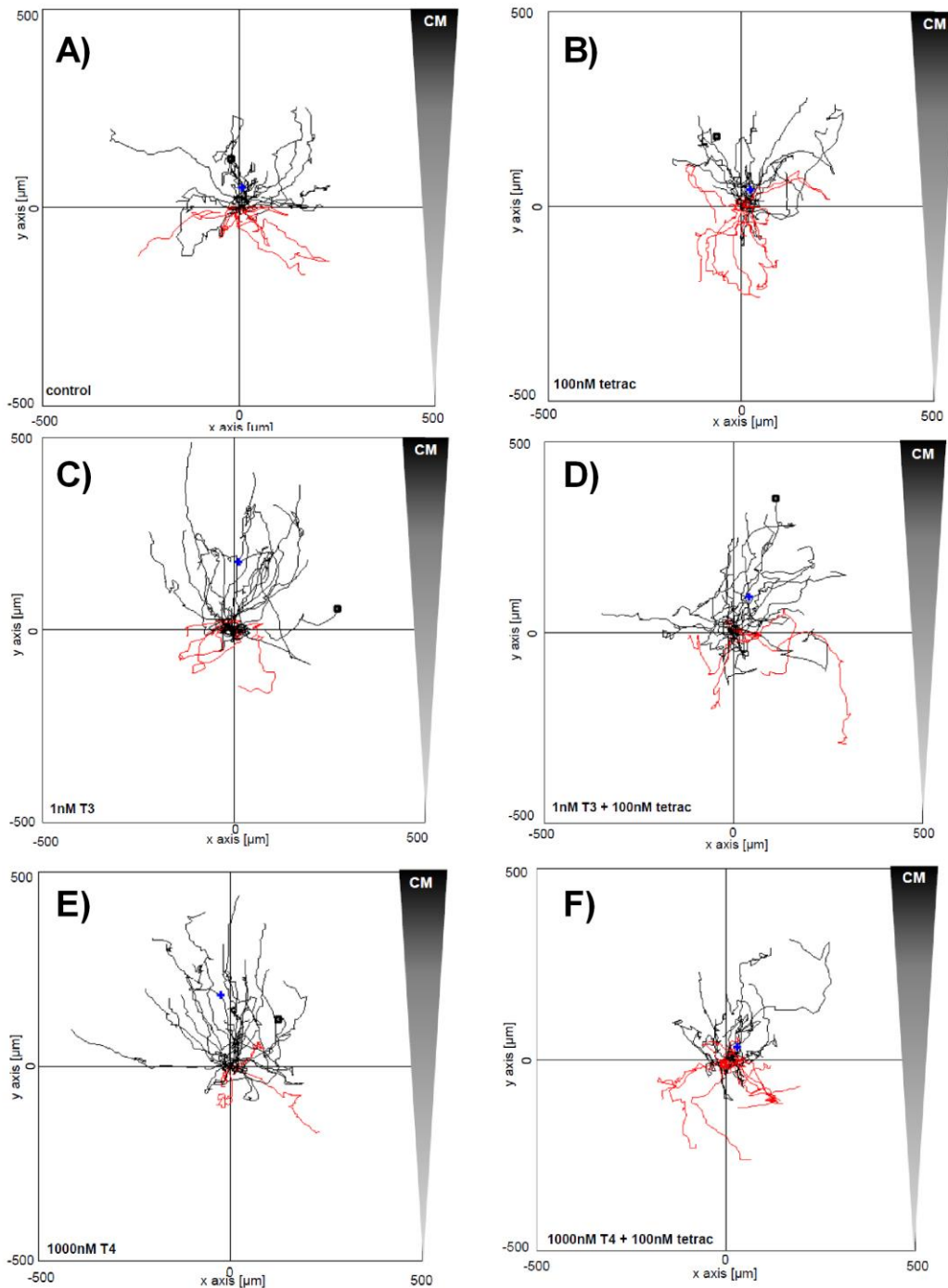


Figure 38: T3 and T4 increase tumor directed chemotaxis of MSCs in a Tetrac dependent manner: **A)** Exemplary trajectory plot of untreated MSCs showing little tumor directed migration. **B)** Exemplary trajectory plot of MSCs treated with 100nM Tetrac showing a trajectory plot comparable to untreated MSCs. **C) and D)** Exemplary trajectory plots of MSCs treated with 1nM T3 with or without 100nM Tetrac for 24 hrs showing increased chemotaxis for 1nM T3 compared to unstimulated MSCs and unaffected chemotaxis for MSCs treated with T3 and Tetrac. **E) and F)** Exemplary trajectory plots of MSCs treated with 1 μM T4 with or without 100nM Tetrac for 24 hrs showing increased chemotaxis for 1000nM T4 compared to unstimulated MSCs and unaffected chemotaxis for MSCs treated with T4 and Tetrac. *Black pathways along the chemical gradient, red pathways against the chemical gradient; blue cross represents the center of mass. CM stands for HUH7 conditioned medium. The results are representative of three independent experiments.*

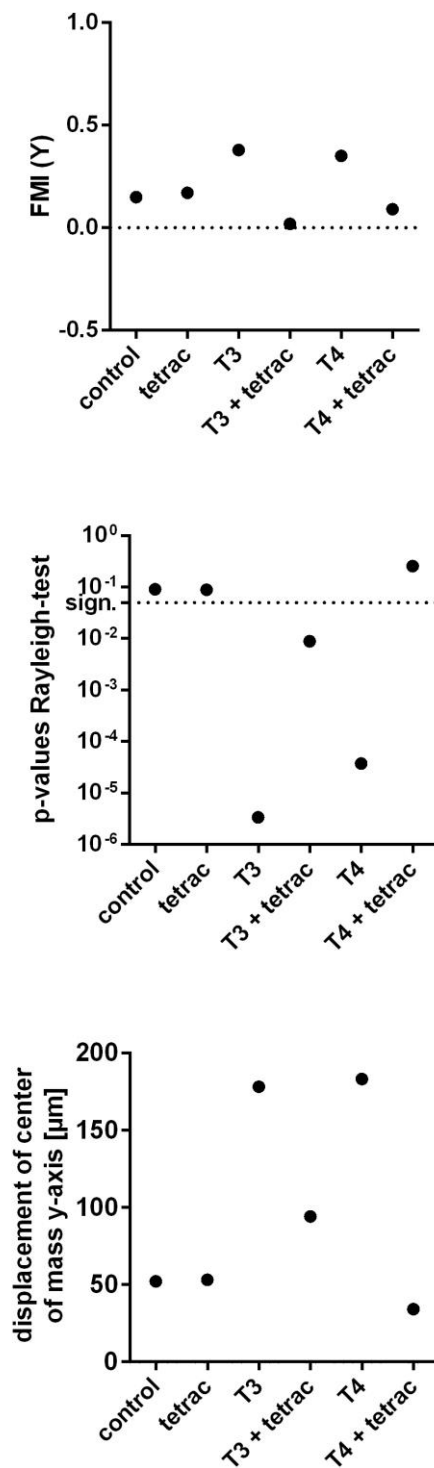


Figure 39: T3 and T4 increase tumor directed chemotaxis of MSCs in a Tetrac dependent manner characterized by FMI, displacement of CoM and Rayleigh test for vector data: FMI (A) and displacement of CoM (C) indicate increased chemotaxis for MSCs treated with 1nM T3 or 1000nM T4. This effect was reversible through treatment with 100nM Tetrac. Rayleigh Test for vector data (B) proved significant chemotaxis for 1nM T3 and 1000nM T4 treated MSCs in a Tetrac dependent manner as well. *CM* stands for HUH7 conditioned medium. The results show one of three independent experiments. Statistics calculated with Rayleigh test for vector data. $p < 0.05$ indicating significant chemotaxis. Results expressed as mean.

3.5. Effects of thyroid hormones, HUH7 tumor cell conditioned medium (CM) and oxygen level on MSC viability

Thyroid hormones, CM and oxygen levels can alter MSC biology, specifically their growth rate and viability. It was therefore necessary to exclude major effects of the stimulants on MSC growth and viability. To test the potential effect of thyroid hormones on these parameters, MTT-assays were used to assess effects on MSC mitochondrial activity as a means of measuring cell proliferation. MSCs were plated into 96 well plates and stimulated for 24, 48 and 72 hrs. Changes in viability were detected by colorimetric quantification using an ELISA reader. After 72 hrs significant changes in proliferation were seen.

When looking at the effects of CM on MSC growth, replacing 10% or 20% of the respective culture medium with CM increased MSC viability after 24 and 48 hrs as well as significantly after 72 hrs ($p=0.0162$) above control level. As next step, the effects of various oxygen concentrations on MSC growth with and without 20% CM were tested. Anoxic incubation significantly ($p=0.0388$) decreased the replication of MSCs after 72 hrs with reduced cell viability after 24 hrs. The addition of CM appeared to have adverse effects on cell growth in the absence oxygen ($p=0.0232$). However, MSCs showed significantly ($p=0.025$) increased viability when incubated with 2.5% O₂ for 72 hrs. This increase could be enhanced by addition of CM ($p=0.0384$). (Figure 40)

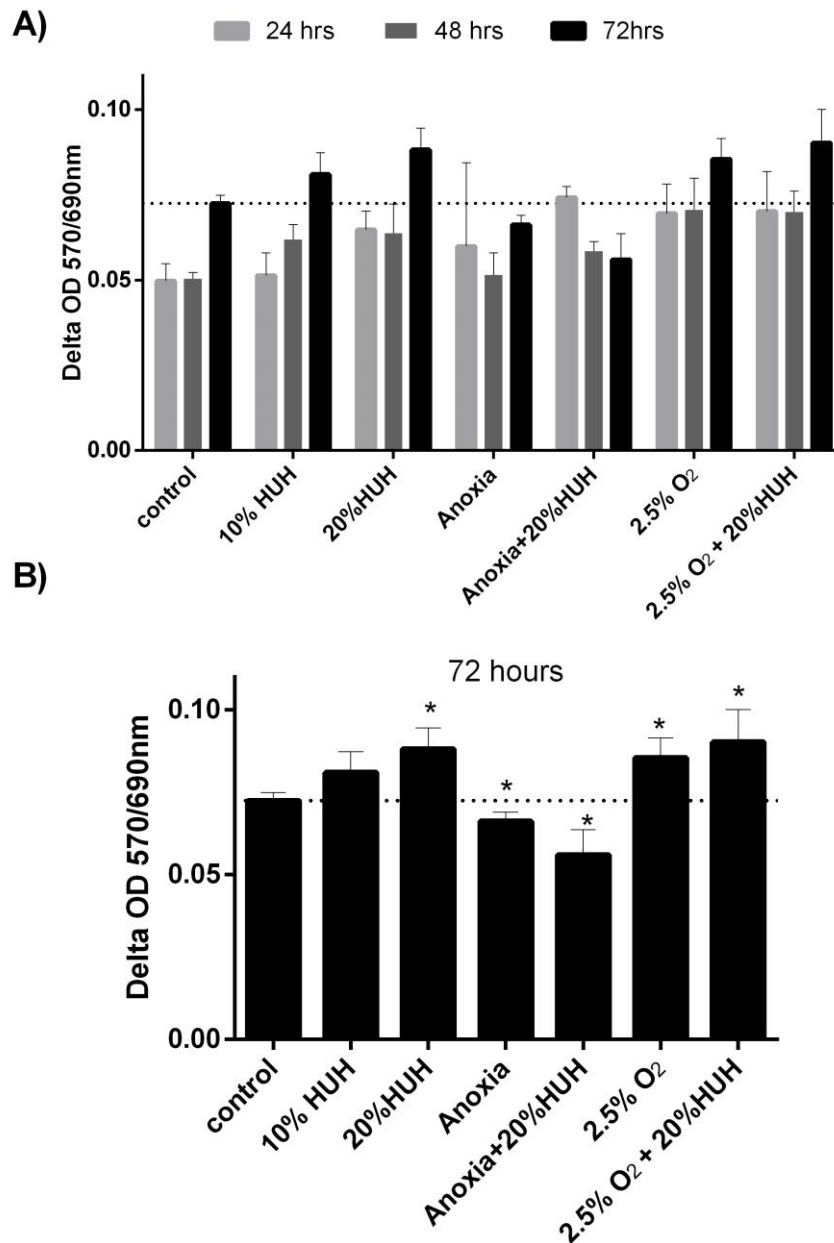


Figure 40: Stimulation with HUH7 conditioned medium (CM) and hypoxia leads to significant increase in MSC viability after 72hrs: A) Differences in optical density after 24, 48 and 72 hrs incubation with 21%, 2,5% and 0% O₂ as well as 10% and 20% CM. **B)** Significant differences in optical density after 72 hrs incubation with 20% CM ($p=0.0162$) or 2,5% O₂ ($p=0.025$) alone as well as 2,5% O₂ in combination with 20% CM ($p=0.0384$). Anoxia significantly ($p=0.0388$) decreased MSC proliferation, even more ($p=0.0232$) when combined with CM. Dotted line represents 72 hrs unstimulated control level. Experiment performed in triplicates, repeated three times; statistics calculated with two-tailed Student's *t*-test, reported as mean \pm SD, $p<0.05$ *, $p<0.01$ **, $p<0.001$ ***, $p<0.0001$ ****.

The potential effects of thyroid hormones on MSC viability in normoxia were then evaluated with and without addition of CM. In the absence of CM, thyroid hormones significantly increased MSC viability after 72 hrs above control level (1nM T3 $p=0.011$; 100nM T3 $p=0.0487$; 1000nM T4 $p=0.0031$). Tetrac dependency could not be established for all concentrations. Stimulation with CM alone increased MSC viability above the unstimulated control level ($p=0.0162$). In the presence of CM only 1000nM T4 increased MSC viability significantly ($p=0.0403$) above the CM stimulated control. Comparing thyroid hormone effects in the absence and presence of CM

results showed enhanced thyroid hormone and Tetrac effects for all samples. Significantly higher MSC viability was found for stimulation with 100nMT3 ($p=0.0205$), 10nMT4 ($p=0.0191$) and 1000nM T4 ($p=0.0482$) in the presence of CM. Suggesting that the tumor microenvironment may enhance thyroid hormone effects. A significant Tetrac effect was only detected for 10nM T4 ($p=0.0462$).

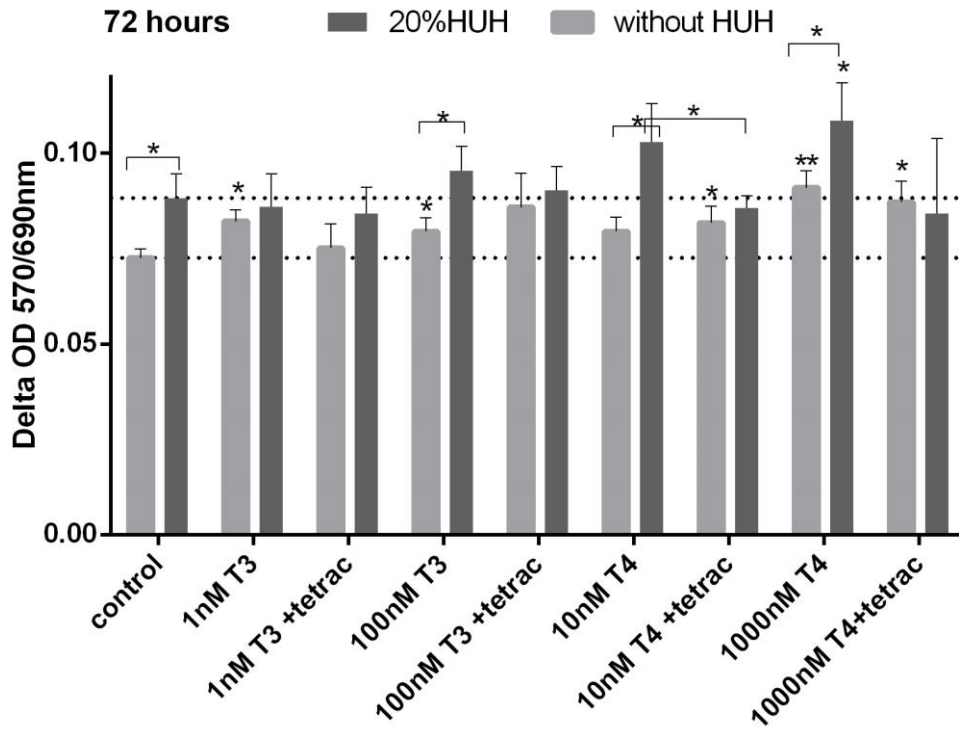


Figure 41: Stimulating effects of thyroid hormones and HUH7 conditioned medium (CM) on MSC proliferation: Differences in optical density (MSC viability) after 72 hrs incubation with 1/100nM T3, 10/1000nM T4 with and without 100nM Tetrac and 20% CM.

Thyroid hormones increase MSC proliferation significantly after 72 hrs in the absence of (CM) (1nM T3 $p=0.011$; 100nM T3 $p=0.0487$; 1000nM T4 $p=0.0031$). (light grey bars)

CM increases MSC proliferation significantly ($p=0.0162$) after 72hrs. (control)

CM enhances thyroid hormone and Tetrac effects on MSC proliferation after 72 hrs. In the presence of CM 1000nM T4 increased MSC proliferation significantly ($p=0.0403$) above the CM stimulated control. Comparing thyroid hormone effects in the absence and presence of CM results showed enhanced thyroid hormone and Tetrac effects for all samples. Significantly higher MSC proliferation was found for stimulation with 100nM T3 ($p=0.0205$), 10nM T4 ($p=0.0191$) and 1000nM T4 ($p=0.0482$) in the presence of CM.

Tetrac dependency could not be established for all conditions. 10nM and 1000nM T4 increased MSC viability above control level as well in combination with 100nM Tetrac. For 10nM T4 a **significant ($p=0.0462$) reverse of the stimulation through Tetrac could only be detected in the presence of CM.**

Dotted lines represent control levels with (upper) and without (lower) addition of CM. Experiment performed in triplicates, repeated three times; statistics calculated with two-tailed Student's *t*-test, reported as mean \pm SD, $p<0.05$ *, $p<0.01$ **, $p<0.001$ ***, $p<0.0001$ ****.

In conclusion, both the tumor microenvironment and thyroid hormones have viability-increasing effects on MSCs in general.

4. Discussion

4.1. New targeting strategies for MSC-based cancer gene therapy

Despite advances in our understanding and therapy of tumors, there is still an obvious need for new approaches of therapeutic intervention. Various methods using MSC-based cancer therapy have advanced to clinical trials, but the technology is still in an early stage of development (Niess et al. 2015). Based in part on their unique biology, MSCs have been adapted as therapy vehicles for the treatment of solid tumors. MSCs are immunoprivileged, and are easy to grow and engineer. These cells have a natural tropism for solid neoplasias, which has been used to adapt them to act as potential therapy vehicles - something akin to a “trojan horse” that delivers therapeutic agents into tumors (Bao et al. 2012).

MSCs have been evaluated in diverse animal models for a variety of clinical applications including therapy of bone segmental defects, osteogenesis imperfecta, brain insults, infarcted myocardium, muscle defects and graft versus host disease (Fritz et al. 2008). Other groups have evaluated the use of antitumor agents in MSC-based cancer therapy. Among the therapy genes tested, are antitumor proteins such as interferon- β or TRAIL (Studený et al. 2004, Keung et al. 2013) or suicide gene systems encoding for enzymes acting on prodrugs (Knoop et al. 2011, Bao et al. 2012). MSC-based therapy may not be free of side effects, as MSCs can naturally home to normal tissues as a consequence of tissue homeostasis (Hagenhoff et al. 2016). The tumor-specificity of MSC therapy can be enhanced by using genetically engineered MSCs that express their therapeutic transgenes in response to tumor-derived signals. This has been achieved through the use of specific gene promoters for transgene expression, that respond to tumor signals, thus restricting transgene expression to the tumor milieu. The promoters tested to date include the Tie2 promoter/enhancer and the RANTES/CCL5 promoter. The Tie2 promoter is activated by angiogenic signals delivered to the tumor-recruited MSCs (Bao et al. 2012), while the RANTES/CCL5 promoter is induced as MSCs response to inflammatory factors released into the tumor microenvironment (Zischek 2011). Both promoters have been shown to enhance tumor-specificity of the MSC-based therapy. Generally, the outcome in various mouse tumor models was shown to be more effective using the RANTES/CCL5 promoter, which targets metastases as well the primary tumor (Knoop et al. 2015).

A central goal of this thesis was to evaluate in more detail, a new potential promoter targeted approach, and to compare its induction to existing protocols. Solid tumors can have large regions of hypoxia, and necrosis. This occurs when tumor growth outpaces the generation of new vessels, which happens in most solid neoplasias. For example, HCC is a fast growing tumor that generally contains large regions of hypoxia and necrosis (Forner et al. 2012, Liu et al. 2014). Due to its aggressive growth, this cancer is largely chemo resistant especially in more advanced stages (Yang et al. 2011). In addition, this tumor is highly dependent on its supporting stromal microenvironment to sustain growth rates, making the tumor stroma a promising target (Yang et al. 2011, Heindryckx et al. 2015). These observations led to the idea of targeting hypoxic areas in tumor microenvironment.

4.1.1. Existing protocols do not target hypoxic tumor stroma

The concept of MSC-based cancer gene therapy discussed here makes use of two important principles. The first is the directed recruitment (homing) of MSCs into the tumor environment, and the second, is the induced expression of therapeutic transgenes within the tumor stroma. MSCs migrate to sites of tissue damage. Cancer

is thought to resemble, in many ways, a chronic wound as it shows hypoxia, necrosis, inflammation, and new vessel growth (Dvorak 2015). MSCs can act as progenitors for many of the cell types that form the tumor stroma. MSCs are attracted by local inflammatory chemokines and growth factors (Knoop et al. 2013). However, as was previously discussed, MSCs also naturally migrate into other tissues like the lung, spleen, thymus, lymph nodes, liver, mucosa of the small intestine, skin and salivary glands as a part of normal tissue homeostasis (Fritz et al. 2008, Bao et al. 2012). The results described in this thesis show that the RANTES/CCL5 promoter does not become activated in response to hypoxic conditions (Figure 42), even though the promoter contains potential HIF1 α -responsive elements (Yeligar et al. 2009). This may be clinically relevant as hypoxic regions are largely resistant to chemotherapy. For this reason, it was important to identify an approach that targets these tumor regions more effectively.

4.1.2. Establishing tools to target hypoxic solid tumors

Hypoxia has been proposed to help fuel tumor progression, and to drive metastasis formation and therapy resistance. Thus, targeting the hypoxia response system represents an attractive new concept (Casazza et al. 2014). Other research groups have explored the potential of hypoxia for cancer treatment by employing HIF1 α inhibitors (Patiar et al. 2006), HIF1 α stability suppressors (Kim et al. 2013a) or a hypoxia activated prodrug called Q6. This drug significantly reduces proliferation-induced apoptosis (Liu et al. 2014). Oxygen levels also play an important role in MSC biology. It has been reported that hypoxia contributes to MSC homing as it promotes inflammatory signals emitted by the tumor stroma (Spaeth et al. 2008). In addition, the circulating pool of MSCs increases under hypoxic conditions (Salem et al. 2010). The main regulators of the hypoxia response are the hypoxia induced transcription factors such as HIF1 α (Benita et al. 2009). HIF1 α levels in MSCs under different oxygen concentrations were characterized using western blot. Hypoxic (1-2.5% O₂ or 50-100 μ M CoCl₂) conditions led to increased levels of HIF1 α (3.1.2.) in comparison to normoxia (21% O₂). This serves as basis for gene activation in hypoxic tumor areas.

The next step in this characterization was comparison of HIF1 α -responsive reporter gene activation under hypoxic conditions (1-2.5% O₂ or 100 μ M CoCl₂), to the potential hypoxic activation of the RANTES/CCL5 promoter. In contrast to the RANTES/CCL5 promoter, the synthetic hypoxia responsive promoter efficiently induced reporter gene expression in response to hypoxia *in vitro* (3.1.3.). These findings suggest that the HIF1 α -responsive promoter, or related promoters, could be suitable for transgene-based therapy of hypoxic tumor areas.

To study the potential activation of the HIF1 α -responsive promoter in a tumor model system, HUH7 and HT29 (HCC and colorectal adenocarcinoma derived) tumor spheroids were used as *in vitro* tumor models. These spheroids showed central necrosis and hypoxia (3.1.4.). Transgenic MSCs showed invasion into this central area. Anna Hagenhoff (AG Klinische Biochemie, Prof. Nelson) has shown activation of HIF1 α -driven reporter genes in the center of these experimental tumors. *Andrea Müller et al.* subsequently provided *in vivo* proof of this concept in subcutaneous and orthotopic HCC xenograft mouse models (Muller et al. 2016).

Evaluation of MSC proliferation under tumor conditions showed significantly increased MSC proliferation in response to hypoxia (2.5% O₂), and after addition of HUH7 conditioned medium. These results suggest that MSCs may survive, replicate and differentiate in the hypoxic tumor microenvironment, but they may not be as active in areas of normoxia. These findings are supported by reports discussing that

MSCs can directly stimulate tumor growth (Torsvik et al. 2013), and the cells normally reside in hypoxic niches in the human bone marrow (Palomaki et al. 2013).

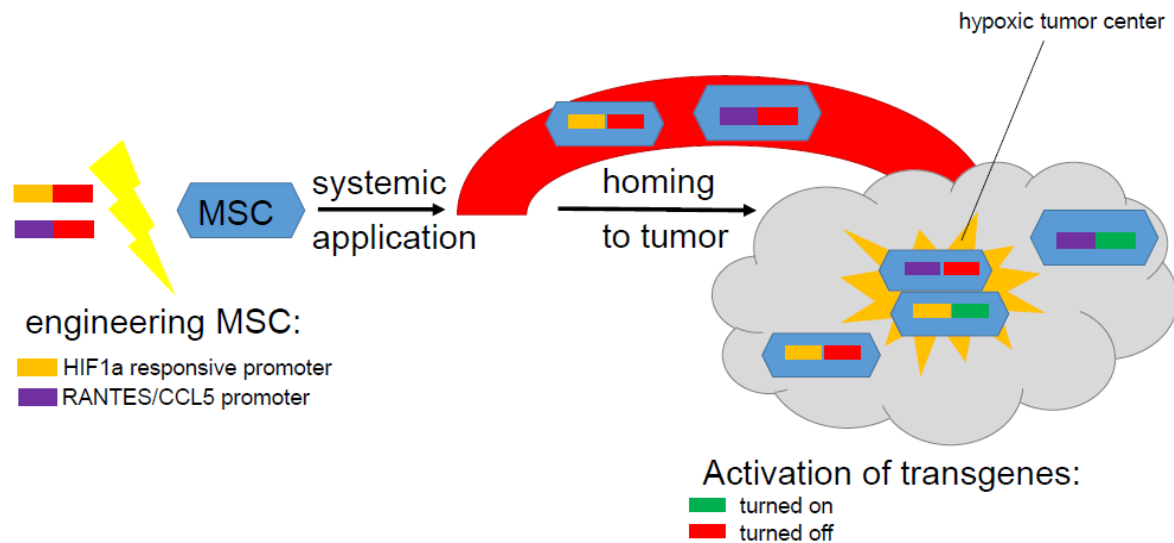


Figure 42: Principle of hypoxia targeted MSC-based cancer gene therapy in comparison to RANTES/CCL5 targeted approach: MSCs engineered with RANTES/CCL5 or HIF1 α -responsive promoter are applied systemically and naturally home into the tumorous site. Hypoxia driven transgenes activate inside the hypoxic tumor center whereas RANTES/CCL5 does not activate in this area.

The results of this thesis provide sufficient *in vitro* evidence that hypoxia targeting is a promising strategy for MSC-based cancer therapy that should be pursued further.

4.2. Non-genomic thyroid hormone effects on MSC biology in the context of Hepatocellular Carcinoma (HCC)

The current MSC-based therapy approach under development in our laboratory makes use of the sodium iodide symporter (NIS). NIS is a theranostic gene that can be used for specific, non-invasive imaging using ^{123}I scintigraphy, ^{123}I SPECT/CT and ^{124}I PET or even MRI as well as efficient therapy through application of radionuclides (^{131}I or ^{188}Re) (Knoop et al. 2015). ^{131}I plays a dual role as therapeutic β -emitter and detectable γ -emitter. Both radionuclides cause a substantial bystander effect on surrounding tissue surpassing that of other effector genes like the HSV-TK/Ganciclovir system. Recent reports by our laboratory and collaborators have shown that NIS dramatically improves the effectiveness of MSC-based cancer therapy (Knoop et al. 2011, Knoop et al. 2013, Knoop et al. 2015). To date, MSC-based NIS therapy has been successfully demonstrated in experimental liver cancer using the constitutive CMV promoter or the tumor milieu-induced RANTES/CCL5 promoter. The latter also showed a robust therapeutic effect for experimental metastatic colon cancer. The NIS gene is strongly expressed in the thyroid gland. It is a transmembrane glycoprotein that helps bring iodine into the thyroid for the generation of thyroid hormones. The use of diverse methods for transcriptionally targeted gene transfer of NIS has subsequently opened the door for a wide range of extra thyroidal tumor applications (Knoop et al. 2011, Knoop et al. 2013, Knoop et al. 2015). Importantly, when using NIS-based approaches for the treatment of non-thyroid tumors, it becomes necessary to protect the thyroid gland against radioiodine-mediated damage, by pre-treatment of patients with the thyroid hormones T3 and T4. Hyperthyroid levels of these hormones lead to the loss of NIS from the cell surface of the thyroid cells. These hormones can have other physiologic effects that are relevant in the context of MSC-NIS-based therapy. We have previously shown that

T3 and T4 can have direct effects on the migratory capacity of MSCs (Schmohl et al. 2015). These hormones can also have effects on HIF1 α (Otto et al. 2008). Furthermore thyroid hormones have been shown to play a key role in the tumor stroma formation (Davis et al. 2011). In the context of this thesis work, these hormones may also thus directly influence hypoxia response in MSCs.

Approximately 20 years ago, a non-genomic pathway of thyroid hormone action was identified. It was found to influence various effects including angiogenesis (Bergh et al. 2005, Davis et al. 2014b, Cayrol et al. 2015), proliferation, (Lin et al. 2009, Davis et al. 2011) tumor cell growth and inflammation (Sharma et al. 2014, Straub 2014). The pathway initiates at the cell surface receptor integrin $\alpha\beta$ 3, which has binding sites for both T3 and T4 (Davis et al. 2011). Upon binding to its site, T4 can influence angiogenesis via activation of the mitogen-activated protein kinase (MAPK) and ERK1/2 (Davis et al. 2005). At the second binding site, T3 can activate phosphatidylinositol 3-kinase (PI3-K). It also influences angiogenesis, but stimulates tumor cell division and possibly stabilization of HIF1 α in addition (Hiroi et al. 2006, Patiar et al. 2006, Davis et al. 2009).

Interestingly, integrin $\alpha\beta$ 3 is already a target for antitumor therapies. Tetrac, an inhibitor of integrin $\alpha\beta$ 3, leads to disordered cell defensive pathways and inhibition of neovascularization (Davis et al. 2009, Davis et al. 2014b, Lin et al. 2015). Treatment with Tetrac also alters the steady-state levels of mRNAs including VEGFa, EGFR, MMP9 and HIF1 α genes. Additionally, Tetrac was found to increase radiosensitivity of cancer cells (Davis et al. 2014b).

Integrins are involved in the adhesion and migration of cells. MSCs and fibroblasts use these cell surface molecules (De Wever et al. 2003, Fox et al. 2007, Salem et al. 2010). Thyroid hormones have been shown to influence the invasiveness, adhesion and migratory capacities of different tumor cells via the integrin $\alpha\beta$ 3 (Cohen et al. 2014). We have recently shown that thyroid hormone stimulation through $\alpha\beta$ 3 can also dramatically alter the tropism of MSCs for experimental tumors (Schmohl et al. 2015).

Within the scope of this thesis work, it was important to investigate possible interactions between hypoxia and thyroid hormones as both influence the tumor microenvironment and MSCs. Additionally, the effect of the thyroid hormones on MSC growth and differentiation were evaluated to round up the investigation.

MSC biology was examined in the context of a specific tumor model, in this case HCC. The HCC derived cell line HUH7 served a model cancer. Importantly, this cell line allows a distinction between effects on MSCs and potential confounding effects on the tumor, as the HUH7 cell line lacks expression of integrin $\alpha\beta$ 3.

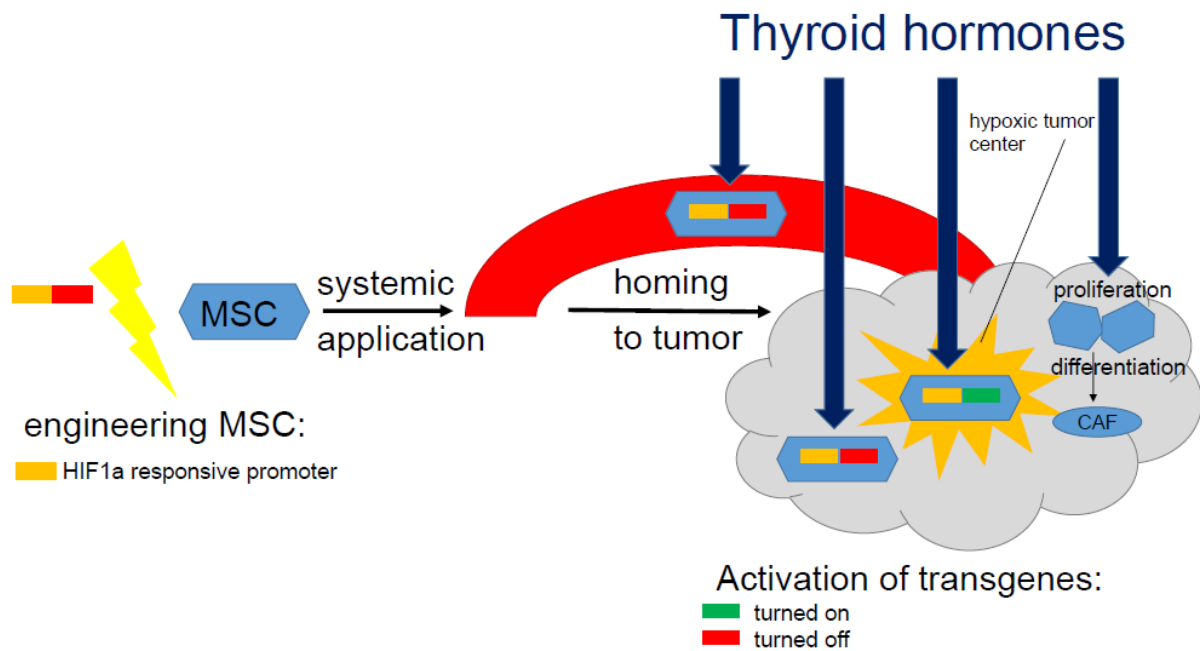


Figure 43: Influence of thyroid hormones on MSC-based hypoxia targeted cancer gene therapy: Thyroid hormones enhance MSC homing into tumors *in vitro* as well as *in vivo*. They also enhance hypoxia regulated gene activation in the tumor milieu under normoxic and hypoxic conditions. Moreover, MSC proliferation and differentiation can be influenced.

4.2.1. Potential effect of thyroid hormones on MSC proliferation

Thyroid hormones can stimulate cell proliferation (Davis et al. 2009). The results described here show that thyroid hormones can also increase MSC proliferation significantly after 72 hrs, as can treatment with HUH7 conditioned medium. Combining both stimuli enhances MSC proliferation even further. The stronger effector appears to be tumor conditioned medium, but thyroid hormones show additive effects. 10nM and 1000nM T4 increased MSC viability above control level. Tetrac dependency could not be clearly established in this experiment. This could be due in part to the formulation of Tetrac used. It has been shown to travel into the cell's interior and cause intrinsically stimulating effects itself leading to further stimulation instead of inhibition. These effects could be avoided by using nanoparticulate version of Tetrac, which is covalently bound to poly-lactic-coglycolic acid and cannot penetrate the cell membrane (Davis et al. 2014b). However, this agent was not available for the experiments shown here.

In conclusion, MSCs showed increased proliferation in response to tumor-derived signals and under thyroid hormone treatment. These observations suggest that thyroid hormone treatment may enhance the use of MSCs as cancer therapy vehicles.

4.2.2. Potential effects of thyroid hormones on MSC differentiation

The tumor microenvironment can drive MSC differentiation to TAFs or pericyte-like cells. Thyroid hormones can also influence MSC differentiation. They have been described to enhance MSC differentiation into chondrocytes or oligodendrocytes (Mackay et al. 1998, Kaka et al. 2012, Karl et al. 2014). Moreover, MSCs can also influence tumor growth by their secretion of growth factors such as VEGF, CXCL12, EGF, IL6 and CCL5 (Knoop et al. 2013). We have shown that thyroid hormones and tumor-conditioned medium may enhance the differentiation of MSCs into TAF-like cells via the integrin $\alpha\beta3$ pathway as demonstrated by an upregulation of respective markers (Schmohl et al. 2015). Davis et al. also showed a non-genomic regulation of angiogenesis via VEGFa as well as FGF and EGFR (Davis et al. 2014b).

Neovascularization is stimulated by hypoxic conditions via stabilization of the HIF1 α transcription factor. The stabilization of HIF1 α is also enhanced by T4, which occurs in a Tetrac dependent manner (Mousa et al. 2014). Hypoxia also leads to an upregulation of CXCL12, FGF, HGF, IL6 and TGF β by MSCs (Hagenhoff et al. 2016). Moreover, integrin α v β 3-controlled MAPK has been linked to increased MMP9 expression (Cohen et al. 2014). In conclusion, thyroid hormones can influence gene regulation and differentiation in MSCs.

In the context of this thesis, mRNA levels of a series of HIF1 α regulated genes were examined. Under normoxic conditions, thyroid hormones increased mRNA levels of HIF1 α and CCL5 genes in a Tetrac dependent manner. Other genes evaluated (IL6, VEGFa, MMP2, MMP9, CTGF, CXCL12, ID1, TGF β , HGF) showed no induction of mRNA levels. Treatment with hypoxia increased mRNA levels of all genes examined. This increase was even higher when adding HUH7 conditioned medium (CM) simultaneously.

When applying thyroid hormones, a Tetrac dependent increase in mRNA levels could be established for HIF1 α and FGF2 genes, and for HIF1 α , CCL5, IL6, VEGFa, FGF2 and CXCL12 genes when stimulating MSCs with tumor conditioned medium in addition. T3 produced higher levels of induction, which could be possibly be due in part to the different binding sites for the thyroid hormones on the integrin α v β 3 receptor. Only T3 has been shown to activate PI3K (with downstream effects on HIF1 α). Steady state mRNA levels of other relevant genes (TGF β , HGF, ID1, TIMP1, MMP9) did not increase through stimulation with thyroid hormones. The mentioned results described in Schmohl et al. (2015) substantiate this data. The tumor microenvironment enhances MSC differentiation as evidenced by the changes in specific mRNA levels. Thyroid hormones enhance and modulate the response of the cells to tumor-derived signals. The Tetrac dependency of the effects is indicative of a non-genomic thyroid hormone pathway mediated effect.

These findings suggest that thyroid hormones play an important role in the growth of the tumor stroma. They may enhance MSC differentiation and thus possibly indirectly promote growth of the cancer. Hypoxia stimulates MSC differentiation as well. However, the additive effects seen between the three general stimulants (hypoxia, CM and thyroid hormones) still have to be better defined. The general findings support the potential use of a hypoxia targeting strategy as a promising candidate for *in vivo* experiments.

4.2.3. MSC hypoxia response: HIF1 α protein level and HIF1 α -driven reporter gene activation

Signaling through PI3K and MAPK can influence HIF1 α expression (Moeller et al. 2005). Both pathways can be activated through stimulation of the integrin α v β 3 (Davis et al. 2009) suggesting that non-genomic thyroid hormone effects may also influence HIF1 α metabolism and HIF1 α regulated gene expression in MSCs. Under "maximum" hypoxic activation, no increase in HIF1 α protein levels in response to thyroid hormones could be detected. However, under normoxic conditions, thyroid hormones, especially T3, were found to increase HIF1 α protein levels. This effect was not strongly influenced by Tetrac treatment. Tumor milieu conditions (medium hypoxic stimulation with 20% HUH7 conditioned medium) also increased HIF1 α protein levels. Adding T3 in this setting produced a Tetrac dependent increase of HIF1 α protein levels.

In addition, the results described here showed a significant Tetrac dependent induction of HIF1 α -associated reporter genes under normoxic conditions. Under

hypoxic conditions (1% O₂) the increase in hypoxia controlled gene activation was not statistically significant.

In conclusion, thyroid hormones, especially T3, were found to stimulate the hypoxia response system in MSCs leading to a more efficient hypoxia driven transgene expression. As detailed above, thyroid hormones can increase mRNA levels of hypoxia regulated genes in MSCs, especially under tumor milieu conditions. The discrepancy between T3- and T4-mediated effects could again be in part possibly due to the different binding sites for the thyroid hormones on the integrin $\alpha\beta3$ receptor. Only T3 has been shown to activate PI3K (with downstream effects on HIF1 α).

4.2.4. MSC chemotaxis

Local concentrations of inflammatory chemokines and growth factors can be chemotactic attractants for MSCs (Knoop et al. 2013). This is especially true for the chemokine CXCL12, which is thought to play an important role in MSC migration (Spaeth et al. 2008, Penzo et al. 2014). This chemokine is upregulated during tissue damage or injury, and is linked to the response of a tissue to hypoxia (Semaan et al. 2017). In addition, growth factors like EGF can stimulate MSC chemotaxis (Lourenco et al. 2015).

Thyroid hormones can regulate the adhesion and migration of certain cells, e.g. multiple myeloma cells, via integrin $\alpha\beta3$ (Cohen et al. 2014). In chemotaxis assays HUH7 conditioned medium efficiently attracted MSCs. 24-hrs-prestimulation of MSCs with 1nM T3 and 1000nM T4 could increase this basic tumor directed migration in a Tetrac dependent manner. Thus, the results suggest that integrin $\alpha\beta3$ -mediated stimulation can increase the general chemotaxis of MSCs.

Continued stimulation with thyroid hormones during the chemotaxis assay produced integrin $\alpha\beta3$ -mediated stimulation of MSC chemotaxis as well suggesting that the thyroidal status of a patient treated with MSC-based gene therapy should be taken into consideration to maximize therapeutic efficiency.

4.2.5. MSC tumor spheroid invasion, *in vivo* homing and activation of transgenes in tumor stroma

A lab colleague, Svenja Rühland has extensively evaluated the effects of thyroid hormones on MSC invasion *in vitro*. The HUH7 tumor spheroid model used is the same as described in 3.1.5. MSCs showed significantly deeper and more frequent invasion into 3D HUH7 spheroids upon 1nM T3 and 1000nM T4 treatment in a Tetrac dependent manner (Schmohl et al. 2015), which substantiates the findings of the chemotaxis assays described in this thesis (3.4.).

Moreover, Schmohl et al found out the thyroidal status influences MSC recruitment into experimental tumors *in vivo* significantly (nude mice harboring HUH7 xenografts). MSCs were recruited increasingly to perivascular regions of the tumor and invaded the surrounding tumor tissue in hyperthyroid mice as compared to euthyroid mice. Both recruitment and invasion were reduced in hypothyroid mice, and even further reduced in Tetrac treated mice. Neither alteration of the thyroidal status nor Tetrac treatment had an effect on tumor growth (HUH7) in these experiments. (Schmohl et al. 2015)

4.3. Hypoxia targeting and thyroid hormones during MSC-based cancer gene therapy

MSCs and thyroid hormones are key players in the formation of tumor stroma (Barcellos-de-Souza et al. 2013). Therefore, the interaction of this biology imposes important consequences for the therapeutic efficiency of MSC-based therapy approaches. MSC biology has been exploited to treat solid malignancies. Thyroid hormones influence both MSC migration into the tumor as well as tumor-specific activation of antitumor transgenes.

4.3.1. Using hypoxia targeting for MSC-based cancer gene therapy

Hypoxia targeting as a MSC targeting strategy, especially for fast growing solid tumors like HCC, represents an interesting new therapeutic approach. These tumors can be resistant to conventional therapies (Liu et al. 2014). The established MSC-based therapeutic protocol using RANTES/CCL5 promoter to drive transgene expression shows no activation under hypoxic conditions. The activation of the HIF1 α -responsive promoter was shown to upregulate the NIS transgene *in vivo* (Muller et al. 2016). However, the experiments showed that for general tumor reduction and *in vivo* survival the synthetic HIF1 α -responsive promoter was not yet as effective as the RANTES/CCL5 promoter while it's *in vitro* effectiveness was significantly higher. This may be linked in part to the use of a synthetic promoter here. These promoters reach specific targets very efficiently while native promoters respond to a wider range of signals, which leads to reduced specificity (Muller et al. 2016). Limiting promoter activation to one specific pathway requires a promoter structure built of tandem repeats (in this case HIF1 α -responsive elements). However, this structural built up also enhances *in vivo* recombination due to the multiple repeats, which limits *in vivo* promoter function. Furthermore, the potential targeting of tumor metastases using hypoxia driven approaches remains to be evaluated (Knoop et al. 2015). While at present, the RANTES/CCL5 promoter is the most efficient tumor-specific promoter *in vivo*, new native promoters strongly associated with inflammation and hypoxia represent very promising approaches for future experiments.

To enhance *in vivo* therapeutic effectiveness of hypoxia targeting, the current focus is to identify native gene promoters that are responsive to a wider range of tumor signals. RANTES/CCL5 is not activated by hypoxia, but is activated by other tumor-associated signals allowing effective MSC-based tumor reduction and prolongation of survival. Potential native promoter candidates may be found among the hypoxia regulated genes identified in this thesis. HIF1 α , CCL5, IL6, VEGFa, FGF2 and CXCL12 genes are all activated in part by hypoxia, in combination with tumor derived signals. Angiogenesis associated gene promoters (VEGFa) are interesting targets for tumor therapy. Angiogenesis has been used to target MSC-based therapy successfully using the Tie2 gene promoter/enhancer to drive tumor-specific suicide gene expression (Niess et al. 2011). VEGFa contributes to MSC tropism for glioma and pancreatic cancer (Barcellos-de-Souza et al. 2013). Another interesting option is the IL6 gene. It is among the cytokines that are associated with attracting MSCs to breast cancer (Barcellos-de-Souza et al. 2013). The potential efficacy of these native promoters are currently being evaluated.

Importantly, the above-mentioned genes were also inducible by thyroid hormone treatment. Therefore, in the context of NIS-based therapy, the hyperthyroid status used to limit damage to the thyroid gland, could also enhance therapeutic effectiveness, when using one of these gene promoters.

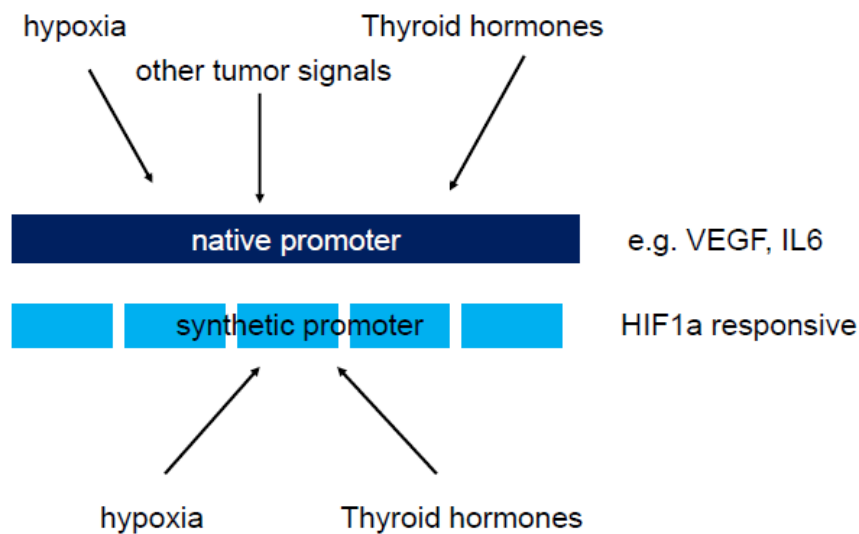


Figure 44: Effective tumor-specific promoters for MSC-based cancer gene therapy – synthetic versus native promoters: The synthetic HIF1 α -responsive promoter evaluated in this thesis has the disadvantage of potentially being unstable *in vivo* due to the tandem repeat structure. Moreover, it did not reduce tumor load *in vivo* as effectively as the RANTES/CCL5 promoter did due to limited activation through only one pathway (hypoxia). One advantage of this approach is the induction of the system by thyroid hormones. The goal now is to find a stable native promoter activated by hypoxia, thyroid hormones and other tumor signals to reach a higher therapeutic efficiency than RANTES/CCL5 promoter provides. Among the potential candidates are the gene promoters for VEGF α and IL6.

4.3.2. Influence of thyroid hormones on MSC-based cancer gene therapy

Thyroid hormone treatment enhances tumor directed MSC chemotaxis *in vitro*, as well as MSC invasion into tumor spheroid models. A hyperthyroid status *in vivo* enhances MSC homing into HUH7 xenograft tumors. Tetrac treatment and hypothyroid status reduced the effectiveness of MSC homing dramatically *in vivo* (Schmohl et al. 2015). These findings suggest that for any MSC-based cancer therapy, it may be important to assess the patient's thyroidal status. Indeed, the patient's thyroidal status may be relevant when considering the general use of engineered MSCs for tumor therapy.

A survey of the literature shows that hypothyroidism has been associated with cancer outcome. It has been linked to tumor invasiveness and metastatic development and has been shown to influence the course of glioblastoma multiforme, breast cancer and renal cell carcinoma negatively (Martinez-Iglesias et al. 2009, Mousa et al. 2014). A potential tumor promoting effect of thyroid hormones has to be taken into account as well.

4.3.3. Tetrac as antitumor agent

Tetrac is undergoing testing as an anticancer agent. In a nanoparticulate formulation, it exclusively binds to the surface receptor integrin $\alpha_v\beta_3$ (Davis et al. 2014b). For $\alpha_v\beta_3$ expressing tumors, Tetrac has been shown to alter proliferation and apoptosis and sensitize the tumor to conventional treatment (Lin et al. 2016). This is in addition to indirectly reducing angiogenesis (Davis et al. 2014b).

Most of the *in vitro* and *in vivo* effects of thyroid hormones shown in this thesis were found to be Tetrac dependent. *In vivo* Tetrac mimics a hypothyroid status, which leads to reduced MSC-based tumor stroma growth (Schmohl et al. 2015). This occurs by reducing the migration and differentiation of MSCs (Schmohl et al. 2015).

Tetrac may limit angiogenesis, and in $\alpha\beta3$ -expressing tumors, directly limit growth. The results shown here suggest that Tetrac may also show therapeutic efficacy for integrin $\alpha\beta3$ -negative solid tumors as well (Schmohl et al. 2015).

4.3.4. Possible therapeutic improvements by prestimulation of MSCs with thyroid hormones

Another possible amendment to MSC-based gene therapy is the prestimulation of exogenously administered MSCs with thyroid hormones. As shown in this thesis pretreatment of MSCs with thyroid hormones enhanced their tumor directed chemotaxis *in vitro*. It has to be established if prestimulation of MSCs enhances tumor migration *in vivo*. Furthermore, other effects of prestimulation remain to be evaluated, including increased viability and resilience. Integrin $\alpha\beta3$ -mediated pathways have to be examined in more detail to discover the full potential of thyroid hormone effects on MSC biology.

4.4. Outlook

MSC-based cancer gene therapy is still in its early stages. We still need to better understand general MSC and tumor stromal biology. The applicability and effectiveness of MSC-based cancer gene therapy can also be enhanced by the identification of better tumor-specific promoters for each tumor entity. Furthermore, possible immunosuppressive and cancer promoting abilities of MSCs should be addressed in parallel.

Finally, MSC-based cancer gene therapy represents a next generation therapy for solid cancers. Due to the complicated nature of the biology at work, and the many steps needed for effective therapy, further optimization is required to advance the approach into the clinic.

4.4.1. Effects of chronic tumor disease on patient's thyroidal status and relevance for MSC therapy

When the NIS gene is used as theranostic transgene, patients need to be treated with thyroid hormones in order to reduce NIS expression in the thyroid gland. This helps protect the organ from treatment with radioiodine. As detailed earlier, hypothyroidism can influence cancer outcome (Nelson et al. 2006, Martinez-Iglesias et al. 2009). Hyperthyroidism has also been linked to the prevalence of certain cancer types (Lin et al. 2016). How then to interpret T4 substitution need for MSC/NIS-based cancer therapy? Transient T4 substitution in cancer patients needs to be better evaluated.

4.4.2. Current limitations and risks of MSC-based cancer therapy and application of thyroid hormones

While MSC-based cancer therapy is a promising new approach, it is also important to keep risks and challenges in balance with the advantages. The isolation and expansion of MSCs is still challenging, and the isolated cells are fragile and heterogeneous. The best source for MSCs for cancer therapy has yet to be determined. MSCs can be isolated from bone marrow, umbilical cord blood, cord blood and adipose tissue (Brown et al. 2014, Hagenhoff et al. 2016). Generally, MSCs isolated from the bone marrow of patients or healthy donors are used. Immortalization, safety and the general characteristics of the modified cells need to be examined further. Targeting metastases also imposes further challenges in finding appropriate tumor-specific promoters. Possible tumor promoting effects of exogenous MSC application have to be considered, which have proven to be minor in comparison to the therapeutic effect so far (Schmohl et al. 2015). However, several

studies showed enhancement of tumor growth through MSC application. One explanation for tumor promotion could be MSCs' immunosuppressive functions. Innate and adaptive immune system are influenced likewise altering the endogenous antitumor immunity.

However, for transient application all these alterations seem to be of minor relevance. (Knoop et al. 2011). To date, clinical trials have shown mild or no adverse effects from MSC treatment (D'souza et al. 2015).

5. Addendum

5.1. Abbreviations and Symbols

5-FU	5-fluorouracil
ADP	adenosine diphosphate
AG	research group
ARNT	aryl-hydrocarbon receptor nuclear transporter
ATP	adenosine triphosphate
BCA	acid
BSA	bovine serum albumin
°C	degree Celsius
C57BL/6 mice	C57 black 6 mice
CAF	cancer associated fibroblasts
CCL3	chemokine ligand 3
CCL5	chemokine ligand 5
CCL19	chemokine ligand 19
CCL21	chemokine ligand 21
CD14	cluster of differentiation 14
CD19	cluster of differentiation 19
CD34	cluster of differentiation 34
CD45	cluster of differentiation 45
CD73	cluster of differentiation 73
CD90	cluster of differentiation 90
CD105	cluster of differentiation 105
cDNA	complementary DNA
CE/CPT-11	carboxyl esterase with irinotecan
CM	HUH7 conditioned medium
CMDA	4-[(2-chloroethyl) (2-mesyloxyethyl) amino] -benzoyl-L-glutamic acid
CMFDA	5-chloromethylfluorescein diacetate
CMV	cytomegalovirus
CO ₂	carbon dioxide
CoCl ₂	cobalt-(II)-chloride
CoM	center of mass
CPG2/CMDA	carboxypeptidase G2/4-[(2-chloroethyl) (2-mesyloxyethyl) amino] -benzoyl-L-glutamic acid
CT	cycle threshold
CTGF	connective tissue growth factor
CX3CL1	CX3 chemokine ligand 1
CXCL12	chemokine (C-X-C Motif) Ligand 12
CXCL16	chemokine (C-X-C Motif) Ligand 16
CXCR4	chemokine receptor type 4
DAPI	4',6-diamidino-2-phenylindole
dl	deciliter
DMEM	Dulbecco's modified eagle medium
DMSO	dimethyl sulfoxide
DNA	deoxyribonucleic acid
DTT	dithiothreitol
EDTA	ethylenediaminetetraacetic acid
EGF	epidermal growth factor
EGFP	green fluorescent protein

EGFR	epidermal growth factor receptor
ELISA	enzyme-linked immunosorbent assay
EMT	epithelial mesenchymal transition
ERK1/2	extracellular-signal regulated kinases
FACS	fluorescence-activated cell sorting
FCS	fetal calf serum
FGF2	fibroblast growth factor 2
FMI	forward migration index
hBMSC	human bone marrow derived mesenchymal stem cell
HCC	hepatocellular carcinoma
HCl	hydrochloric acid
HE	haematoxylin-eosin
HEMA	2-hydroxyethyl methacrylate
HEPES	(4-(2-hydroxyethyl)-1-piperazineethanesulfonic acid)
HGF	hepatocyte growth factor
HIF1 α	hypoxia inducible factor 1 α
HIFs	hypoxia induced transcription factors
HLA-DR	human leukocyte antigen - D related
HRE	hypoxia responsive element
hrs	hours
HSV-TK	herpes simplex virus thymidine kinase
HUH7	human hepatoma cell line 7 (HCC derived)
I	iodine
ID1	DNA-binding protein inhibitor 1
IGF-2	Insulin-like growth factor 2
IL6	interleukin 6
kDA	kilodalton
L	liter
M	molar
MAPK	mitogen-activated protein kinase
MHC II	major histocompatibility complex II
Min	minute
ml	mililiter
MMP9/2	matrix metalloprotease 9/2
Mio	million
MRI	magnetic resonance imaging
mRNA	messenger RNA
MSCs	human mesenchymal stem cells
MTA	medical-laboratory assistant
mTOR	mechanistic target of Rapamycin
MTT	3-(4,5-dimethylthiazol-2-yl)-2,5-diphenyltetrazolium bromide
n	number
NaOH	sodium hydroxide
ng	nanogram
NIS	sodium iodine symporter
nM	nanomolar
NTC	no template control
NTR/CB1954	nitroreductase Nfsb with 5-(aziridin-1-Y1)-2 4-dinitrobenzamide
O ₂	oxygen
p	probability value
PBS	phosphate buffered saline

PCR	polymerase chain reaction
PET	positron emission tomography
Pg	pikogram
PI3K	phosphatidylinositol 3-kinase
PIPES	piperazine-N,N'-bis(2-ethanesulfonic acid)
PLB	passive lysis buffer
μF	microfarad
μl	microliter
μM	micromole
qPCR	quantitative polymerase chain reaction
qRT-PCR	quantitative real time polymerase chain reaction
rcf	relative centrifugal force
Re	rhenium
RNA	ribonucleic acid
Rpm	rounds per minute
rRNA	ribosomal RNA
RT	reverse transcriptase
SD	standard deviation
SDF1	stromal cell-derived factor 1
SDS	sodium dodecyl sulfate
Sec	second
sFCS	stripped fetal calf serum
SPECT	single photon emission computed tomography
SV40	simian virus 40
T3	3,3',5-triiodo-L-thyronine
T4	L-thyroxine
TAF	tumor associated fibroblasts
Tetrac	tetraiodothyroacetic acid
TGF β	transforming growth factor β
Tie2	angiopoetin receptor
Timp1	metallopeptidase inhibitor 1
TPP	techno plastic products
TR	thyroid hormone receptor
TRAIL	tumor necrosis factor related apoptosis inducing ligand
UV	ultraviolet
V	volt
VEGF	vascular endothelial growth factor
Vzvtk/Aram	varicella zoster virus thymidine kinase with 6-methoxypurine arabinonucleoside
WB	western blot

5.2. List of Figures

Figure 1: MSC sources for tumor stroma.....	2
Figure 2: MSC tumor promoting functions	3
Figure 3: A) Tissue specific MSC differentiation B) Tumor-specific expression of engineered genes in MSCs	6
Figure 4: Molecular structure of T3 and T4.....	7
Figure 5: Overlap of non-genomic and genomic thyroid hormone effects	9
Figure 6: Molecular structure of Tetrac	9
Figure 7: Role of integrin receptors in MSC recruitment and tumor homing	10
Figure 8: Circle of tumor hypoxia.....	11
Figure 9: Hypoxia response system	12
Figure 10: MSCs showing adipogenic (after 20 days) and osteogenic (after 12 days) differentiation	17
Figure 11: Formula for cell counting with Neubauer Chamber.....	28
Figure 12: Integrin $\alpha\beta 3$ expression on MSCs is not influenced by T3/T4/Tetrac treatment	29
Figure 13: Plating plan for osteogenic (left) and adipogenic (right) differentiation	30
Figure 14: Plasmid map of pIRES-EGFP-SV40 used to immortalize primary MSCs	31
Figure 15: pGL3-based luciferase reporter vectors: A) RANTES/CCL5 promoter (pGL3-RFL) B) HIF1 α -responsive promoter (pGL3-6xHRE-luc-Blasti_clock-wise)...	40
Figure 16: Establishment of western blot conditions for analysis of MSC hypoxia response.....	42
Figure 17: Principle of μ -slide chemotaxis 3D	44
Figure 18: Parameters for evaluation of MSC migration.....	48
Figure 19: Example of 5-day-old HUH7 tumor spheroid <i>in vitro</i>	49
Figure 20: Explanation of p-values in Rayleigh-test.....	52
Figure 21: Increased intracellular HIF1 α protein level under hypoxic conditions in MSCs after 12 hrs.....	53
Figure 22: Principle of promoter induced reporter gene activity.....	54
Figure 23: Significant induction of HIF1 α -responsive promoter in MSCs after 48 hrs of hypoxic exposure, with and without additional exposure to HUH7 conditioned medium (CM). No induction of RANTES/CCL5 promoter driven luciferase in hypoxia after 48 hrs	55
Figure 24: Necrotic center of 19-day-old HUH7 tumor spheroid	56
Figure 25: Hypoxic belt around the necrotic center of HT29 tumor spheroids	57
Figure 26: CMFDA stained MSCs show strong tropism for HUH7 tumor spheroid center.....	57
Figure 27: HIF1 α western blot in HUH7 cells shows no effect of thyroid hormone treatment on HIF1 α protein levels under different oxygen conditions	58
Figure 28: HIF1 α -dependent reporter gene activity in HUH7 cells not influenced by thyroid hormones under hypoxic or normoxic conditions	59
Figure 29: Thyroid hormones increase normoxic HIF1 α protein levels in MSCs after 12 hrs.....	60
Figure 30: T3 increases HIF1 α protein levels in MSCs in a Tetrac dependent manner under tumor milieu conditions.....	60
Figure 31: Significant Tetrac dependent increase of HIF1 α -driven reporter gene activation through thyroid hormone treatment in MSCs under normoxic conditions .	61
Figure 32: Increase of HIF1 α -driven reporter gene activation through thyroid hormone treatment in MSCs under hypoxic conditions.....	62

Figure 33: Steady state mRNA level of HIF1 α and CCL5 genes in MSCs increases in a Tetrac dependent manner through thyroid hormone treatment under normoxic conditions	63
Figure 34: Induction of mRNA expression of HIF1 α , CCL5, IL6, VEGFa, FGF2 and CXCL12 genes in MSCs through thyroid hormone treatment in a Tetrac dependent manner under tumor milieu conditions.....	64
Figure 35: Stable directed migration of MSCs along a gradient of HUH7 conditioned medium (CM)	66
Figure 36: T3 increases tumor directed chemotaxis of MSC	68
Figure 37: T4 increases tumor directed chemotaxis of MSCs	69
Figure 38: T3 and T4 increase tumor directed chemotaxis of MSCs in a Tetrac dependent manner.	70
Figure 39: T3 and T4 increase tumor directed chemotaxis of MSCs in a Tetrac dependent manner characterized by FMI, displacement of CoM and Rayleigh test for vector data.....	71
Figure 40: Stimulation with HUH7 conditioned medium (CM) and hypoxia leads to significant increase in MSC viability after 72hrs.....	73
Figure 41: Stimulating effects of thyroid hormones and HUH7 conditioned medium (CM) on MSC proliferation	74
Figure 42: Principle of hypoxia targeted MSC-based cancer gene therapy in comparison to RANTES/CCL5 targeted approach	77
Figure 43: Influence of thyroid hormones on MSC-based hypoxia targeted cancer gene therapy.....	79
Figure 44: Effective tumor-specific promoters for MSC-based cancer gene therapy – synthetic versus native promoters	83

5.3. List of Tables

Table 1: Media for osteogenic and adipogenic differentiation of MSCs	30
Table 2: Reaction mixture for reverse transcription of 2 μ g RNA.....	37
Table 3: Reaction mixture used for qRT-PCR using premixed Taqman assay.....	37
Table 4: Reaction mixture used for qRT-PCR with separate forward and reverse primers.....	38
Table 5: Reaction mixture used for qRT-PCR using SYBRgreen method	39
Table 6: Recipe for 6-8% resolving gel.	43
Table 7: Basic recipe for collagen I gel matrix	45

6. References

- Ahmed, F., Steele, J. C., Herbert, J. M., Steven, N. M., Bicknell, R. (2008).** "Tumor stroma as a target in cancer." *Curr Cancer Drug Targets* 8(6):447-453.
- Bao, Q., Zhao, Y., Niess, H., Conrad, C., Schwarz, B., Jauch, K. W., Huss, R., Nelson, P. J., Bruns, C. J. (2012).** "Mesenchymal stem cell-based tumor-targeted gene therapy in gastrointestinal cancer." *Stem Cells Dev* 21(13):2355-2363.
- Barcellos-de-Souza, P., Gori, V., Bambi, F., Chiarugi, P. (2013).** "Tumor microenvironment: bone marrow-mesenchymal stem cells as key players." *Biochim Biophys Acta* 1836(2):321-335.
- Benita, Y., Kikuchi, H., Smith, A. D., Zhang, M. Q., Chung, D. C., Xavier, R. J. (2009).** "An integrative genomics approach identifies Hypoxia Inducible Factor-1 (HIF-1)-target genes that form the core response to hypoxia." *Nucleic Acids Res* 37(14):4587-4602.
- Bergh, J. J., Lin, H. Y., Lansing, L., Mohamed, S. N., Davis, F. B., Mousa, S., Davis, P. J. (2005).** "Integrin $\alpha 5\beta 3$ contains a cell surface receptor site for thyroid hormone that is linked to activation of mitogen-activated protein kinase and induction of angiogenesis." *Endocrinology* 146(7):2864-2871.
- Brown, P. T., Squire, M. W., Li, W. J. (2014).** "Characterization and evaluation of mesenchymal stem cells derived from human embryonic stem cells and bone marrow." *Cell Tissue Res* 358(1):149-164.
- Bruick, R. K. (2003).** "Oxygen sensing in the hypoxic response pathway: regulation of the hypoxia-inducible transcription factor." *Genes Dev* 17(21):2614-2623.
- Casazza, A., Di Conza, G., Wenes, M., Finisguerra, V., Deschoemaeker, S., Mazzone, M. (2014).** "Tumor stroma: a complexity dictated by the hypoxic tumor microenvironment." *Oncogene* 33(14):1743-1754.
- Cayrol, F., Diaz Flaque, M. C., Fernando, T., Yang, S. N., Sterle, H. A., Bolontrade, M., Amoros, M., Isse, B., Farias, R. N., Ahn, H., Tian, Y. F., Tabbo, F., Singh, A., Inghirami, G., Cerchietti, L., Cremaschi, G. A. (2015).** "Integrin $\alpha v\beta 3$ acting as membrane receptor for thyroid hormones mediates angiogenesis in malignant T cells." *Blood* 125(5):841-851.
- Chaturvedi, P., Gilkes, D. M., Wong, C. C., Luo, W., Zhang, H., Wei, H., Takano, N., Schito, L., Levchenko, A., Semenza, G. L. (2013).** "Hypoxia-inducible factor-dependent breast cancer-mesenchymal stem cell bidirectional signaling promotes metastasis." *J Clin Invest* 123(1):189-205.
- Chen, M., Zhang, H., Wu, J., Xu, L., Xu, D., Sun, J., He, Y., Zhou, X., Wang, Z., Wu, L., Xu, S., Wang, J., Jiang, S., Zhou, X., Hoffman, A. R., Hu, X., Hu, J., Li, T. (2012).** "Promotion of the induction of cell pluripotency through metabolic remodeling by thyroid hormone triiodothyronine-activated PI3K/AKT signal pathway." *Biomaterials* 33(22):5514-5523.

- Cody, V., Davis, P. J., Davis, F. B. (2007).** "Molecular modeling of the thyroid hormone interactions with $\alpha\beta 3$ integrin." *Steroids* 72(2):165-170.
- Cohen, K., Flint, N., Shalev, S., Erez, D., Baharal, T., Davis, P. J., Hercbergs, A., Ellis, M., Ashur-Fabian, O. (2014).** "Thyroid hormone regulates adhesion, migration and matrix metalloproteinase 9 activity via $\alpha\beta 3$ integrin in myeloma cells." *Oncotarget* 5(15):6312-6322.
- Conrad, C., Gupta, R., Mohan, H., Niess, H., Bruns, C. J., Kopp, R., von Luettichau, I., Guba, M., Heeschen, C., Jauch, K. W., Huss, R., Nelson, P. J. (2007).** "Genetically engineered stem cells for therapeutic gene delivery." *Curr Gene Ther* 7(4):249-260.
- Conrad, C., Husemann, Y., Niess, H., von Luettichau, I., Huss, R., Bauer, C., Jauch, K. W., Klein, C. A., Bruns, C., Nelson, P. J. (2011).** "Linking transgene expression of engineered mesenchymal stem cells and angiopoietin-1-induced differentiation to target cancer angiogenesis." *Ann Surg* 253(3):566-571.
- Conrad, C., Niess, H., Huss, R., Huber, S., von Luettichau, I., Nelson, P. J., Ott, H. C., Jauch, K. W., Bruns, C. J. (2009).** "Multipotent mesenchymal stem cells acquire a lymphendothelial phenotype and enhance lymphatic regeneration in vivo." *Circulation* 119(2):281-289.
- Conrad, C., Zeindl-Eberhart, E., Moosmann, S., Nelson, P. J., Bruns, C. J., Huss, R. (2008).** "Alkaline phosphatase, glutathione-S-transferase-P, and cofilin-1 distinguish multipotent mesenchymal stromal cell lines derived from the bone marrow versus peripheral blood." *Stem Cells Dev* 17(1):23-27.
- D'souza, N., Rossignoli, F., Golinelli, G., Grisendi, G., Spano, C., Candini, O., Osturu, S., Catani, F., Paolucci, P., Horwitz, E. M. (2015).** "Mesenchymal stem/stromal cells as a delivery platform in cell and gene therapies." *BMC medicine* 13(1):186.
- Davis, P. J., Davis, F. B., Cody, V. (2005).** "Membrane receptors mediating thyroid hormone action." *Trends Endocrinol Metab* 16(9):429-435.
- Davis, P. J., Davis, F. B., Lin, H. Y., Mousa, S. A., Zhou, M., Luidens, M. K. (2009).** "Translational implications of nongenomic actions of thyroid hormone initiated at its integrin receptor." *Am J Physiol Endocrinol Metab* 297(6):E1238-1246.
- Davis, P. J., Davis, F. B., Mousa, S. A., Luidens, M. K., Lin, H. Y. (2011).** "Membrane receptor for thyroid hormone: physiologic and pharmacologic implications." *Annu Rev Pharmacol Toxicol* 51:99-115.
- Davis, P. J., Glinsky, G. V., Lin, H. Y., Leith, J. T., Hercbergs, A., Tang, H. Y., Ashur-Fabian, O., Incerpi, S., Mousa, S. A. (2014a).** "Cancer Cell Gene Expression Modulated from Plasma Membrane Integrin $\alpha\beta 3$ by Thyroid Hormone and Nanoparticulate Tetrac." *Front Endocrinol (Lausanne)* 5:240.

- Davis, P. J., Lin, H. Y., Sudha, T., Yalcin, M., Tang, H. Y., Hercbergs, A., Leith, J. T., Luidens, M. K., Ashur-Fabian, O., Incerpi, S., Mousa, S. A. (2014b).** "Nanotetrac targets integrin $\alpha v \beta 3$ on tumor cells to disorder cell defense pathways and block angiogenesis." *Onco Targets Ther* 7:1619-1624.
- De Wever, O., Mareel, M. (2003).** "Role of tissue stroma in cancer cell invasion." *J Pathol* 200(4):429-447.
- Dimarino, A. M., Caplan, A. I., Bonfield, T. L. (2013).** "Mesenchymal stem cells in tissue repair." *Front Immunol* 4:201.
- Dominici, M., Le Blanc, K., Mueller, I., Slaper-Cortenbach, I., Marini, F., Krause, D., Deans, R., Keating, A., Prockop, D., Horwitz, E. (2006).** "Minimal criteria for defining multipotent mesenchymal stromal cells. The International Society for Cellular Therapy position statement." *Cytotherapy* 8(4):315-317.
- Droujinine, I. A., Eckert, M. A., Zhao, W. (2013).** "To grab the stroma by the horns: from biology to cancer therapy with mesenchymal stem cells." *Oncotarget* 4(5):651-664.
- Dvorak, H. F. (2015).** "Tumors: wounds that do not heal-redux." *Cancer Immunol Res* 3(1):1-11.
- Fessele, S. (2001).** "Funktionelle Charakterisierung und in silico-Modellierung LPS-induzierbarer Elemente des RANTES-Promoters in humanen Monocyten." *univ. Diss., Universität Stuttgart.*
- Forner, A., Llovet, J. M., Bruix, J. (2012).** "Hepatocellular carcinoma." *Lancet* 379(9822):1245-1255.
- Fox, J. M., Chamberlain, G., Ashton, B. A., Middleton, J. (2007).** "Recent advances into the understanding of mesenchymal stem cell trafficking." *Br J Haematol* 137(6):491-502.
- Fritz, V., Jorgensen, C. (2008).** "Mesenchymal stem cells: an emerging tool for cancer targeting and therapy." *Curr Stem Cell Res Ther* 3(1):32-42.
- Fujita, M., Yasuda, M., Kitatani, K., Miyazawa, M., Hirabayashi, K., Takekoshi, S., Iida, T., Hirasawa, T., Murakami, M., Mikami, M., Ishiwata, I., Shimizu, M., Osamura, R. Y. (2007).** "An up-to-date anti-cancer treatment strategy focusing on HIF-1 α suppression: its application for refractory ovarian cancer." *Acta Histochem Cytochem* 40(5):139-142.
- Gammon, L., Biddle, A., Heywood, H. K., Johannessen, A. C., Mackenzie, I. C. (2013).** "Sub-sets of cancer stem cells differ intrinsically in their patterns of oxygen metabolism." *PLoS One* 8(4):e62493.
- Grisendi, G., Spano, C., D'Souza, N., Rasini, V., Veronesi, E., Prapa, M., Petrachi, T., Piccinno, S., Rossignoli, F., Burns, J. S., Fiorcari, S., Granchi, D., Baldini, N., Horwitz, E. M., Guarneri, V., Conte, P., Paolucci, P., Dominici, M. (2015).** "Mesenchymal progenitors expressing TRAIL induce apoptosis in sarcomas." *Stem Cells* 33(3):859-869.

- Hagenhoff, A., Bruns, C. J., Zhao, Y., von Luttichau, I., Niess, H., Spitzweg, C., Nelson, P. J. (2016).** "Harnessing mesenchymal stem cell homing as an anticancer therapy." *Expert Opin Biol Ther*:1-14.
- Hammes, S. R., Davis, P. J. (2015).** "Overlapping nongenomic and genomic actions of thyroid hormone and steroids." *Best Pract Res Clin Endocrinol Metab* 29(4):581-593.
- Heindryckx, F., Gerwins, P. (2015).** "Targeting the tumor stroma in hepatocellular carcinoma." *World J Hepatol* 7(2):165-176.
- Hiroi, Y., Kim, H. H., Ying, H., Furuya, F., Huang, Z., Simoncini, T., Noma, K., Ueki, K., Nguyen, N. H., Scanlan, T. S., Moskowitz, M. A., Cheng, S. Y., Liao, J. K. (2006).** "Rapid nongenomic actions of thyroid hormone." *Proc Natl Acad Sci U S A* 103(38):14104-14109.
- Horwitz, E., Le Blanc, K., Dominici, M., Mueller, I., Slaper-Cortenbach, I., Marini, F., Deans, R., Krause, D., Keating, A. (2005).** "Clarification of the nomenclature for MSC: The International Society for Cellular Therapy position statement." *Cytotherapy* 7(5):393-395.
- Hung, S. C., Deng, W. P., Yang, W. K., Liu, R. S., Lee, C. C., Su, T. C., Lin, R. J., Yang, D. M., Chang, C. W., Chen, W. H., Wei, H. J., Gelovani, J. G. (2005).** "Mesenchymal stem cell targeting of microscopic tumors and tumor stroma development monitored by noninvasive in vivo positron emission tomography imaging." *Clin Cancer Res* 11(21):7749-7756.
- ibidi GmbH, H., Elias. (2012).** "Application Note 17: 3 D Chemotaxis Assays Using μ -Slide Chemotaxis 3D." Retrieved 10.11.2015, from http://ibidi.com/fileadmin/support/application_notes/AN17_Chemotaxis3D.pdf.
- Kaka, G. R., Tiraihi, T., Delshad, A., Arabkheradmand, J., Kazemi, H. (2012).** "In vitro differentiation of bone marrow stromal cells into oligodendrocyte-like cells using triiodothyronine as inducer." *Int J Neurosci* 122(5):237-247.
- Karl, A., Olbrich, N., Pfeifer, C., Berner, A., Zellner, J., Kujat, R., Angele, P., Nerlich, M., Mueller, M. B. (2014).** "Thyroid hormone-induced hypertrophy in mesenchymal stem cell chondrogenesis is mediated by bone morphogenetic protein-4." *Tissue Eng Part A* 20(1-2):178-188.
- Karp, J. M., Leng Teo, G. S. (2009).** "Mesenchymal stem cell homing: the devil is in the details." *Cell Stem Cell* 4(3):206-216.
- Keung, E. Z., Nelson, P. J., Conrad, C. (2013).** "Concise review: genetically engineered stem cell therapy targeting angiogenesis and tumor stroma in gastrointestinal malignancy." *Stem Cells* 31(2):227-235.
- Kim, K. H., Jung, H. J., Kwon, H. J. (2013a).** "A new anti-angiogenic small molecule, G0811, inhibits angiogenesis via targeting hypoxia inducible factor (HIF)-1 α signal transduction." *Biochem Biophys Res Commun* 441(2):399-404.
- Kim, W. G., Cheng, S. Y. (2013b).** "Thyroid hormone receptors and cancer." *Biochim Biophys Acta* 1830(7):3928-3936.

- Kizaka-Kondoh, S., Tanaka, S., Harada, H., Hiraoka, M. (2009).** "The HIF-1-active microenvironment: an environmental target for cancer therapy." *Adv Drug Deliv Rev* 61(7-8):623-632.
- Knoop, K., Kolokythas, M., Klutz, K., Willhauck, M. J., Wunderlich, N., Draganovici, D., Zach, C., Gildehaus, F. J., Boning, G., Goke, B., Wagner, E., Nelson, P. J., Spitzweg, C. (2011).** "Image-guided, tumor stroma-targeted ¹³¹I therapy of hepatocellular cancer after systemic mesenchymal stem cell-mediated NIS gene delivery." *Mol Ther* 19(9):1704-1713.
- Knoop, K., Schwenk, N., Dolp, P., Willhauck, M. J., Zischek, C., Zach, C., Hacker, M., Goke, B., Wagner, E., Nelson, P. J., Spitzweg, C. (2013).** "Stromal targeting of sodium iodide symporter using mesenchymal stem cells allows enhanced imaging and therapy of hepatocellular carcinoma." *Hum Gene Ther* 24(3):306-316.
- Knoop, K., Schwenk, N., Schmohl, K., Muller, A., Zach, C., Cyran, C., Carlsen, J., Boning, G., Bartenstein, P., Goke, B., Wagner, E., Nelson, P. J., Spitzweg, C. (2015).** "Mesenchymal stem cell-mediated, tumor stroma-targeted radioiodine therapy of metastatic colon cancer using the sodium iodide symporter as theranostic gene." *J Nucl Med* 56(4):600-606.
- Kumar, D. (2009).** "Signal and tissue specific functional characterization, and in silico modelling of the CCL5 promoter in human natural killer and glomerular mesangial cells." *Dr. rer. nat., Ludwig-Maximilians Universität München.*
- Laemmli, U. K. (1970).** "Cleavage of structural proteins during the assembly of the head of bacteriophage T4." *Nature* 227(5259):680-685.
- Lazennec, G., Jorgensen, C. (2008).** "Concise review: adult multipotent stromal cells and cancer: risk or benefit?" *Stem Cells* 26(6):1387-1394.
- Lee, B. H., Kim, M. H., Lee, J. H., Seliktar, D., Cho, N. J., Tan, L. P. (2015).** "Modulation of Huh7.5 spheroid formation and functionality using modified PEG-based hydrogels of different stiffness." *PLoS One* 10(2):e0118123.
- Lee, J. G., Kang, C. M., Park, J. S., Kim, K. S., Yoon, D. S., Choi, J. S., Lee, W. J., Kim, B. R. (2006).** "The actual five-year survival rate of hepatocellular carcinoma patients after curative resection." *Yonsei Med J* 47(1):105-112.
- Lin, H. Y., Chin, Y. T., Yang, Y. C., Lai, H. Y., Wang-Peng, J., Liu, L. F., Tang, H. Y., Davis, P. J. (2016).** "Thyroid Hormone, Cancer, and Apoptosis." *Compr Physiol* 6(3):1221-1237.
- Lin, H. Y., Glinsky, G. V., Mousa, S. A., Davis, P. J. (2015).** "Thyroid hormone and anti-apoptosis in tumor cells." *Oncotarget* 6(17):14735-14743.
- Lin, H. Y., Sun, M., Tang, H. Y., Lin, C., Luidens, M. K., Mousa, S. A., Incerpi, S., Drusano, G. L., Davis, F. B., Davis, P. J. (2009).** "L-Thyroxine vs. 3,5,3'-triiodo-L-thyronine and cell proliferation: activation of mitogen-activated protein kinase and phosphatidylinositol 3-kinase." *Am J Physiol Cell Physiol* 296(5):C980-991.

- Liu, W., Shen, S. M., Zhao, X. Y., Chen, G. Q. (2012).** "Targeted genes and interacting proteins of hypoxia inducible factor-1." *Int J Biochem Mol Biol* 3(2):165-178.
- Liu, X. W., Cai, T. Y., Zhu, H., Cao, J., Su, Y., Hu, Y. Z., He, Q. J., Yang, B. (2014).** "Q6, a novel hypoxia-targeted drug, regulates hypoxia-inducible factor signaling via an autophagy-dependent mechanism in hepatocellular carcinoma." *Autophagy* 10(1):111-122.
- Liu, Z. J., Zhuge, Y., Velazquez, O. C. (2009).** "Trafficking and differentiation of mesenchymal stem cells." *J Cell Biochem* 106(6):984-991.
- Lourenco, S., Teixeira, V. H., Kalber, T., Jose, R. J., Floto, R. A., Janes, S. M. (2015).** "Macrophage migration inhibitory factor-CXCR4 is the dominant chemotactic axis in human mesenchymal stem cell recruitment to tumors." *J Immunol* 194(7):3463-3474.
- Mackay, A. M., Beck, S. C., Murphy, J. M., Barry, F. P., Chichester, C. O., Pittenger, M. F. (1998).** "Chondrogenic differentiation of cultured human mesenchymal stem cells from marrow." *Tissue Eng* 4(4):415-428.
- Martinez-Iglesias, O., Garcia-Silva, S., Regadera, J., Aranda, A. (2009).** "Hypothyroidism enhances tumor invasiveness and metastasis development." *PLoS One* 4(7):e6428.
- Maxson, S., Lopez, E. A., Yoo, D., Danilkovitch-Miagkova, A., Leroux, M. A. (2012).** "Concise review: role of mesenchymal stem cells in wound repair." *Stem Cells Transl Med* 1(2):142-149.
- Moeller, L. C., Dumitrescu, A. M., Refetoff, S. (2005).** "Cytosolic action of thyroid hormone leads to induction of hypoxia-inducible factor-1alpha and glycolytic genes." *Mol Endocrinol* 19(12):2955-2963.
- Moore, B. R. (1980).** "A Modification of the Rayleigh Test for Vector Data." *Biometrika* 67(1):175-180.
- Mosmann, T. (1983).** "Rapid colorimetric assay for cellular growth and survival: application to proliferation and cytotoxicity assays." *J Immunol Methods* 65(1-2):55-63.
- Mousa, S. A., Lin, H. Y., Tang, H. Y., Hercbergs, A., Luidens, M. K., Davis, P. J. (2014).** "Modulation of angiogenesis by thyroid hormone and hormone analogues: implications for cancer management." *Angiogenesis* 17(3):463-469.
- Muller, A. M., Schmohl, K. A., Knoop, K., Schug, C., Urnauer, S., Hagenhoff, A., Clevert, D. A., Ingrisch, M., Niess, H., Carlsen, J., Zach, C., Wagner, E., Bartenstein, P., Nelson, P. J., Spitzweg, C. (2016).** "Hypoxia-targeted 131I therapy of hepatocellular cancer after systemic mesenchymal stem cell-mediated sodium iodide symporter gene delivery." *Oncotarget*.

- Muller, I., Kordowich, S., Holzwarth, C., Spano, C., Isensee, G., Staiber, A., Viebahn, S., Gieseke, F., Langer, H., Gawaz, M. P., Horwitz, E. M., Conte, P., Handgretinger, R., Dominici, M. (2006).** "Animal serum-free culture conditions for isolation and expansion of multipotent mesenchymal stromal cells from human BM." *Cytotherapy* 8(5):437-444.
- Nelson, M., Hercbergs, A., Rybicki, L., Strome, M. (2006).** "Association between development of hypothyroidism and improved survival in patients with head and neck cancer." *Arch Otolaryngol Head Neck Surg* 132(10):1041-1046.
- Niess, H., Bao, Q., Conrad, C., Zischek, C., Notohamiprodjo, M., Schwab, F., Schwarz, B., Huss, R., Jauch, K. W., Nelson, P. J., Bruns, C. J. (2011).** "Selective targeting of genetically engineered mesenchymal stem cells to tumor stroma micro-environments using tissue-specific suicide gene expression suppresses growth of hepatocellular carcinoma." *Ann Surg* 254(5):767-774; discussion 774-765.
- Niess, H., von Einem, J. C., Thomas, M. N., Michl, M., Angele, M. K., Huss, R., Gunther, C., Nelson, P. J., Bruns, C. J., Heinemann, V. (2015).** "Treatment of advanced gastrointestinal tumors with genetically modified autologous mesenchymal stromal cells (TREAT-ME1): study protocol of a phase I/II clinical trial." *BMC Cancer* 15:237.
- Otto, T., Fandrey, J. (2008).** "Thyroid hormone induces hypoxia-inducible factor 1alpha gene expression through thyroid hormone receptor beta/retinoid x receptor alpha-dependent activation of hepatic leukemia factor." *Endocrinology* 149(5):2241-2250.
- Palomaki, S., Pietila, M., Laitinen, S., Pesala, J., Sormunen, R., Lehenkari, P., Koivunen, P. (2013).** "HIF-1alpha is upregulated in human mesenchymal stem cells." *Stem Cells* 31(9):1902-1909.
- Patiar, S., Harris, A. L. (2006).** "Role of hypoxia-inducible factor-1alpha as a cancer therapy target." *Endocr Relat Cancer* 13 Suppl 1:S61-75.
- Penzo, M., Habel, D. M., Ramadass, M., Kew, R. R., Marcu, K. B. (2014).** "Cell migration to CXCL12 requires simultaneous IKKalpha and IKKbeta-dependent NF-kappaB signaling." *Biochim Biophys Acta* 1843(9):1796-1804.
- Pittenger, M. F., Mackay, A. M., Beck, S. C., Jaiswal, R. K., Douglas, R., Mosca, J. D., Moorman, M. A., Simonetti, D. W., Craig, S., Marshak, D. R. (1999).** "Multilineage potential of adult human mesenchymal stem cells." *Science* 284(5411):143-147.
- Pomo, J. M., Taylor, R. M., Gullapalli, R. R. (2016).** "Influence of TP53 and CDH1 genes in hepatocellular cancer spheroid formation and culture: a model system to understand cancer cell growth mechanics." *Cancer Cell Int* 16:44.
- Rajab, K., Nelson, P., Keung, E. Z., Conrad, C. (2013).** "Suicide Gene Therapy against Cancer." *J Genet Syndr Gene Ther* 4(187):2.
- Reiser, J., Zhang, X. Y., Hemenway, C. S., Mondal, D., Pradhan, L., La Russa, V. F. (2005).** "Potential of mesenchymal stem cells in gene therapy approaches for inherited and acquired diseases." *Expert Opin Biol Ther* 5(12):1571-1584.

- Ruhland, S., Wechselberger, A., Spitzweg, C., Huss, R., Nelson, P. J., Harz, H. (2015).** "Quantification of in vitro mesenchymal stem cell invasion into tumor spheroids using selective plane illumination microscopy." *J Biomed Opt* 20(4):040501.
- Salem, H. K., Thiemermann, C. (2010).** "Mesenchymal stromal cells: current understanding and clinical status." *Stem Cells* 28(3):585-596.
- Sanger, F., Nicklen, S., Coulson, A. R. (1992).** "DNA sequencing with chain-terminating inhibitors. 1977." *Biotechnology* 24:104-108.
- Sasportas, L. S., Kasmieh, R., Wakimoto, H., Hingtgen, S., Van De Water, J. A., Mohapatra, G., Figueiredo, J. L., Martuza, R. L., Weissleder, R., Shah, K. (2009).** "Assessment of therapeutic efficacy and fate of engineered human mesenchymal stem cells for cancer therapy." *Proceedings of the National Academy of Sciences* 106(12):4822-4827.
- Schmohl, K. A., Muller, A. M., Wechselberger, A., Ruhland, S., Salb, N., Schwenk, N., Heuer, H., Carlsen, J., Goke, B., Nelson, P. J., Spitzweg, C. (2015).** "Thyroid hormones and tetrac: new regulators of tumour stroma formation via integrin $\alpha v \beta 3$." *Endocr Relat Cancer*.
- Semaan, A., Dietrich, D., Bergheim, D., Dietrich, J., Kalff, J. C., Branchi, V., Matthaei, H., Kristiansen, G., Fischer, H. P., Goltz, D. (2017).** "CXCL12 expression and PD-L1 expression serve as prognostic biomarkers in HCC and are induced by hypoxia." *Virchows Arch* 470(2):185-196.
- Semenza, G. L. (2003).** "Targeting HIF-1 for cancer therapy." *Nat Rev Cancer* 3(10):721-732.
- Sharma, P., Levesque, T., Boilard, E., Park, E. A. (2014).** "Thyroid hormone status regulates the expression of secretory phospholipases." *Biochem Biophys Res Commun* 444(1):56-62.
- Shweta, Mishra, K. P., Chanda, S., Singh, S. B., Ganju, L. (2015).** "A comparative immunological analysis of CoCl₂ treated cells with in vitro hypoxic exposure." *Biomaterials* 28(1):175-185.
- Spaeth, E., Klopp, A., Dembinski, J., Andreeff, M., Marini, F. (2008).** "Inflammation and tumor microenvironments: defining the migratory itinerary of mesenchymal stem cells." *Gene Ther* 15(10):730-738.
- Spaeth, E. L., Dembinski, J. L., Sasser, A. K., Watson, K., Klopp, A., Hall, B., Andreeff, M., Marini, F. (2009).** "Mesenchymal stem cell transition to tumor-associated fibroblasts contributes to fibrovascular network expansion and tumor progression." *PLoS One* 4(4):e4992.
- Srinivasan, S., Dunn, J. F. (2011).** "Stabilization of hypoxia-inducible factor-1 α in buffer containing cobalt chloride for Western blot analysis." *Anal Biochem* 416(1):120-122.

Stewart, B. W., Wild, C. P. (2014). World Cancer Report 2014, *IARC Nonserial Publication*.

Straub, R. H. (2014). "Interaction of the endocrine system with inflammation: a function of energy and volume regulation." *Arthritis Res Ther* 16(1):203.

Studený, M., Marini, F. C., Dembinski, J. L., Zompetta, C., Cabreira-Hansen, M., Bekele, B. N., Champlin, R. E., Andreeff, M. (2004). "Mesenchymal stem cells: potential precursors for tumor stroma and targeted-delivery vehicles for anticancer agents." *J Natl Cancer Inst* 96(21):1593-1603.

Thalmeier, K., Meissner, P., Reisbach, G., Falk, M., Brechtel, A., Dormer, P. (1994). "Establishment of two permanent human bone marrow stromal cell lines with long-term post irradiation feeder capacity." *Blood* 83(7):1799-1807.

Torsvik, A., Bjerkvig, R. (2013). "Mesenchymal stem cell signaling in cancer progression." *Cancer Treat Rev* 39(2):180-188.

Towbin, H., Staehelin, T., Gordon, J. (1979). "Electrophoretic transfer of proteins from polyacrylamide gels to nitrocellulose sheets: procedure and some applications." *Proc Natl Acad Sci U S A* 76(9):4350-4354.

Vaupel, P. (2004). "The role of hypoxia-induced factors in tumor progression." *Oncologist* 9 Suppl 5:10-17.

Waleh, N. S., Brody, M. D., Knapp, M. A., Mendonca, H. L., Lord, E. M., Koch, C. J., Laderoute, K. R., Sutherland, R. M. (1995). "Mapping of the vascular endothelial growth factor-producing hypoxic cells in multicellular tumor spheroids using a hypoxia-specific marker." *Cancer Res* 55(24):6222-6226.

Yang, J. D., Nakamura, I., Roberts, L. R. (2011). "The tumor microenvironment in hepatocellular carcinoma: current status and therapeutic targets." *Semin Cancer Biol* 21(1):35-43.

Yeligar, S. M., Machida, K., Tsukamoto, H., Kalra, V. K. (2009). "Ethanol augments RANTES/CCL5 expression in rat liver sinusoidal endothelial cells and human endothelial cells via activation of NF-kappa B, HIF-1 alpha, and AP-1." *J Immunol* 183(9):5964-5976.

Yen, P. M., Ando, S., Feng, X., Liu, Y., Maruvada, P., Xia, X. (2006). "Thyroid hormone action at the cellular, genomic and target gene levels." *Mol Cell Endocrinol* 246(1-2):121-127.

Zischek, C. (2011). "Das Tumorstroma als Angriffspunkt einer stammzellbasierten CCL5-Promoter/HSV-TK Suizidtherapie in einem murinen Pankreastumormodell." *LMU Munich*.

Zischek, C., Niess, H., Ischenko, I., Conrad, C., Huss, R., Jauch, K. W., Nelson, P. J., Bruns, C. (2009). "Targeting tumor stroma using engineered mesenchymal stem cells reduces the growth of pancreatic carcinoma." *Ann Surg* 250(5):747-753.

7. Publications

Work associated with the experiments of this thesis was published 2015 under the title "Thyroid hormones and tetrac: new regulators of tumour stroma formation via integrin $\alpha v \beta 3$ " in the journal "endocrine-related cancer" together with Schmohl, K. A., Muller, A. M., Wechselberger, A., Rühland, S., Schwenk, N., Heuer, H., Carlsen, J., Goke, B., Nelson, P. J. and Spitzweg, C. (Schmohl et al. 2015)

8. Acknowledgements

The work for this thesis was funded by FöFoLe (Förderprogramm für Forschung und Lehre) at Ludwig-Maximilians University Munich. The project was also funded by the Deutsche Forschungsgemeinschaft within the Priority Program SPP1629 to C. Spitzweg and P.J. Nelson (SP 581/6-1, SP581/6-2, NE 648/5-2).

I want to thank:

Prof. Nelson for the outstanding supervision and support at all levels. I feel honored that I could work with such an inspiring researcher on a very interesting topic.

The good souls of the lab: Alexandra Wechselberger, Monika Hofstetter, Anke Fischer and Sylke Rohrer who supported me with their expertise and positive attitude in so many ways.

Anna Hagenhoff for the good cooperation and prework.

Svenja Rühland for the good cooperation.

Prof. Spitzweg and her team, especially Andrea Müller and Kathrin Schmohl for the fruitful meetings and cooperation.

Carsten Jäckel for the IT-support.

The Föfole Team for funding and many opportunities to learn and exchange advice with fellow students.

Apceth GmbH for the isolated MSCs.

My family for their continued support and love through all challenges.

Eidesstattliche Versicherung

Ich, **Nicole Salb, geb. Schöbinger**, erkläre hiermit an Eides statt, dass ich die vorliegende Dissertation mit dem Thema **Application of engineered mesenchymal stem cells as therapeutic vehicles for the treatment of solid tumors: HIF1 α -based targeting and the influence of thyroid hormones** selbständig verfasst, mich außer der angegebenen keiner weiteren Hilfsmittel bedient und alle Erkenntnisse, die aus dem Schrifttum ganz oder annähernd übernommen sind, als solche kenntlich gemacht und nach ihrer Herkunft unter Bezeichnung der Fundstelle einzeln nachgewiesen habe.

Ich erkläre des Weiteren, dass die hier vorgelegte Dissertation nicht in gleicher oder in ähnlicher Form bei einer anderen Stelle zur Erlangung eines akademischen Grades eingereicht wurde.

München, den 08.10.2018

Nicole Salb
(Unterschrift Doktorandin)